PONTIFICIA UNIVERSIDAD JAVERIANA

DOCTORAL THESIS

NOVEL DATA-DRIVEN CONTROL APPROACHES

Application in essential oil extraction processes

Author:

Eng. Freddy F. Valderrama Gutiérrez, M.Sc

Advisor:

Prof. Fredy O. Ruiz, Ph.D.

A thesis submitted in fulfillment of the requirements for the degree of Ph.D. in Engineering
in the

Departamento de Electrónica
Facultad de ingeniería
Pontificia Universidad Javeriana

December 12, 2019

Abstract

In this dissertation are developed new methods for the design of controllers from data for linear systems, useful when the plant model is unavailable, two frameworks have been considered using set-membership techniques (SMT) and the Youla-Kucera parametrization (YK-DDC). The developed methods have been extensively evaluated in simulation and experimental settings. In SMT, the Unknown But Bounded (UBB) noise structure affecting the experimental data has been assumed, and a proper data-based criterion is stated according to the reference model criterion problem. Such formulation allows to state hard bounds on controller parameters via linear programming techniques. SMT approach has been experimentally validated on an active suspension system via a Monte-Carlo experiment, and it has been compared with VRFT methodology. Results have shown that using the same information about the plant to be controlled, the VRFT controllers are strongly affected by the size of the dataset while the SMT controllers exhibit good performances, even when they are estimated from reduced datasets.

Two SMT extensions have been proposed, the first one allows to design limited-complexity controllers using sparse identification methods, the proposed algorithm avoids solving big combinatorial problems that arise when the dimension of the vector parametrizing the candidate controllers is large and the number of desired parameters is much lower. A benchmark flexible transmission model is employed to illustrate the performance of the proposed methodology in comparison to the sparse correlation based tuning approach (SCbT). It is found that both approaches offer similar performance when the size of the data set is much larger than the dimension of the controller parameters vector. Notwithstanding, the SCbT controllers are strongly affected when data set size is reduced, while SMT controllers exhibit good performances even when the controller parameters are estimated from reduced data sets. The second extension proposes a procedure to estimate controllers capable of approaching a given closed-loop reference model and a sensitivity transfer function (Two-degree-of-freedom controllers). To do this, an efficient solution based on convex optimization is proposed. In literature, this the first attempt that employs a SM formulation. In order to validate our approach, the Errors-in-Variables approach proposed in literature for one DoF controllers has been adapted to solve the two degree-of-freedom problem. Our method and the adapted method are developed within a Set Membership framework. Results indicate that the computational cost, in terms of execution time of the adapted approach is higher than in our setting, even three hundred times bigger, while similar estimation errors are presented in both approaches.

The Youla-Kucera parametrization has been employed to solve the problem of controllers design without requiring a process model. The main contribution of this part of the thesis is that the proposed controller structure allows reaching more stringent reference models than those proposed previously in the literature, maintaining a convex formulation and a procedure to estimate the closed-loop stability. An extension of YK-DDC methodology to the MIMO case is also proposed. Such a methodology has been experimentally validated on a 2-DoF Helicopter. This is an important model from the control engineering point of view due to its wide non-linear characteristics, highly cross-coupling effects, and instability in open-loop. Experimental results showed that our approach achieves better results compared with the LQR+I controller proposed by the system manufacturer since the former meets the control requirement with lower settling time and smaller maximum overshoot. However, given that the 2DOF helicopter is unstable an initial stabilizing controller is required to collect the dataset and to construct a cascade control strategy.

The modeling and control of essential oil extraction processes are comprehensively studied, and novel strategies for optimal extraction operation and temperature regulation are proposed. A lab-scale ohmic distiller able to extract the essential oil from $100[g]$ of vegetal mass (aromatic herb) has been designed and constructed by the author. The selected characteristics of the distiller allowed to obtain measurable essential oil quantity from Eucalyptus, in order to obtain the kinetic extraction curves. In steam distillation, an optimal control problem has been formulated and solved in order to save energy during the extraction

process while maintaining the yield of extraction. Our solutions show that optimal steam flow trajectories are not necessarily constant, as previously mentioned in the literature. Given some phenomenological similarities between steam distillation and Ohmic assisted hydrodistillation (OAHD), the optimal input trajectories found to the former were extended to OAHD. Experimental results indicate that our input trajectory allows important energy savings, maintaining the yield statistically equal to the yield with a constant input. In addition, the proposed YK-DDC approach is applied for the regulation of temperature in an ohmic-heater, where experimental results show that our controller offers better tracking results than a procedure extracted from recent literature.

Acknowledgement

Contents

List of Tables

List of Figures

Chapter 1

Introduction

Currently, data acquisition technology permits to collect a large amount of measurements from industrial plants. When enough plant data are available in order to design a controller, there exist two main approaches in the scientific literature. In the standard model-based controller design procedure, a plant model is estimated (identified) and then employed to design a controller (two-step design). This controller is not necessarily optimal because the control loop performance is restricted by modeling errors. On the other hand, the available data can be employed to directly design a controller, avoiding the plant model estimation. This approach has been named Direct Data-Driven controllers (DDC) tuning. DDC is of particular interest in real-world practical applications. The interested reader can referred to Formentin et al. (2014), where an interesting comparison between Model-based controller design and DDC tuning is presented.

There exist adaptive (iterative) and non-iterative DDC techniques, in the first ones the controller parameters are adjusted at each time instant, in the last ones the controller is designed based on the information contained in one batch of experimental data (one-shot), these approaches are known also as off-line techniques. In this work, we are interested in off-line techniques in order to avoid the typical problems of adaptive control, moreover, since a single set of data is employed in several model-based control design methods, a fair comparison between off-line DDC techniques and model-based design can be carried out.

In the linear setting, some non-iterative controller design methods for direct data-driven controller tuning are shown and compared in (Van Heusden et al., 2011b), the studied methods are correlation approach (CbT), periodic errors in variables (EiV), the inverse controller (IC) and prediction error methods (PEM). All of them are constructed within a stochastic framework. A more recent review work of DDC methods can be found in (Hou and Wang, 2013). The authors perform a qualitative comparison and briefly explain each one technique. A different approach to solve the DDC problem follows a deterministic formulation using Set-membership techniques. There exist few results that follow this approach, one solution can be found in Cerone et al. (2017), also, for control of non-linear plants a technique named as Direct feedback control (DFK) has been developed in Novara et al. (2013a). DFK method can be used only in the restrictive case where the full state is measurable.

The more relevant techniques for this thesis are virtual reference feedback tuning (VRFT) and correlation-based tuning (CbT). VRFT was proposed in (Guardabassi and Savaresi, 2000), it is a non-iterative data-driven method that can be used to select the controller parameters for a LTI system, the problem is formulated as a controller parameters identification problem via introducing a virtual reference signal. Principal characteristics of VRFT are: (i) It is one-shot method in the linear case (noise free). (ii) The controller to find is linearly parametrized. (iii) When the measurements are noisy, the solution is addressed via instrumental variables. This requires a second experiment or a plant model.

(iv) The resulting optimization problem is convex. (v) There exist many extensions of VRFT, for instance, in (Campestrini et al., 2016) the MIMO case is tackled, and a non-linear framework is studied in (Formentin and Savaresi, 2011). In (Rojas, 2011) other extensions and applications of VRFT are studied, such author, indicates that in data-driven control it is difficult to find a controller that assures stability, and he proposes a stability test, this test requires previous identification of the plant, this is undesirable because in direct data-driven controller techniques the aim is to avoid developing a model of the plant.

Regarding to CbT, it is worth to mention that exist two correlation based approaches for data-driven controller design, one of them is iterative (iCbT) (Karimi et al., 2002), another is non-iterative (CbT-GS) (van Heusden et al., 2011), as above mentioned, in this work our interest is limited to non-iterative techniques, that is why principal characteristics of CbT-GS are listed: (i) The problem is solved via model reference criterion, but it doesn't need a virtual reference signal, (ii) In the same way that in VRFT, the controller is linearly parametrized, (iii) It is one-shot method and is better suited to deal with measurement noise (iv) In CbT-GS a sufficient conditions is proposed to guarantee closed-loop stability, (v) This method has not been extend to non linear framework. Few extensions on non-iterative CbT have been found in literature, one of them is about the tuning of controller parameters taking into account stability constraints for non-minimum phase plants (Matsuo et al., 2013), meanwhile in (Yubai et al., 2009) and (Usami, 2010) was addressed the MIMO case.

In all the methods mentioned above, the main ingredients of a DDC problem are a set of input-output data generated by the plant to be controlled, a closed-loop reference model where performance specifications are embedded, and a given controller structure, usually parametrized by a fixed set of basis functions. When the set of bases is not consistent with the reference model, the resulting controller can yield to closed-loop instability. In this sense, in Kergus et al. (2019) a set of conditions to define the behaviours that the closed-loop can reach are proposed, in order to select an achievable reference model. According to Novara (2019) the drawbacks of DDC are: (i)Only sufficient conditions are currently available to guarantee closed-loop stability. (ii) Direct design is statistically less efficient than model-based design with correct model parametrization, and (iii) If the controller can be freely chosen, the problem of model parametrization is not skipped, but simply transformed into that of controller selection.

Several applications of DDC have been reported in the literature, but none of them has considered the essential oil extraction process, this process is of high interest for this thesis. Essential Oil (EO) is an agro product which has a great prospect to be developed (Kusuma et al., 2018). The essential oils market accounted for USD 4.46 Billion in 2016, according to the Observatory of Economic Complexity (Simoes, 2018), and it is projected to reach USD 11.19 Billion by 2022. Essential oils are complex mixtures of volatile compounds extracted from a large number of plants. EO is stored in different parts of plants, for example in leaves, flowers, stems, roots, etc. There exist multiple essential oil extraction techniques (Stashenko, 2009). The most employed ones are hydro-distillation, steam distillation, and steam-water distillation. Some new techniques have been proposed, such as supercritical fluids extraction (SFE), microwave-assisted hydrodistillation (MWD), and ohmic-assisted hydrodistillation (OAHD). In this thesis, we are interested in OAHD since its main advantage over conventional distillation is that, shorter extraction times and lower energy consumption are obtained, thereby, it is environmentally friendly.

The dissertation is organized in chapters and each one can be read independently. Figure 1.1 depicts the organization of the thesis, numbered by the respective chapter and their roles in the framework of this thesis.

First, in Chapter 2, considering previous results by the author in Valderrama and Ruiz (2014) a set-membership approach to give solution to DDC design problem is proposed, our formulation is named Set-Membership tuning (SMT). In SMT, the Unknown But Bounded (UBB) noise structure affecting the
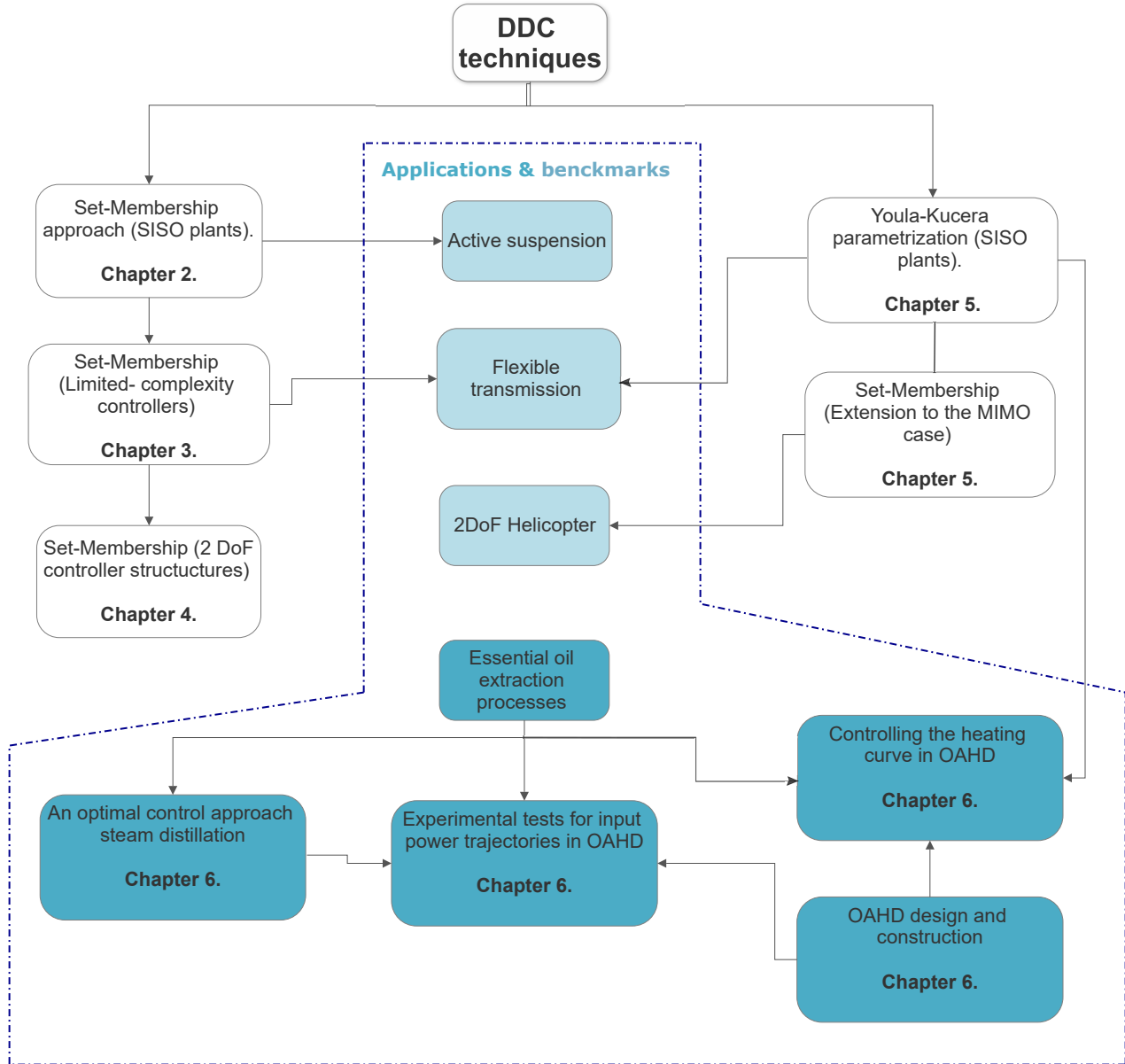
Figure 1.1: Thesis organization

experimental data has been assumed, and a proper data-based criterion is stated according to the reference model criterion problem. Such formulation allows to state hard bounds on controller parameters via linear programming techniques. We compare our approach with the Virtual Reference Feedback Tuning (VRFT) technique which assumes an stochastic description of the unknown signals. The two approaches are evaluated on an experimental case study, consisting of the controller tuning for an active suspension system. The results are obtained via a Monte-Carlo experiment, one hundred controllers are tuned by both methods employing different noise realizations and the performance is measured experimentally. Results show that both approaches offer a similar performance when the size of the dataset is much larger than the dimension of the controller parameters vector. However, for reduced datasets, the SMT approach gives consistent results while the VRFT method is not able to extract useful information. The same behavior is observed when the two approaches are applied to datasets affected by process disturbances. It is observed that the Root Mean Squared Error of the resulting loops can be up to 30 times

lower using the Set Membership method for reduced datasets. The results of this Chapter were published in (Valderrama and Ruiz, 2019).

In Chapter 3 an approach based on the set-membership techniques to tune limited-complexity controllers from data for linear systems is proposed. The controller is parametrized as a linear combination of a large set of basis functions and the proposed algorithm allows to select a sparse subset of bases, guaranteeing a bounded approximation error. A feasibility condition allows to adjust the trade-off between accuracy and sparsity. The controller design is performed by solving a set of linear programming problems, allowing to handle large data-sets. The proposed strategy is evaluated by means of a Monte-Carlo simulation experiment on a flexible transmission benchmark model. Results show that the proposed solution offers similar results than previous approaches for large data-sets, requiring less adjustable parameters. However, for reduced data-sets, the presented algorithm shows better performance than the compared approaches. The results of this Chapter have been submitted for peer review to the European Journal of Control.

In Chapter 4 an approach based on Output-Error formulation to the design of Two-Degree-of-Freedom (2DoF) controllers is proposed. We compare our approach with Errors-in-Variables formulation (EiV), assuming unknown but bounded noise sequences. First, it is derived a setting to estimate from data controllers capable of approaching a given closed-loop reference model and a sensitivity transfer function. Then, the controller estimation problems are transformed in equivalent Set-Membership Errors-in-Variables and Output-Error identification setups. Finally, we compare our approach with EiV employing two numerical examples and it is observed that a similar performance is obtained by the two methods, while our formulation is more than one hundred times faster. The results of this Chapter were presented in (Valderrama et al., 2019).

In chapter 5 the Youla-Kucera parametrization is employed to solve the DDC tuning problem, without requiring a process model. It is shown that the Youla-Kucera parametrization gives more degrees of freedom than the solutions of the previous chapters, then, it allows to achieve more stringent closed-loop performances than previous works in literature, maintaining a procedure to estimate the closed-loop stability. The proposed design methodology does not imply a plant identification step and the solution can be obtained by least-squares algorithms in the case of stochastic additive noise. The proposed solution is evaluated through Monte Carlo simulations on a flexible transmission benchmark model for the regulation problem of an under-damped system. Also in this chapter, Youla-Kucera parametrization in DDC is extended to the MIMO case, this approach is experimentally evaluated on a 2-DoF Helicopter. Our approach achieves good results compared with the LQR+I controller proposed by the system manufacturer. However, given that the 2DOF helicopter is unstable an initial stabilizing controller is required to collect the dataset. In this case, a cascade control was proposed in order to achieve loop specifications. Partial results of this Chapter have been submitted to the IFAC world congress 2020.

In chapter 6, the modeling and control of essential oil extraction processes are comprehensively studied, and novel strategies for optimal extraction operation and temperature regulation are proposed. First, in the steam distillation case, an optimal steam flow trajectory for essential oils extracted from aromatic plants is derived, minimizing energy consumption. A phenomenological dynamic model of the oil extraction process is adopted from literature and a multi-objective optimal control problem is formulated, in order to minimize energy consumption and at the same time maximize the yield of extraction. The solutions obtained show that optimal steam flow trajectories are not necessarily constant, as previously mentioned in the literature. Such solutions are extended to the OAHD method via phenomenological analysis, where the experimental results for OAHD indicate that a decreasing input power maintains an extraction yield statistically equal to the yield with constant input power. To perform the mentioned tests an ohmic distiller for 100 [g] of vegetal mass, and maximum extraction power of 1 [kW] is designed and

constructed. Finally, the DDC method proposed in Chapter 5 is employed to control the temperature in the camera of the ohmic distiller. In order to evaluate the performance of our method, the CbT method is used. Both approaches allowed tuning controllers with the same structure; however, in light of results, our controller offers better tracking results than CbT controller, specifically, the rise time is three times lower, maintaining null overshot and null steady-state error. Some results of this chapter have been published in (Valderrama and Ruiz, 2018) and (Valderrama, 2018).

Chapter 2

A set-membership approach to DDC

As mentioned above, in VRFT and CbT the measurement noise is addressed via stochastic mechanisms. In systems identification, it is well known that the counterpart of the stochastic theory (ST) is the set-membership theory (SM), a deep review can be found in (Milanese and Novara, 2011). The SM framework assumes only that the noise is bounded, in contrast with stochastic approaches, which rely on stochastic assumptions such as stationarity, uncorrelation, type of distribution,etc.

SM estimation techniques have been satisfactorily applied in system identification Milanese and Novara (2004); Milanese and Taragna (2005), filter design from data (Milanese et al., 2010; Ruiz et al., 2010; Novara et al., 2013b). The problem of data-driven controller tuning for linear systems has been investigated in Cerone et al. (2017) and Valderrama and Ruiz (2014) the latter as a precedent of this dissertation. In Cerone et al. (2017), the SM Errors-in-Variables (SMEiV) identification method is applied to solve the controller tuning problem. Convex relaxations are employed to solve the resulting polynomial optimization problems, leading to computationally demanding solutions and therefore limiting the amount of experimental data that can be considered, even for a reduced set of controller parameters. In Valderrama and Ruiz (2014), set over-bounding techniques are used to derive efficient linear programming problems from the original non-convex problem, allowing to manage larger data sets. In the non-linear framework also exist relevant studies, for instance in (Novara et al., 2013a; Tanaskovic et al., 2015) it was formulated a novel method to data-driven controllers tuning, main characteristics of such work are: (i) The authors developed theoretical framework for the stability analysis of non-linear feedback control systems, (ii) It is presented a technique for the direct design of a controller from data, (iii) Under some assumptions the closed-loop stability is guaranteed for a set of trajectories of interest, (iii) A drawback of the method is that all state variables are assumed to be measured and a feasible state trajectory is required as reference signal, generated for example by an expert human operator.

The aim of this chapter of the dissertation is to design a novel DDC tuning approach. The key idea behind this approach is employing previous results of set-membership identification theory to find a proper controller such that loop specifications are met, avoiding the model of the plant.

This chapter is organized as follows. In section 2.1 the problem is formulated, assumptions and main theorems are proposed in Section 2.2, finally a case study with the active suspension and the experimental results are shown in Section 2.3.

As the first part of this chapter, the problem is formulated as follows.
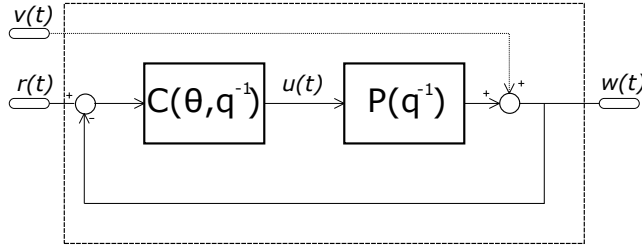
Figure 2.1: Assumed feedback control structure

2.1 Statement of the problem

Consider the discrete-time linear-time invariant (LTI) single-input single-output (SISO) feedback control scheme, depicted in Fig. 2.1, where q^{-1} denotes backward shift operator, $P(q^{-1})$ is the plant transfer function, $C(\theta, q^{-1})$ is the controller transfer function, and θ is vector of controller parameters.

For the system interconnection shown in Fig. 2.1, the aim of the controller tuning procedure is to select an optimal controller C^o minimizing some performance criterion. For example, an optimization problem can be stated as:

$$C^o(\theta^o, q^{-1}) = \arg \min_{C(\theta, q^{-1}) \in \mathcal{C}} J(C(\theta, q^{-1})) \tag{2.1}$$

For the cost function

$$J(\theta) = \left\| M(q^{-1}) - \frac{P(q^{-1})C(\theta, q^{-1})}{1 + P(q^{-1})C(\theta, q^{-1})} \right\|_{\mathfrak{s}} \tag{2.2}$$

Being $\mathfrak{s}$ a proper system norm, $\mathcal{C}$ the set of LTI systems where the controller is selected, θ a real vector parameterizing $C(\theta, q^{-1})$ and $M(q^{-1})$ a reference model for the closed-loop system, where performance specifications are embedded.

If $P(q^{-1})$ is known, Problem 2.1 can be seen as a loop-shaping problem and, for $\mathcal{H}_2$, $\mathcal{H}_\infty$ and l_1 norms, known techniques exist to solve it under proper controllability (reachability) and observability (detectability) conditions see e.g. in Skogestad and Postlethwaite (2005), Zhou and Doyle (1998).

If system $P(q^{-1})$ is unknown, Problem (2.1) can not be solved directly. The common procedure to controller design for unknown plants is to follow a two-step procedure where first a system model $\hat{P}(q^{-1})$ is estimated from data, possibly with some uncertainty measure and then a controller is obtained solving problem (2.1) for $\hat{P}(q^{-1})$.

The following assumptions define the framework of the data-driven controller tuning problem.

Assumption 1. $P(q^{-1})$ *is unknown. The available information on* $P(q^{-1})$ *is a set of input-output data generated by* $P(q^{-1})$, *initially at rest,*

$$\mathcal{D} = \{w(t), u(t), t = 1, 2, ..., N\} \tag{2.3}$$

Where

$$w(t) = \sum_{j=0}^{t} h_j u(t - j) + v(t) = y(t) + v(t),$$

16

h_j are the impulse response coefficients of $P(q^{-1})$, $y(t) = \sum_{j=0}^{t} h_j u(t-j)$ is the noise-free output and $v(t)$ is the plant output noise/disturbance.

Remark 1. *Input $u(t)$ is assumed sufficiently informative, i.e., it allows to obtain bounded sets of controller parameters. However, no hypotheses are established about the plant operation during the experiment. Either open or closed loop data can be employed.*

Assumption 2. *An internally stabilizing controller $C(\theta^*, q^{-1})$ exists such that the minimum of (3.2) is 0, that is:*

$$M(q^{-1}) = \frac{P(q^{-1})C(\theta^*, q^{-1})}{1 + P(q^{-1})C(\theta^*, q^{-1})}$$

for some $\theta^* \in \Theta$

Assumption 2 is required only for the derivation of theoretical results of the controller tuning method.

In the framework analysed, the controller is parametrized as a linear combination of fixed basis functions, that is,

$$C(\theta, q^{-1}) = \sum_{i=1}^{m} \theta_i \beta_i(q^{-1}) \tag{2.4}$$

Then, the controller that solves problem (2.1) is selected from the set:

$$\mathcal{C} = \left\{ C(\theta, q^{-1}) : \theta \in \Theta \subseteq \mathfrak{R}^n \right\}$$

Based on the previous assumptions, the DDC tuning problem can be stated as follows:

Problem 1. Data-Driven Controller tuning: *Given a dataset $\mathcal{D}$ generated as in Assumption 1, a reference model $M(q^{-1})$, a set of basis functions $\beta_i, i = 1, ..., m$, and some assumptions about noise/disturbance $v(t)$, find a vector $\hat{\theta}$ that approximately solves problem (2.1).*

For the second part of this section, we are in a position to propose an approach to solve the problem 1 employing set-membership theory.

2.2 Set-Membership approach

In this method, the noise sequence is modeled as an unknown but bounded (UBB) signal without any statistical assumption about it, as defined in the following Assumption.

Assumption 3. *Noise $v(t)$ is an (UBB) signal, such that*

$$\|v(t))\|_{\ell_p} \leq \epsilon_p$$

with $\ell_p \in [2, \infty]$. In this framework, energy and amplitude limited noise sequences can be considered. The following Lemma allows to transform the model-based controller design problem in eq. (2.1) into an data-driven controller tuning problem.

Lemma 1. *Given a data set $\mathcal{D}$ generated as in assumption 1, affected by noise bounded as in assumption 3. Then, any controller $C(\theta)$, guaranteeing an internally stable loop, satisfies the time-domain relation,*

$$e(\theta, t) = M(1-M)u(t) - C(\theta)(1-M)^2 y(t) + d(t) \tag{2.5}$$

where $e(\theta, t)$ is the output of the model matching error transfer function

$$E_m(q^{-1}) = M(q^{-1}) - \frac{P(q^{-1})C(\theta, q^{-1})}{1 + P(q^{-1})C(\theta, q^{-1})}. \tag{2.6}$$

and the unknown signal $d(t)$ is bounded as,

$$\|d(t)\|_{\ell_p} \leq \left\|C(\theta)(1-M)^2\right\|_{\ell_p, \ell_p} \epsilon_p = \delta_p \tag{2.7}$$

being $\left\|C(\theta)(1-M)^2\right\|_{\ell_p, \ell_p}$ the proper induced norm of the system relating $v(t)$ and $d(t)$. Note that, for $p = 2$, the induced norm is the H_∞ norm of the system and for $p = \infty$, the induced norm is the ℓ_1 norm of the system.

Proof: Using Assumption 2, the model matching transfer function becomes

$$E_m = \frac{C(\theta^*)P}{1 + C(\theta^*)P} - \frac{C(\theta)P}{1 + C(\theta)P} = \frac{C(\theta^*)P - C(\theta)P}{(1 + C(\theta^*)P)(1 + C(\theta)P)} \tag{2.8}$$

where the backward shift operator q^{-1} has been removed for simplicity.
Assuming that the sensitivity function for any controller close to the optimum approximates the desired one, i.e.,

$$\frac{1}{1 + PC(\theta)} \approx \frac{1}{1 + PC(\theta^*)} = (1 - M), \tag{2.9}$$

from (2.8) it follows that

$$E_m \approx \frac{C(\theta^*)P - C(\theta)P}{(1 + C(\theta^*)P)^2} = (1 - M)^2 \left[C(\theta^*)P - C(\theta)P\right] \tag{2.10}$$

Note that, from assumption 2, $C(\theta^*)P = M/(1 - M)$. Therefore,

$$E_m \approx M(1 - M) - C(\theta)(1 - M)^2 P. \tag{2.11}$$

Now, in order to avoid using the plant transfer function, the input signal $u(t)$ is applied to the system in eq. (2.11), as depicted in the block diagram of Fig. 2.2. In this case, the following model-free equation is obtained:
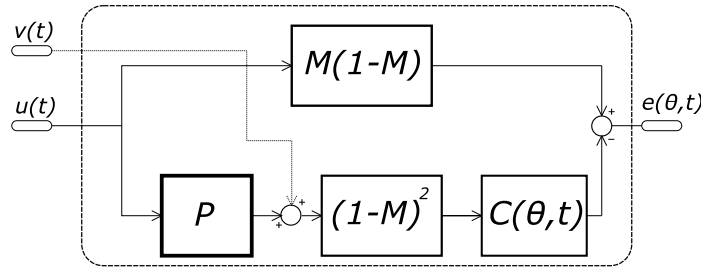
Figure 2.2: Tuning problem block diagram

$$
\begin{aligned}
e(\theta, t) &= M(1 - M)u(t) - C(\theta)(1 - M)^2 Pu(t) \\
&= M(1 - M)u(t) - C(\theta)(1 - M)^2 (y(t) + v(t)) \\
&= M(1 - M)u(t) - C(\theta)(1 - M)^2 y(t) + d(t)
\end{aligned}
\tag{2.12}
$$

Finally, the noise $d(t)$ is given by $d(t) = -C(\theta)(1 - M)^2 v(t)$.

From the previous analysis, we are in position to define the Feasible Controller Set (FCS), that is, the set of all controllers $C(\theta)$ that are compatible with hypotheses and data.

Definition 1. *Feasible Controller Set (FCS):*

$$FCS = \left\{ C(\theta) \in \mathcal{C} : \left\| M(1 - M)u(t) - C(\theta)(1 - M)^2 w(t) \right\|_{\ell_p} \leq \delta_p \right\} \tag{2.13}$$

Notice that, in a noise-free case, i.e., $d(t) = 0$, it is possible to find a controller $C(\theta) = C(\theta^*)$, such that $e(\theta, t) = 0$. However, in any practical setting we have $\delta_p > 0$, then the set-membership approach is suitable to find a set containing all the controllers $C(\theta, t)$ that are compatible with data, noise bound δ_p and *a priori* information on the reference model M and the controller structure defined by the basis set. Similarly, the Feasible Parameters Set (FPS) is the set of all parameters $\theta \in \Theta$ that are compatible with hypotheses and data:

$$FPS = \left\{ \theta \in \Theta : \left\| M(1 - M)u(t) - C(\theta)(1 - M)^2 w(t) \right\|_{\ell_p} \leq \delta_p \right\} \tag{2.14}$$

Under this definition and previous assumptions, the next theorem is stated.

Theorem 1. *Given a dataset $\mathcal{D}$, a reference model $M(q^{-1})$ and a set of basis functions $[\beta_1(q^{-1}), \ldots, \beta_m(q^{-1})]$. If $\delta_p \geq \delta_p^*$, for δ_p^* the solution to the convex optimization problem*

$$\delta_p^* = \qquad\qquad \min_{\theta \in \Theta, \varepsilon \in \Re} \delta \tag{2.15}$$
$$s.t.$$
$$\left\| M(1 - M)u(t) - \sum_{i=1}^m \theta_i \beta_i (1 - M)^2 w(t) \right\|_{\ell_p} \leq \delta$$
$$\delta \geq 0$$

Then, $FPS \neq \emptyset$.

Proof. See Milanese et al. (1996) $\qquad\qquad\qquad\qquad\qquad\qquad\qquad\qquad\qquad\qquad\qquad$ $\square$

Remark 2. *A non-empty FPS guarantees a non-empty FCS.*

The previous theorem gives a tool to determine if a set of *a priori* hypotheses is compatible with the available dataset. For example, it allows to evaluate if a reference model is achievable with the selected basis functions with acceptable error.

Given a non-empty FPS, the problem of choosing a vector of parameters, and thus a controller, inside this set arises. According to the Set Membership literature, Milanese et al. (1996), any element inside the FPS is compatible with the available information and is a valid candidate as optimal controller $C(\theta^*, q^{-1})$. Working within the parameters space, for any vector $\hat{\theta}$ define its estimation error as

$$E_e(\hat{\theta}) = \|\theta^* - \hat{\theta}\|_r \tag{2.16}$$

For any vector norm r. However, it can not be evaluated because the optimal parameters vector θ^* is unknown. The worst-case estimation error of $\hat{\theta}$ is defined as

$$E_{WC}(\hat{\theta}) = \max_{\theta \in FPS} \|\theta - \hat{\theta}\|_r \tag{2.17}$$

E_{WC} is the maximum distance between the selected solution and any parameters vector compatible with the available information. An estimate $\hat{\theta}^o$ is optimal if it minimizes E_{WC}, i.e.,

$$E_{WC}(\hat{\theta}^o) = \min_{\vartheta \in \Theta} E_{WC}(\vartheta)$$

The following theorem gives a method to find an optimal estimate of θ^* in a worst-case setting.

Theorem 2. *The vector*

$$\theta^c = \frac{\overline{\theta} + \underline{\theta}}{2}$$

is the Chebyshev center of the FPS and then an optimal estimate of θ^* for $r = \infty$, being $\overline{\theta}$ and $\underline{\theta}$ hard bounds of the parameters feasible intervals, defined as

$$\overline{\theta_i} = \max \theta_i \tag{2.18}$$
$$s.t.$$
$$\theta \in FPS$$

and

$$\underline{\theta_i} = \min \theta_i \tag{2.19}$$
$$s.t.$$
$$\theta \in FPS$$

for $i = 1, 2, \ldots, m$.

Remark 3. *Note that θ^c belongs to the FPS, then*

$$C(\theta^c, q^{-1}) \in FCS$$

and therefore $C(\theta^c, q^{-1})$ is an interpolatory estimate for any system norm, i.e.

$$\|C^*(\theta^*, q^{-1}) - C(\theta^c, q^{-1})\|_{\mathfrak{s}} \leq 2\mathbf{RI}$$

RI *being the Radius of Information, i.e., the lowest achievable uncertainty provided by the Chebyshev center of the FCS measured in a given system norm,* Milanese et al. (1996).

Based on the results presented above, the following algorithm summarizes the proposed procedure for the tuning of controllers for unknown linear plants. It has been named Set-Membership Tuning (SMT).

Algorithm 1. SMT Algorithm

1. *Collect a dataset $\mathcal{D}$ performing an experiment starting with plant at rest.* Note that the assumptions on noise do not require open-loop operation.

2. *Select a proper reference model $M(q^{-1})$ and basis functions $\beta_i(q^{-1})$.*

3. *Solve the feasibility problem in eq. (4.33). If the lower bound on noise δ^* is acceptable go to next step, otherwise go back to step 2.*

4. *Build the estimate θ^c solving problems(2.18) and (2.19) for each component of the parameters vector.*

5. *Select as controller the system*

$$C^c(\theta^c, q^{-1}) = \sum_{i=1}^{m} \theta_i^c \beta_i(q^{-1})$$

Finally, an application to illustrate the approach is developed.

2.3   Active suspension Tuning Case Study

The design of controlled suspension systems for road vehicles aims to enhance the vehicle performances with regard to comfort and road handling. Active suspension systems have the ability to store, dissipate and introduce energy to the system. As a result, the trade-offs among conflicting design goals can be better resolved. Comprehensive studies have been published that evaluate the performances of active and semiactive suspensions (see Lu and DePoyster (2002), Savaresi et al. (2003)).

In this experimental case study, an active suspension platform (AS), from Quanser^{TM} is employed. The AS is a bench-scale plant to emulate a quarter-car model, controlled by an active mechanism. As is shown in Fig. 2.3, the plant consists of three floors/plates on top of each other. The top floor resembles the vehicle body, the middle plate represents the wheel and the bottom plate corresponds to the road. The plates are connected through springs that model a passive suspension and the tire elasticity. A DC motor is also standing between the top and middle plates to emulate the active suspension mechanism.

The chassis and the wheel are modeled as rigid bodies and static linear characteristics are assumed for the suspension. The spring-mass model is shown in Fig. 2.4. The parameters characterizing the model are the sprung mass M_s, representing the mass of the vehicle body while the unsprung mass, M_{us} represents the tire in the quarter-car model. The spring K_{us} and the damper B_{us} model the stiffness of the tire in contact with the road. The spring K_s and the damper B_s support the body weight over the tire. Values of parameters are shown in Table 2.1.

Data-driven controller tuning strategy developed here is compared with VRFT.The latter strategy was proposed in Lecchini et al. (2002b), and their main characteristics are recalled in Annex A.1.

2.3.1   Controller tuning problem

The objectives of controlled suspensions are to enhance comfort and handling. Comfort is related to the sprung mass acceleration, while handling is assured by the contact force between the unsprung mass and the road. In this work, a tracking problem is posed, where the aim is to follow a given suspension displacement. The force F_c (provided by the DC motor) is the manipulated variable (u), measured in Newtons (N), and the output variable is the *suspension travel ($y = x_2 - x_1$)* measured in cm (i.e separation between the top and middle plates).
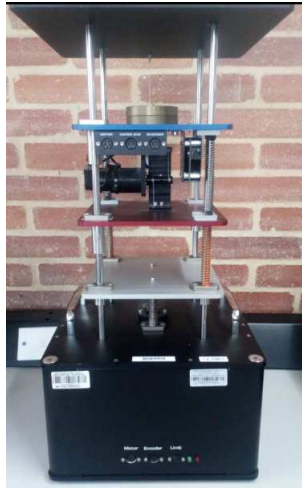
Figure 2.3: Active suspension platform
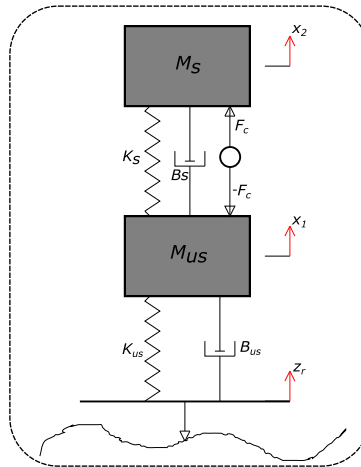
Figure 2.4: Active suspension model

The open-loop step response of the actual plant is shown in Fig. 2.5. The frequency response of the lumped component model of the system is shown in Fig. 2.6, where the nominal parameters in Table 2.1 are employed. The shape of the step and frequency responses show that the AS exhibits an oscillating under-damped behavior.

Table 2.1: Active suspension parameters

Parameter	Value	Unit
M_s	2.45	Kg
K_s	960	N/m
B_s	7.5	$N.s/m$
M_{us}	1	Kg
K_{us}	2500	N/m
B_{us}	0.01	$N.s/m$

The loop performance specifications are defined as a critically damped second order reference model M, parametrized by α, as shown in (2.20).

$$M(q^{-1}) = \frac{(1-\alpha)^2 q^{-1}}{1 - 2\alpha q^{-1} + \alpha^2 q^{-2}} \tag{2.20}$$

Note that α indicates the location of the poles defining the desired loop speed and bandwidth. The desired step response for some values of α are shown in Fig. 2.7. The sampling frequency is fixed as $F_s = 30[Hz]$, that is, one decade after the second resonance peak of the model.

In accordance with the above conditions and requirements, and in order to test the performance of the VRFT and SMT methods, two sets of experiments have been performed. The first one is a Monte-Carlo experiment, where the effect of the length of the dataset and the repetitiveness of the methods are evaluated. The second one evaluates the behavior of the approaches in front of process disturbances. In all the tests, $\ell_p = 2$ is fixed for the SMT algorithm (SMT_2), in order to have similar noise treatments in both approaches.

2.3.2   Monte-Carlo experiment

In this set of experiments, one hundred controllers have been obtained and tested on the AS, for each tuning method. Three cases are addressed, $N = 1000$, $N = 200$ and $N = 100$.

Datasets $\mathcal{D}$ required for both algorithms are obtained as follows, firstly a pseudo-random binary sequence (PRBS) signal with N samples is used as input (u) and suspension travel ($x_2 - x_1$) is measured. Output w is obtained adding white noise $v(t)$ with normal distribution. One hundred noise realizations $v(t)$ allow to obtain 100 datasets. Note that, the measured signal $x_2 - x_1$ has very low noise because the sensor
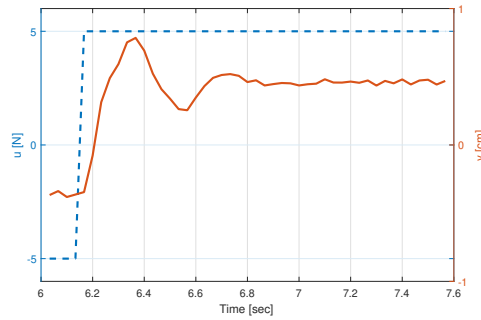
Figure 2.5: Open-loop step response of the active suspension.
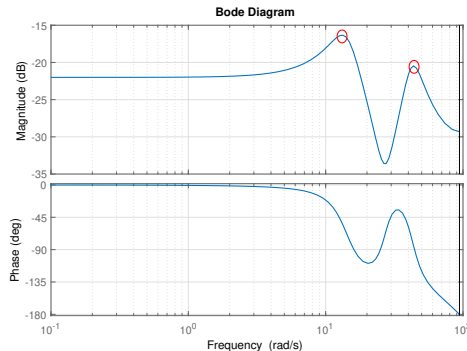
Figure 2.6: Active suspension nominal frequency response.

resolution is $4.87\mu m$. For each N, the noise variance is selected such that the Signal to Noise Ratio (SNR) is approximately $20dB$. The SNR is calculated as

$$SNR = 10log\frac{\sum_{t=1}^{N} y(t)^2}{\sum_{t=1}^{N} v(t)^2}.$$

As an example, one of the realizations with $N = 1000$ is shown in fig. 2.8.

The controllers are selected from an extended PID structure with basis functions β_i of the form

$$\beta_i(q^{-1}) = \frac{q^{1-i}}{1 - q^{-1}}, i = 1, 2, 3.., m$$

The first step in the tuning procedure is to define the number of basis that should be employed. Using one noise realization $v(t)$, datasets $\mathcal{D}$ for different N values are build, and for the SMT_2, feasibility problem (4.33) is solved for different reference model parameters α and increasing m values. The same dataset is used for the VRFT method. In this case, for each m value, the cost function in (A.1) is evaluated. Figs. 2.9 and 2.10 show the results for $N = 1000$ and $N = 100$, respectively.

Note that $m = 7$ is a reasonable number of bases functions when $N = 1000$ for both approaches. Choosing more parameters is unnecessary and would not decrease the error $\delta_2(\theta)$ in equation (3.9) nor the cost
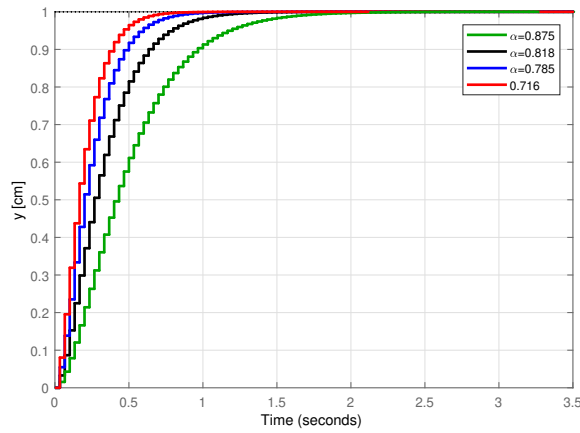
Figure 2.7: Step response of Reference models $M(q^{-1})$ for different α values.
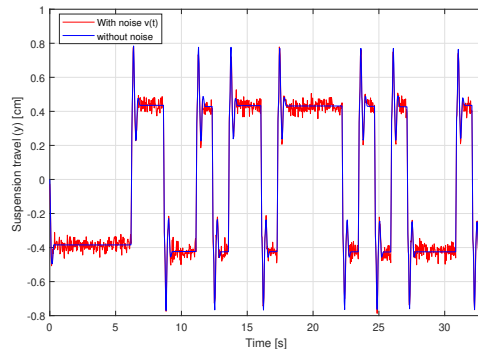
Figure 2.8: Sample of suspension travel with added output noise.

(a) SMT_2 (b) VRFT
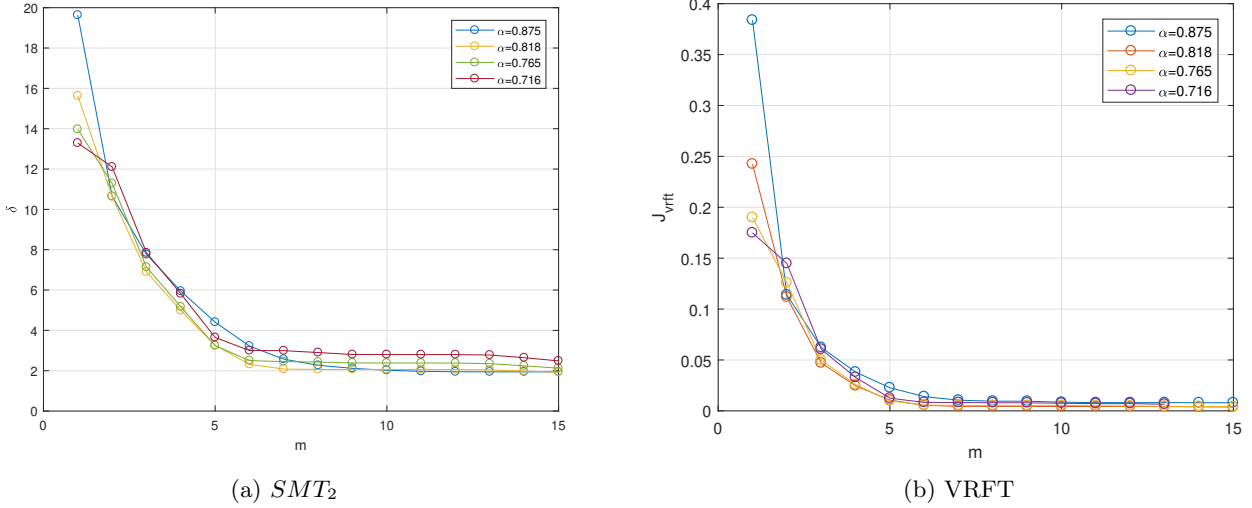
Figure 2.9: Controller structure selection results. Feasibility bounds for SMT and optimal cost for $VRFT$. N=1000.

$J_l(\theta)$. On the other hand, choosing fewer parameters would produce an increment of the error in both cases. However, when $N = 100$, in Fig. 2.10 it can be noted that the selection of the number of bases is not clear for the VRFT approach, while such selection for the case of SMT_2 remains reasonable for all α values of the model reference.

Once the structure of the controller is defined, the estimation of the optimal parameters is performed. For $m = 7$, $N = 1000$ and $\alpha = 0.765$ (i.e rise time 1[s]) a noise bound $\hat{\delta}_2 = 2.7$ is fixed to ensure feasibility (i.e 10% larger than δ_2^*). Both algorithms are executed for each one of 100 dataset $\mathcal{D}$. The obtained controller parameters dispersion is shown in Fig. 2.11. Note that, for this large dataset, both algorithms offer a similar performance with small variations in the obtained parameters. Fig. 2.12 shows the experimental step response for one of the obtained controllers in each case.

Finally, for each dataset size N, the performance of the 100 estimated controllers, with each method, is measured experimentally. The quality of the control action is measured as the maximum error (M_e) and the root mean square error ($RMSE$) of the closed-loop step response. The average and worst-case results are shown in Table 2.2. As can be seen, for the case of $N = 1000$ the results are comparable, but in the cases, $N = 200$ and $N = 100$, both performance measures obtained via SMT_2 algorithm are better than those achieved via $VRFT$ algorithm. Furthermore, it is highlighted that when $N = 100$ the average $RMSE$ of the SMT_2 controllers is about thirty times smaller than the one obtained via $VRFT$. Note also that the behavior of the SMT_2 controllers for small datasets ($N = 100$ and $N = 200$) is superior to the $VRFT$ controllers in a worst-case sense. The maximum $RMSE$ for the SMT_2 solutions, among the 100 experiments, is more than 10 times lower than those of the $VRFT$ ones, and the maximum peak error (M_e) is almost half.

2.3.3 Process disturbance experiment

In the previous experiment the tuning methods were evaluated taking into account output measurement noise only. Although, process disturbances are also present in any practical situation. The active suspension system is able to simulate a road profile by means of a second DC motor driving the lower plate. In
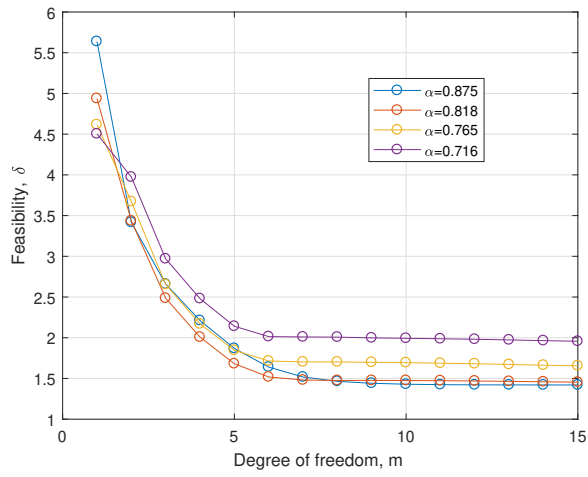
(a) SMT_2
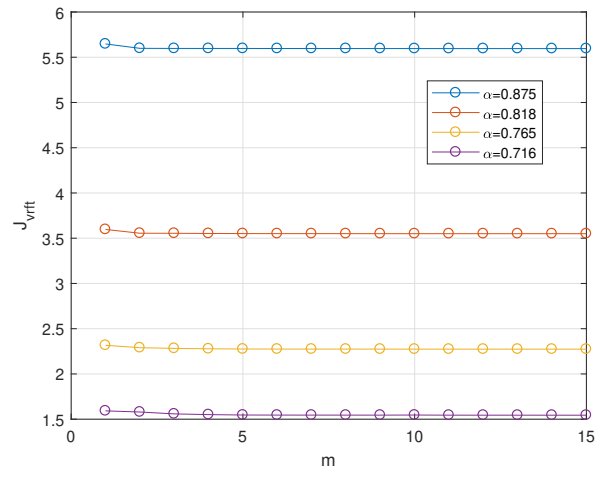
(b) VRFT

Figure 2.10: Controller structure selection results. Feasibility bounds for SMT and optimal cost for $VRFT$. N=100.
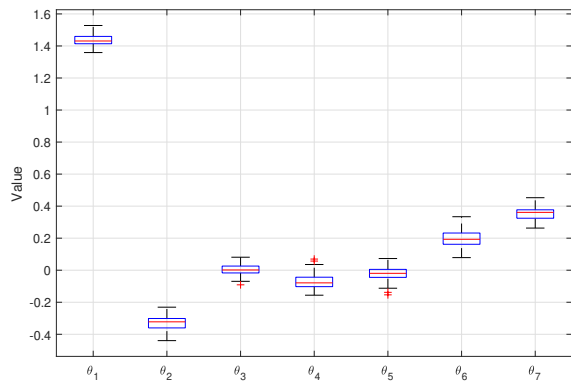
(a) SMT_2
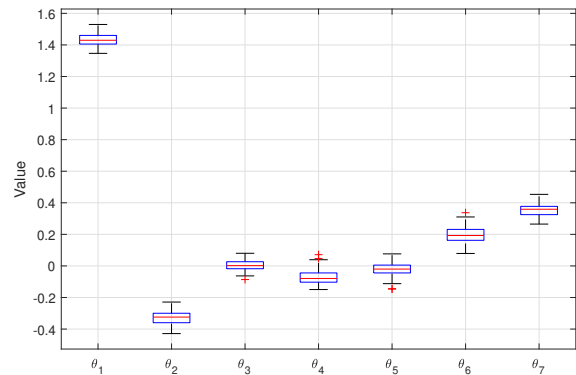
(b) VRFT

Figure 2.11: Controller parameters dispersion from Monte-Carlo experiment. N=1000.

(a) SMT_2 (b) VRFT
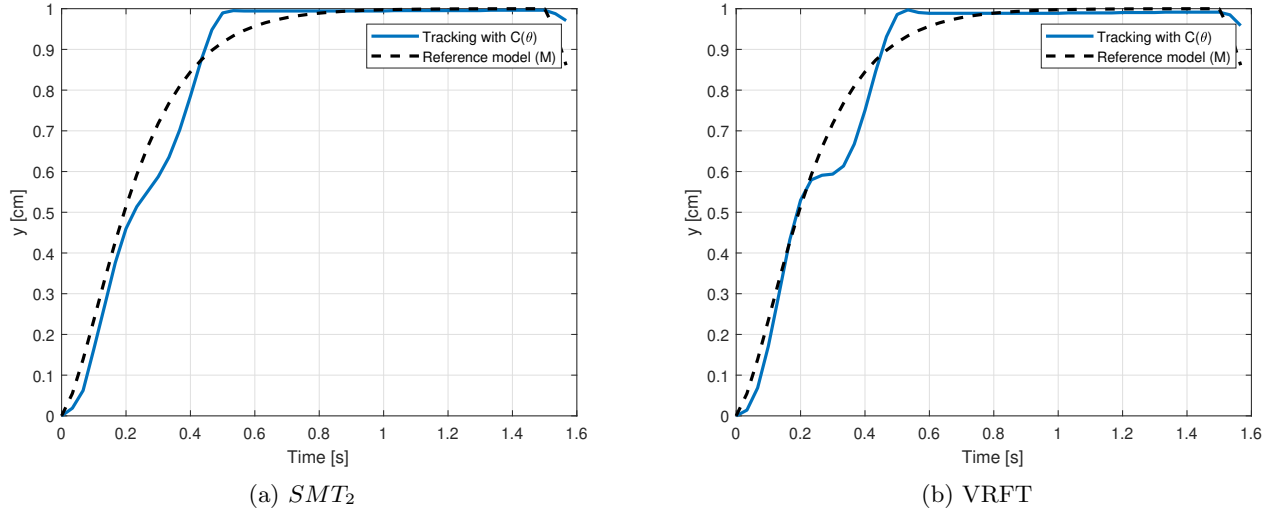
Figure 2.12: Sample closed-loop step response. N=1000.

Table 2.2: Performance results of Monte-Carlo experiment

Case	Measure	SMT_2	$VRFT$
$N = 1000$	$\overline{RMSE}, max(RMSE)$	$0.0031, 0.0039$	$0.0032, 0.0040$
	$\overline{M_e}, max(M_e)$	$0.1503, 0.1788$	$0.1517, 0.1694$
$N = 200$	$\overline{RMSE}, max(RMSE)$	$0.0021, 0.0032$	$0.0202, 0.0410$
	$\overline{M_e}, max(M_e)$	$0.1482, 0.1904$	$0.2889, 0.3581$
$N = 100$	$\overline{RMSE}, max(RMSE)$	$0.0018, 0.0028$	$0.0566, 0.1100$
	$\overline{M_e}, max(M_e)$	$0.1051, 0.1555$	$0.3957, 0.5090$

this case, the road profile shown in Fig.2.13a (filtered Gaussian noise) is applied to the system during the dataset generation experiment, with the same PRBS input $u(t)$ of the first setup. Datasets with lengths $N = 100$, $N = 150$, $N = 200$, $N = 250$ and $N = 300$ are used for testing. As an example, the output signal $y(t)$ obtained when $N = 300$ is depicted in Fig. 2.13b. $m = 7$ is selected for both algorithms and $\delta_2 = 3.5$ is selected for the SMT_2 solution.

The closed-loop step-response achieved by the controllers are depicted in Fig. 2.14. The maximum error (M_e) and $RMSE$ of each controller is shown in Table 2.3. The results indicate that both performance measures obtained via the SMT_2 method are better than those achieved with the $VRFT$ approach, for any N value. Moreover, The step responses show that the SMT_2 method is very robust to the size of the dataset. Similarly to the previous experiment, it is highlighted that when $N = 100$ the $RMSE$ is about sixteen times smaller using SMT_2 controller than the $VRFT$ one. Also note that, the peak error (M_e) is about two times smaller for the SMT_2 solution than the $VRFT$ one, for all N values.
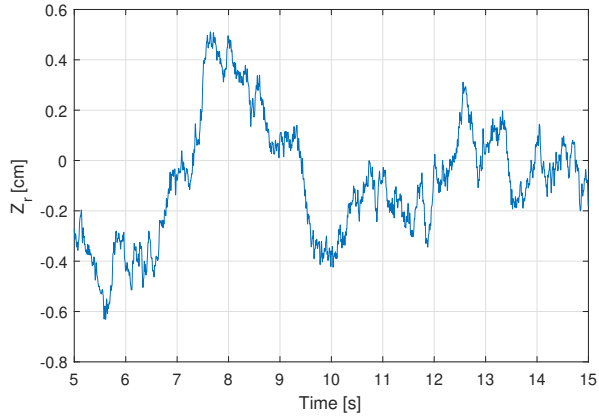
(a) Road profile applied as process disturbance
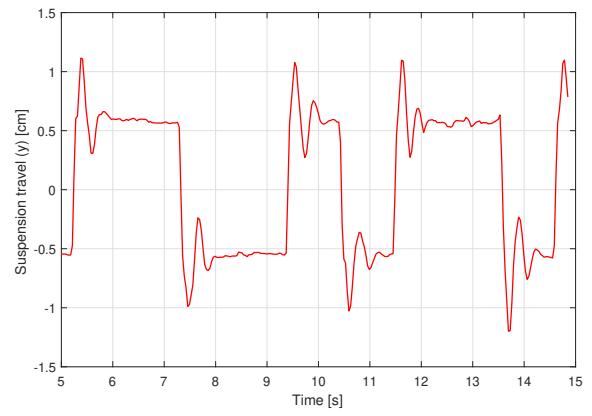
(b) Suspension travel for PRBS input and process disturbance

Figure 2.13: Dataset for process disturbance experiment. N=300.
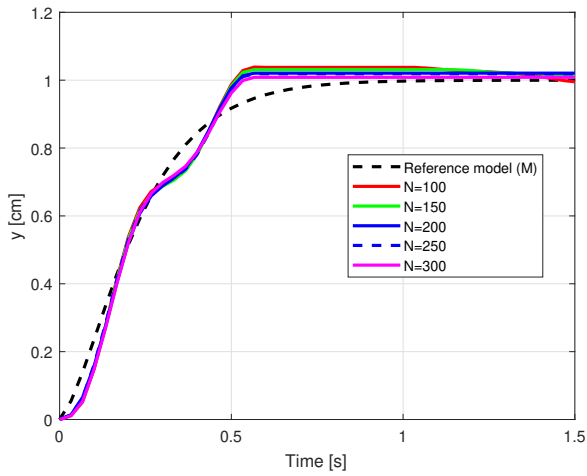
(a) SMT_2.
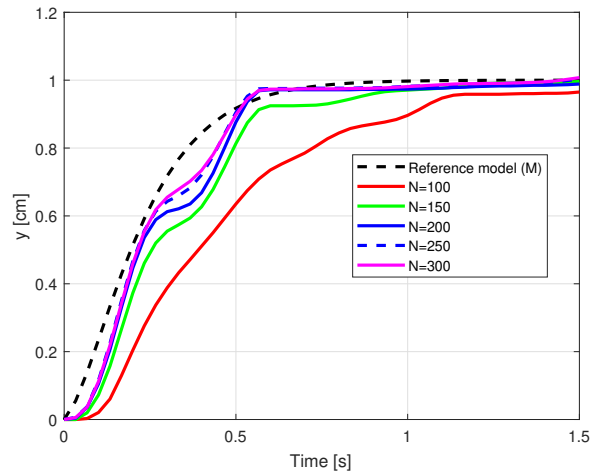
(b) VRFT.

Figure 2.14: Closed-loop step responses.

Table 2.3: Performance results of process disturbance experiment

Case	Measure	SMT_2	$VRFT$
$N = 100$	$RMSE$	0.0023	0.0380
	M_e	0.0948	0.3385
$N = 150$	$RMSE$	0.0021	0.0091
	M_e	0.0892	0.2180
$N = 200$	$RMSE$	0.0016	0.0045
	M_e	0.0797	0.1765
$N = 250$	$RMSE$	0.0015	0.0026
	M_e	0.0769	0.1274
$N = 300$	$RMSE$	0.0012	0.0023
	M_e	0.0881	0.1230

2.4 Conclusions

A novel methodology inspired by Set-Membership identification techniques for controller tuning has been proposed in a discrete-time and linear setting. The algorithm requires experimental information, formed by input-output measured data from the system to be controlled, operated in open or closed-loop. Hard bounds on controller parameters are derived employing linear programming techniques. The Chebyshev center is employed to find an optimal estimate of controller parameters.

We have compared our formulation (SMT) with Virtual Reference Feedback Tuning (VRFT). They do not rely on a plant model to tune the controllers, but the available input-output data, experimentally collected from the plant, is directly used to design the controller. Although they differ in the considered noise model, it is found that that both approaches offer a similar performance when the size of the dataset is much larger than the dimension of the controller parameters vector.

An extended experimental evaluation on an active suspension system has shown that, using the same information about the plant to be controlled, the VRFT controllers are strongly affected by the size of the dataset while the SMT controllers exhibit good performances, even when they are estimated from reduced datasets. For a samples to parameters ratio below 15, the VRFT method is not able to detect the required controller parameters and the performance of the derived controllers can be up to 30 times worse than the SMT results.

The methodology proposed here resorts useful when the plant model is unavailable and the time to extract the data set is relevant since short experiments lead to reduced data-sets for proper sample time. In practice, this would help to save time and money.

Chapter 3

Limited-complexity Controller Tuning

Some analysis and experiments carried out in the previous chapter have shown that exists a relation between the performance and the number of bases selected (i.e. choice of m). A m value as low as possible leads to a low complexity controller. In Formentin and Karimi (2013) is indicated that low complexity controllers are preferred in the industrial applications because the use of high complexity controllers implies essentially two drawbacks:

- When the number of controller parameters is large, many arithmetic operations are required (i.e., many multiplications and additions), thus slowing down the computational processing.

- High-complexity controllers are fragile, i.e. highly sensitive to round-off errors.

A proper selection of bases and m arise as an interesting topic to analyze in the data-driven controller design procedure.

In literature, low complexity controllers design has been addressed via different approaches. In Goro and Anderson (2001), techniques to derive low order controllers by previously performing model order-reduction are exposed. Another alternative is shown in Anderson and Liu (1989) where the high-complexity controllers derived from high-complexity models can be approximated with low-complexity ones by means of controller order-reduction. In Karimi and Galdos (2010), fixed-order controllers are tuned from high-complexity models without explicit order-reduction. All the previous approaches are model-based, requiring a mathematical model of the processs. A data-driven approach to fixed-order controller design was proposed in Formentin and Karimi (2013). Specifically, an iterative algorithm based on CbT and ℓ_1 regularization to design sparse-controllers is proposed.

In this chapter, an alternative DDC approach to design low-complexity controllers using a Set Membership estimation framework is proposed. The main contributions are:

- An efficient algorithm to derive sparse controllers from data is proposed. Linear and quadratic programming programs are employed to estimate optimal controller parameters, avoiding polynomial problems.

- The problem of noisy measurements is addressed without statistical assumptions on the disturbance signals, overcoming the limitations suffered by existing statistical solutions when reduced data sets are available.

- The proposed controller tuning algorithm does not require iterations or multiple experiments. Moreover, a criterion is provided to suitably manage the trade-off between accuracy and sparsity.

The outline of the chapter is as follows. In Section 3.1, the problem formulation is presented. In Section 3.2, a Set Membership framework to sparse-controller tuning is comprehensively described. Finally, in

Section 3.3 the proposed solution is evaluated on a benchmark problem, comparing its performance with an existing approach using sparse CbT. Some conclusions end the chapter in Section 3.4.

3.1 Sparse controller tuning problem
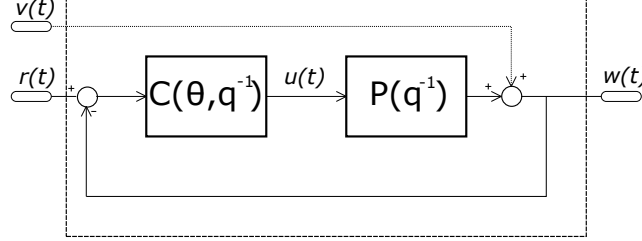
Figure 3.1: Assumed feedback control structure

Similarly to the previous section. Consider a discrete-time linear-time invariant (LTI) single-input single-output (SISO) feedback control scheme, as depicted in Fig. 3.1, where q^{-1} denotes the backward shift operator, $P(q^{-1})$ is the plant transfer function, $C(\theta, q^{-1})$ is the controller transfer function, θ is a vector of controller parameters, $r(k)$ is the reference signal, $v(k)$ is output noise, $u(k)$ and $w(k)$ are the plant input and output signals, respectively.

For the system interconnection in Fig. 3.1, the aim of the controller tuning procedure is to select an optimal controller C^0 minimizing some performance criterion. For example, an optimization problem can be stated as:

$$C^0(\theta^0, q^{-1}) = \arg \min_{C(\theta, q^{-1}) \in \mathcal{C}} J(C(\theta, q^{-1})) \tag{3.1}$$

For the cost function

$$J(\theta) = \left\| M(q^{-1}) - \frac{P(q^{-1})C(\theta, q^{-1})}{1 + P(q^{-1})C(\theta, q^{-1})} \right\|_{\mathfrak{s}} \tag{3.2}$$

Being $\mathfrak{s}$ a proper system norm, $\mathcal{C}$ the set of LTI systems where the controller is selected, θ a real vector parameterizing $C(\theta, q^{-1})$ and $M(q^{-1})$ a reference model for the closed-loop system, where performance specifications are embedded. As in the previous section, the controller is parametrized as a linear combination of fixed basis functions, that is,

$$C(\theta, q^{-1}) = \sum_{i=1}^{m_{max}} \theta_i \beta_i(q^{-1})$$

Where m_{max} is designated as the maximum allowable controller complexity.
Then, the controller is selected from the set:

$$\mathcal{C} = \left\{ C(\theta, q^{-1}) : \theta \in \Theta \subseteq \mathfrak{R}^{m_{max}} \right\}$$

Adding the next assumption to the set of assumptions previously proposed, we will be in a position to formulate the data-driven controller tuning problem in a sparse framework.

Assumption 4. *The optimal controller $C(\theta^*, q^{-1})$ is sparse, in other words*

$$\|\theta^*\|_0 \ll m_{max}$$

where

$$\|\theta\|_0 = card(supp(\theta))$$

$$supp(\theta) \doteq \{i \in \{1, 2, ..., m_{max}\}, \theta_i \neq 0\}$$

and $card(.)$ is the set cardinality.

Assumption 4 is reasonable, because one would expect that from a "large" set of basis functions, only some of them are useful for solving problem (2.1), if the set $\mathcal{C}$ is properly parametrized.

Assumption 5. *Any controller $C(\theta, q^{-1}) \in \mathcal{C}$ can be expressed as:*

$$C(\theta, q^{-1}) = C^*(\theta^*, q^{-1}) \left(1 + \Delta(\theta, q^{-1})\right)$$

with $\Delta(\theta, q^{-1})$ a proper and stable transfer function.

The previous assumption is motivated by the fact that common controller structures are usually stable or marginally stable (with pure integrators). Then, if C^* and C share poles in $z = 1$ with the same multiplicity, the difference between them is always a stable system.

Based on all of the previous assumptions (1-5), we are in position to formulate the data-driven controller tuning problem in sparse setting:

Problem 2. Sparse-controller tuning: *Given a data set $\mathcal{D}$, generated as in Assumptions 1 and 3; a reference model $M(q^{-1})$ and a set of basis functions $\beta_i, i = 1, ..., m_{max}$ satisfying assumptions 2, 4 and 5 identify a coefficient vector θ such that*

1. *θ is sparse*

2. *$J(\theta)$ in (3.2) is "small"*

Note that since $J(\theta)$ depends on the plant but, according to Assumption 1, it is unavailable, therefore is necessary to express the cost function in terms of the available data set.

3.2 A sparse Set Membership framework for controller tuning

Departing from the assumptions stated in the previous section, in this section, Problem 2 is cast into a Set Membership identification framework and an efficient algorithm is proposed to find sparse controllers from data.

Let the model matching error be defined as the argument of the cost function $J(\theta)$ in (3.2):

$$E_m(\theta) = M - \frac{PC(\theta)}{1 + PC(\theta),} \tag{3.3}$$

where the shift operator q^{-1} has been removed for simplicity. This notation is maintained in the following when possible.

First, the model matching error is expressed in a convenient form.

Theorem 3. *For any controller $C(\theta, q^{-1}) \in \mathcal{C}$, satisfying assumption 5, the model matching error $E_m(\theta)$ in (3.2) can be expressed as:*

$$E_m(\theta) = \frac{1}{1 + M\Delta(\theta)} \left(M(1-M) - C(\theta)(1-M)^2 P \right) \tag{3.4}$$

Proof: From assumption 2, it is known that

$$M = \frac{C^* P}{1 + C^* P}$$

and

$$1 - M = \frac{1}{1 + C^* P}.$$

Then, the model matching error system can be expressed as:

$$
\begin{aligned}
E_m(\theta) &= M - \frac{C(\theta)P}{1 + C(\theta)P} \\
&= \frac{C^* P}{1 + C^* P} - \frac{C(\theta)P}{1 + C(\theta)P}
\end{aligned}
$$

After some algebra we have,

$$
\begin{aligned}
&= \frac{C^* P - C(\theta)P}{(1 + C^* P)(1 + C(\theta)P)} \\
&= \frac{C^* P - C(\theta)P}{(1 + C^* P)(1 + (1 + \Delta(\theta))C^* P)} \\
&= \frac{C^* P - C(\theta)P}{(1 + C^* P)^2 (1 + \frac{C^* \Delta(\theta)P}{1 + C^* P})} \\
&= \frac{1}{1 + M\Delta(\theta)} \left(\frac{C^* P}{(1 + C^* P)^2} - \frac{C(\theta)P}{(1 + C^* P)^2} \right) \\
&= \frac{1}{1 + M\Delta(\theta)} \left(M(1-M) - (1-M)^2 C(\theta)P \right)
\end{aligned}
$$

arriving to the stated modelling error system.

Fig. 3.2 shows a block-diagram of the equivalent model matching error system, derived in Theorem 3. Note that the system contains an output inverse multiplicative uncertainty structure that allows to state the following Corollary:
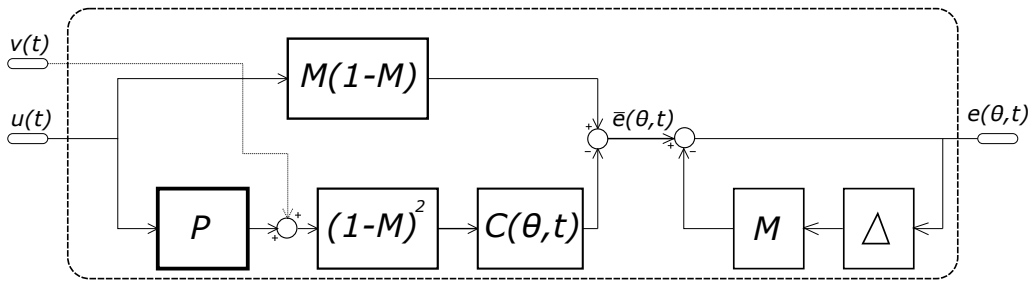
Figure 3.2: Model Matching block diagram

Corollary 1. *Given a controller $C(\theta) \in \mathcal{C}$, the transfer function $E_m(\theta)$ is input-output stable if:*

$$|\Delta(\theta, e^{j\omega})| < |M(e^{j\omega})|, \forall \omega \in [0, \ \pi] \tag{3.5}$$

The result follows from the Nyquist stability condition for the inverse multiplicative uncertainty structure in eq. (3.4).

The following Corollary allows to transform the model-based controller design problem in eq. (2.1) into an identification problem.

Corollary 2. *Given a data set $\mathcal{D}$ generated as in assumption 1, affected by noise bounded as in assumption 3, any controller $C(\theta) \in \mathcal{C}$, guaranteeing an internally stable loop, satisfies the time-domain relations:*

$$
\begin{align}
e_m(\theta, t) &= \frac{1}{1 + M\Delta(\theta)} * \overline{e}_m(t) \tag{3.6} \\
\overline{e}_m(\theta, t) &= [M(1 - M)] * u(t) - \notag \\
&\quad [C(\theta)(1 - M)^2] * w(t) + d(\theta, t) \tag{3.7} \\
d(\theta, t) &= (1 + \Delta(\theta))C^*(1 - M)^2 * v(t) \tag{3.8}
\end{align}
$$

and $d(\theta, t)$ is an UBB signal with bound

$$\|d(\theta, t)\|_{\ell_p} \leq \left\|(1 + \Delta(\theta))C^*(1 - M)^2\right\|_{\ell_p, \ell_p} \epsilon_p = \delta_p \tag{3.9}$$

Moreover, for an optimal controller $C^*(\theta^*)$, it holds:

$$
\begin{align}
e_m(t) &= \overline{e}_m(t) \tag{3.10} \\
M(1 - M) * u(t) + d(t) &= C^*(\theta^*)(1 - M)^2 * w(t) \tag{3.11}
\end{align}
$$

Proof: The results are the time domain relations of applying the signal $u(t)$ to the model matching error system in (3.2) and using the experimentally measured plant output $w(t)$ as input to the sub-system $(1 - M)^2$ in the lower branch of the block-diagram in Fig. 3.2.

The resulting output noise $d(t)$ is bounded because the transfer function in (3.8) is input-output stable under the hypotheses that $\Delta(\theta)$ is stable and $C^*(\theta^*)$ guarantees an internally stable loop.

From the previous development, it is possible to cast the data-driven controller tuning problem into an identification problem.

let

$$
\begin{align}
y_c(t) &= M(1 - M) * u(t) \tag{3.12} \\
u_c(t) &= (1 - M)^2 w(t) \tag{3.13}
\end{align}
$$

Then, for an optimal controller $C(\theta^*)$, eq. (3.11) can be rewritten as

$$y_c(t) + d(t) = C(\theta^*)u_c(t) \tag{3.14}$$

Note that, equation (3.14) corresponds to an identification problem with additive noise, where the system to be estimated is $C(\theta^*)$.

While the available data set is generated within an errors-in-variables setting, with the unknown signal $v(t)$ affecting the controller input, in this work, it is possible to perform an over-bounding of the noise, moving it to the controller output, thanks to the guaranteed input-output stability in (3.9). Previous approaches have used errors-in-variables identification algorithms, that in a Set-Membership setting lead to highly complex optimization problems, see e.g. Cerone et al. (2017).

3.2.1 The Feasible Parameters Set

From the previous analysis, we are in position to define the Feasible Parameters Set (FPS), that is, the set of all controller parameters θ that are compatible with hypotheses and data.

Definition 2. *Feasible Parameter Set (FPS):*

$$FPS = \left\{ \theta \in \Theta : \|Y_c - \Phi\theta\|_{\ell_p} \leq \delta_p \right\} \tag{3.15}$$

where

$$Y_c = [y_c(1), \ y_c(2), \ldots y_c(N)]^T,$$
$$\Phi = [\phi^1, \ \phi^2, \ldots \phi^{m_{max}}]$$

and

$$\phi^i = [y_{\beta i}(1), \ y_{\beta i}(2), \ldots y_{\beta i}(N)]^T,$$

with

$$y_{\beta i}(t) = \sum_{j=0}^{t} h_j^{\beta_i} u_c(t-j),$$

where $h_j^{\beta_i}$ corresponds to impulse response of the basis β_i.

Notice that, in a noise-free case, i.e., $d(t) = 0$, it is possible to find a controller $C(\theta) = C(\theta^*)$, such that $e(\theta, t) = 0$. However, in any practical setting we have $\delta_p > 0$ and then, the Set Membership approach is suitable to find a set containing all the controllers $C(\theta)$ that are compatible with data, noise bound δ_p and *a priori* information on the reference model M and the controller structure, defined by the basis set.

Under the definition of the FPS and previous assumptions, the next theorem is stated.

Theorem 4. *Given a data set $\mathcal{D}$, a reference model $M(q^{-1})$ and a set of basis functions $\{\beta_1(q^{-1}), \ldots, \beta_{m_{max}}(q^{-1})\}$. If $\delta_p \geq \delta_p^{min}$, for δ_p^{min} the solution to the convex optimization problem*

$$\delta_p^{min} = \min_{\theta \in \Theta} \delta \tag{3.16}$$
$$s.t.$$
$$\|Y_c - \Phi\theta\|_{\ell_p} \leq \delta$$
$$\delta \geq 0$$

Then, $FPS \neq \emptyset$.

Proof:
Note that θ^*, the argument minimizing (4.33), guarantees,

$$\|Y_c - \Phi\theta^*\|_{\ell_p} \leq \delta_p$$

Then, $\theta^* \in FPS$. $\qquad\qquad\qquad\qquad\qquad\qquad\qquad\qquad\qquad\qquad\qquad\qquad\qquad\qquad$ □

As theorem 1, the previous theorem gives a tool to determine if a set of *a priori* hypotheses is compatible with the available data. For example, it allows to evaluate if a reference model is achievable with the selected basis functions with acceptable error.

3.2.2 Finding a sparse controller

The FPS defined in the previous subsection does not take into account assumption 4, that is, the feasible controllers can have any cardinality. Under Assumption 4, a feasible parameters set can be defined, where controllers have the structure of $C^*(\theta^*)$, i.e.,

Definition 3. *Feasible Sparse Parameters Set (FSPS):*

$$FSPS = \{\theta \in \Theta : supp(\theta) = supp(\theta^*),$$
$$\|Y_c - \Phi\theta\|_{\ell_p} \leq \delta_p\} \tag{3.17}$$

However, the support of the optimal controller is unknown. The sparsest controller, compatible with hypotheses and experimental data might be found solving the following optimization problem:

$$\theta^* = \arg\min_{\theta \in \Theta} \|\theta\|_0 \tag{3.18}$$
$$s.t.$$
$$\|Y_c - \Phi\theta\|_{\ell_p} \leq \delta_p$$

In fact, maximizing the sparsity of a vector corresponds to minimizing its l_0 quasi-norm. However, the ℓ_0 quasi-norm is a non-convex function and its minimization is, in general, an NP-hard problem. In an identification framework, convex relaxations, see e.g. Tropp (2006); Donoho et al. (2006); Fuchs (2005), and greedy algorithms, see e.g. Tropp (2004), are the main approaches to deal with this problem.

Instead of minimizing the support of the controller, a different approach is to limit the complexity of the controllers set to a fixed number of basis functions m_θ. This leads to the next limited complexity feasible parameters set:

Definition 4. *Limited complexity Feasible Parameter Set (FPS):*

$$FPS(m_\theta) = \left\{\theta \in \Theta : \|Y_c - \Phi\theta\|_{\ell_p} \leq \delta_p \ \wedge \ \|\theta\|_0 = m_\theta\right\} \tag{3.19}$$

Note that $FPS(m_\theta)$ is the union of $\binom{m_{max}}{m_\theta}$ subsets with the same cardinality and, to fully characterize the set, it is necessary to verify the feasibility condition established in Theorem 4 for each sub-set of bases guaranteeing $\|\theta\|_0 = m_\theta$, this is a combinatorial problem intractable for large sets of basis functions.

Instead of verifying the feasibility of each sub-set in $FPS(m_\theta)$, in this work we propose a "smart" selection of active basis functions, following an approach similar to Novara (2016), where a greedy algorithm is proposed in the context of system identification for fault detection.

The proposed limited-complexity controller estimation algorithm has two steps. First, the support of a particular controllers set is estimated and then, an interpolatory solution is provided.

Consider the optimization problem

$$\theta^1 = \arg\min_{\theta \in \Theta} \|\theta\|_1 \tag{3.20}$$
$$s.t.$$
$$\|Y_c - \Phi\theta\|_{\ell_p} \leq \delta_p$$

where δ_p guarantees a non-empty FPS, according to *Theorem 4*. Recall that the ℓ_1 norm is the convex envelope of the ℓ_0 quasi-norm, and its minimization yields a sparse vector θ^1 Tropp (2006); Donoho et al. (2006); Fuchs (2005).

From the optimal solution θ^1 obtained in (3.20), the following definition provides an ordered set of bases.

Definition 5. *Let*

$$r(\theta^1) \doteq \left\{ i_1, \ldots i_{m_{max}} : \left| \theta_{i1}^1 \right| \geq \ldots \geq \left| \theta_{im_{max}}^1 \right| \right\}.$$

For any $m_\theta \in \{1, 2, \ldots, m_{max}\}$, the support of any controller of complexity m_θ is

$$\lambda(m_\theta) = \{i_1, i_2, \ldots, i_{m_\theta}\} \tag{3.21}$$

Note that $r(\theta^1)$ is the set of basis indexes, sorted by the amplitude of the elements of θ^1.
From the previous ordered set of bases, the Feasible Sparse Parameters Set is defined as:

Definition 6. *Feasible Sparse Parameters Set (FSPS) of complexity m_θ:*

$$FSPS(m_\theta) = \Big\{ \theta \in \Theta : \|Y_c - \Phi\theta\|_{\ell_p} \leq \delta_s \ \wedge$$

$$\theta_i = 0, \forall i \notin \lambda(m_\theta) \Big\} \tag{3.22}$$

Lemma 2. *If $\delta_s \geq \delta_s^{min}(m_\theta)$, for $\delta_s^{min}(m_\theta)$ the solution to the convex optimization problem*

$$\delta_s^{min}(m_\theta) = \min_{\theta \in \Theta} \delta \tag{3.23}$$

$$s.t.$$

$$\|Y_c - \Phi\theta\|_{\ell_p} \leq \delta$$

$$\delta \geq 0$$

$$\theta_i = 0, \forall i \notin \lambda(m_\theta)$$

Then, $FSPS(n_\theta) \neq \emptyset$.

Corollary 3. *Let $\epsilon(m_\theta) = \delta_s^{min}(m_\theta) - \delta_p^{min}$, then $\epsilon(m_\theta) \geq 0$.*
Moreover, if $\epsilon(m_\theta) = 0$, then $FSPS(m_\theta) \subset FPS$.

The previous results follow from the fact that, for any δ, the feasible set in optimization problem (4.33) contains the feasible set in problem (3.23).
For any m_θ, such that $\epsilon(m_\theta) = 0$, the selected subset of basis functions guarantee the same accuracy explaining the available data than the full basis set. It follows that the behavior of $\epsilon(m_\theta)$ is an indicator of the trade-off between accuracy and sparsity, allowing the designer to select a proper controller complexity m_θ.
Once the support of the controller is defined, the final step in the controller tuning procedure is to select a vector of parameters $\hat{\theta}$ belonging to $FSPS(m_\theta)$, guaranteeing an small closed-loop error. Two solutions are proposed:

- The following optimization problem allows to identify an interpolatory estimate, minimizing the controller output error on the available data set:

$$\hat{\theta}_I = \arg \min_{\theta \in \Theta} \|Y_c - \Phi(t)\theta\|_{\ell_p} \tag{3.24}$$

$$s.t.$$

$$\theta_i = 0, \forall i \notin \lambda(m_\theta)$$

- A central estimate, given by the Chebyshev center of the $FSPS(m_\theta)$, can also be employed, minimizing the worst-case error in the parameter space, but increasing the computational complexity of the tuning process.

$$\hat{\theta}_C = \arg \min_{\theta} \max_{\theta' \in FSPS(m_\theta)} \|\theta - \theta'\|_{\ell_q} \tag{3.25}$$

$$s.t.$$

$$\theta_i = 0, \forall i \notin \lambda(m_\theta)$$

Now we are in a position to propose a limited-complexity controller estimation algorithm as follows.

Algorithm 2. *Sparse Set Membership tuning algorithm (SSMT)*

1. *Collect a data set $\mathcal{D}$ performing an experiment starting with the plant initially at rest.* Note that the assumptions on noise do not require open-loop operation.

2. *Select a proper reference model M and basis functions set $\{\beta_1, \beta_2, \ldots, \beta_{m_{max}}\}$.*

3. *Obtain a lower noise bound δ_p (see Theorem 4).*

4. *Solve the optimization problem*

$$\theta^1 = \arg \min_{\theta \in \Theta} \|\theta\|_1 \tag{3.26}$$
$$s.t.$$
$$\|Y_c - \Phi\theta\|_{\ell_p} \le \delta_p$$

   and construct vector $r(\theta^1)$ as in Definition 5.

5. *Select an sparsity error tolerance bound ϵ_{max} and perform the following iteration:*

   for $j = 1 : m_{max} - 1$

$$
\begin{aligned}
m_\theta &= m_{max} - j \\
\theta(j) &= \arg \min_{\theta \in \Theta} \|Y_c - \Phi\theta\|_{\ell_p} \\
&\quad s.t. \\
&\quad \theta_i = 0, \forall i \notin \lambda(m_\theta) \\
\text{if} \quad &\|Y_c - \Phi\theta(j)\|_{\ell_p} \le \delta_p + \epsilon_{max} \\
&\hat{\theta} = \theta(j) \\
\text{else} & \\
&\quad break
\end{aligned}
$$

   end

After, arranging the elements of θ^1 in decreasing amplitude order, in step 5 the bases with smaller coefficients are removed, one by one, until the given threshold ϵ_{max} for the output error increment is reached.

Remark 4. *ϵ_{max} can be tuned to suitably manage the trade-off between accuracy and sparsity in step 5, since large values of ϵ_{max} lead to large sparsity, that is, $m_\theta \ll m_{max}$.*

Under suitable conditions on Φ and θ^1, the results in Novara (2012) guarantee that $\hat{\theta}$, derived by Algorithm 1, is maximally sparse with the same support as θ^o.

3.3   Numerical Case Study

In this section, the proposed approach is evaluated on simulated data, generated by a flexible-transmission model, comparing its performance against a sparse-CbT algorithm, proposed in Formentin and Karimi (2013). As far as the authors are aware, it is the only reported method that uses a sparse approach to solve Problem 2.

Consider the flexible transmission system introduced as a benchmark for digital control design in Landau et al. (1995). The plant transfer function is:

$$P(q^{-1}) = \frac{0.28261q^{-3} + 0.50666q^{-4}}{1 - 0.418q^{-1} + 1.589q^{-2} - 1.316q^{-3} + 0.886q^{-4}}$$

The control objective is given in terms of model-reference specifications, given by:

$$M(q^{-1}) = \frac{(1-\alpha)^2 \, q^{-3}}{(1-\alpha q^{-1})^2}$$

where α indicates the location of the poles defining the desired loop speed and bandwidth. As in previous works with this benchmark, it is used $Ts = 0.05 \ s$ and $\alpha = 0.6$. The basis functions parametrizing the controller are:

$$\beta_i(q^{-1}) = \frac{q^{1-i}}{1 - q^{-1}}, i = 1, 2, ..., m_{max}.$$

It is assumed $m_{max} = 12$.

First, a data set of $N = 200$ samples is generated with the system operating in open loop, input $u(t)$ is generated as a i.i.d noise with variance 4. The plant output $w(t)$ is affected by additive output noise $v(t)$ generated as i.i.d. samples of a uniform distribution with zero mean an a Signal to Noise Ratio (SNR) of $20dB$. The SNR is calculated as

$$SNR = 10log\frac{\sum_{t=1}^{N} y(t)^2}{\sum_{t=1}^{N} v(t)^2}.$$

Then, Theorem 4 is employed to determine lower bounds on the output noise norm δ_p^{min}. $p = 2$ is selected as signal norm and different reference models (i.e different α values) are tested for several m_{max} values. In this case, all the m_{max} basis functions are employed. Results are shown in Figure 5.4. Note that, for fast reference models (α small), the noise bound is high even for a large set of basis. On the other side, for $\alpha = 0.6$, $\delta_2^{min} \approx 2.8$ can be selected as a validated bound.
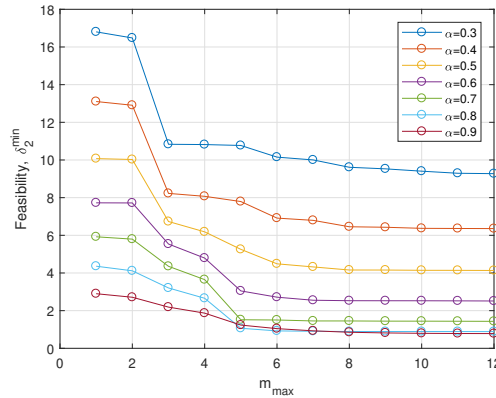
Figure 3.3: Lower noise bounds for different reference models and controller complexities (m_{max}).

The next step is to execute step 5 in *Algorithm 1*. Different ϵ_{max} values are considered, in order to highlight the trade-off between accuracy and sparsity. Results are reported in Figure 3.4. It is shown that increasing ϵ_{max} leads to higher sparsity. When $\epsilon_{max} = 0$, i.e., $FSPS \in FPS$, 10 bases are selected by the algorithm, while $\epsilon_{max} = 0.8$ offers an acceptable trade-off to obtain a "low-complexity" controller. In this case the estimated sparse-controller is:

$$C(\hat{\theta}) = \frac{0.1006 - 0.0308q^{-1} + 0.0625q^{-5}}{1 - q^{-1}}$$

The complexity is $m_\theta = 3$, and the bases selected by the algorithm are $\beta_i(q^{-1}) = \frac{q^{1-i}}{1-q^{-1}}, i = 1, 2, 6$.
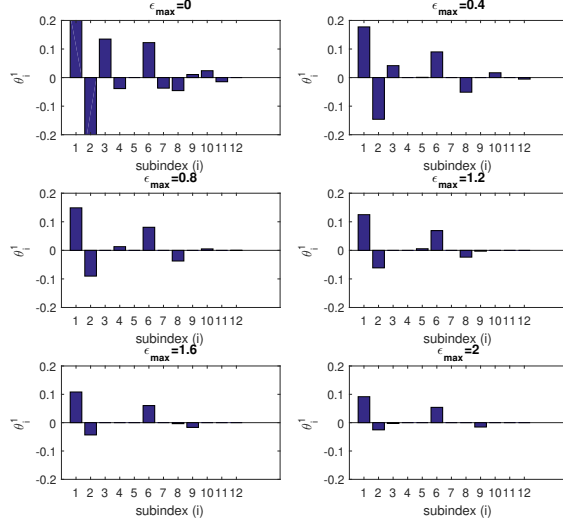
Figure 3.4: Sparsity results for different ϵ_{max} values.

Finally, the solution proposed in Formentin and Karimi (2013) is applied to the available data set. The sparse CbT algorithm relies on ℓ_1 regularization. The cost function to be minimized is:

$$\hat{\theta}^{(j)} = \arg\min_\theta \left[J(\theta) + \lambda \left\| W^{(j)}\theta \right\|_1 \right] \tag{3.27}$$

where $J(\theta)$ is the 2-norm of the correlation signal between a model error and a properly selected instrumental variable, W is a weighing diagonal matrix and j is a counter index.

Parameters $l = 30$ (instrumental variable length), $\lambda_{max} = 0.15$ (upper bound on regularization weight), $j_{max} = 10$ (maximum number of iterations), and $\epsilon = 0.01$ (lower bound of weights in matrix W) are selected, according to the criteria given in Formentin and Karimi (2013). Initially, $\lambda = 0.01$ is employed but the algorithm does not converge (i.e. when $j = j_{max}$, $\|\theta\|_0 > m_\theta$), results are reported in Table 3.1. A second test with $\lambda = 0.12$ is performed and the results are reported in table 3.2. It can be seen that the algorithm converges after 3 iterations.

Table 3.1: SCbT convergence results for $\lambda = 0.01$

iteration	1	2	3	4	5	6	7	8	9	10
$\|\theta\|_0$	12	12	10	8	8	8	8	7	7	7

Table 3.2: SCbT convergence results for $\lambda = 0.12$

iteration	1	2	3	4	5	6	7	8	9	10
$\|\theta\|_0$	12	5	3	3	3	3	3	3	3	3

The sparse-controller obtained is

$$C(\hat{\theta}) = \frac{0.0951 - 0.0235q^{-1} + 0.0643q^{-5}}{1 - q^{-1}}$$

Note that the bases selected by the $SCbT$ algorithm coincide with those identified by the SSMT algorithm.

3.3.1   Monte-Carlo test

A final test is performed, where a Monte-Carlo experiment allows to evaluate the behavior of the algorithm for 100 realizations of noise $v(t)$, leading to 100 data sets $\mathcal{D}$, all of them maintaining a $SNR \approx 20dB$.
For each data set and method, a controller has been tuned and tested on the model of the plant P. Four cases are addressed, $N = 300$, $N = 200$, $N = 100$ and $N = 70$. The controllers have been tuned as described in the previous example. In the $SCbT$ method $l = 30$ or $l = 20$ is used according to data length N.
For each data set size N, the performance of the estimated controllers is measured via simulation. The quality of the resulting control action is measured as the maximum error (M_e) and the root mean square error ($RMSE$) of the closed-loop step response with respect to the reference model. The average and worst-case results are shown in Table 3.3.
As can be seen in Table 3.3, for the case of $N = 300$ the results are comparable for both methods. But, for $N = 200$, the RMSE almost doubles for the $SCbT$ method. For the cases $N = 100$ and $N = 50$, both performance measures for the controllers obtained via $SSMT$ method keep constant, while those achieved via $SCbT$ algorithm increase. It is highlighted that in all cases the $SSMT$ method proposed in this work shown better results than the $SCbT$ method.
Figure 3.5 shows the percentage of experiments (noise realizations) for which, each algorithm properly estimated the optimal basis functions $\beta_i(q^{-1}) = \frac{q^{1-i}}{1-q^{-1}}, i = 1, 2, 6$. For $N = 300$ both methods are able to recover the correct basis. However, for smaller data sets, the $SCbT$ method is not always able to find the correct bases to construct the sparse-controller, even when the number of iterations $j_{max} = 15$ is selected, this was expected because the condition $\ell/N \ll 1$ is not fulfilled, such condition is required for the correlation method (see details in Karimi et al. (2007)). For $N = 70$, correct bases are obtained in less than 50% of the experiments for the $SCbT$ method. Moreover, in some cases it produces unstable closed-loops. However, the performances measures reported in Table 3.3 consider only stable controllers.

Table 3.3: Results for Monte-Carlo experiment

Case	Measure	SSMT	SCbT
N=300,	$\overline{RMSE}/max(RMSE)$	0.0048/0.0051	0.0068/0.0093
l=30	$\overline{M_e}/max(M_e)$	0.1996/0.2025	0.2437/0.2770
N=200,	$\overline{RMSE}/max(RMSE)$	0.0050/0.0051	0.0100/0.0102
l=30	$\overline{M_e}/max(M_e)$	0.1941/0.2053	0.2641/0.2745
N=100,	$\overline{RMSE}/max(RMSE)$	0.0041/0.044	0.0235/0.1153
l=30	$\overline{M_e}/max(M_e)$	0.1914/0.1950	0.3650/0.5602
N=70,	$\overline{RMSE}/max(RMSE)$	0.0048/0.0051	0.0812/0.1133
l=20	$\overline{M_e}/max(M_e)$	0.1914/0.1950	0.2599/0.2776

3.4   Conclusions

We have developed a new Data-Driven approach to design limited-complexity controllers for linear systems using Set Membership techniques and sparse identification methods. An algorithm has been proposed in order to solve the sparse-controller tuning problem, supported by feasibility theorems that provide a
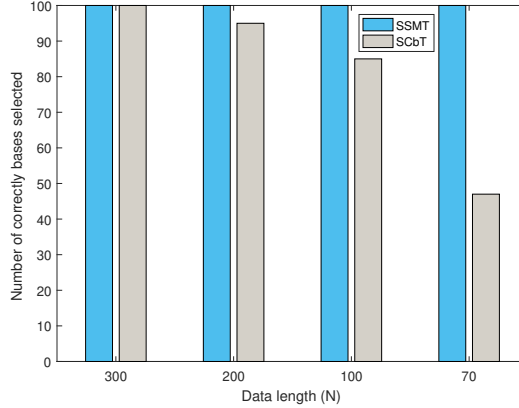
Figure 3.5: Results for bases selection.

single parameter to adjust the complexity-accuracy trade-off.

The proposed algorithm here avoids solving big combinatorial problems that arise when the dimension of the vector parameterizing the candidate controllers is large and the number of desired parameters is much lower.

A benchmark flexible transmission model is employed to illustrate the performance of the proposed methodology (SSMT), in comparison to the sparse correlation based tuning approach (SCbT). It is found that both approaches offer similar performance when the size of the data set is much larger than the dimension of the controller parameters vector. Notwithstanding, the SCbT controllers are strongly affected when data set size is reduced, while the SSMT controllers exhibit good performances even when the controller parameters are estimated from reduced data sets. Moreover, SSMT method has just one parameter to be adjusting and it has a direct interpretation as modeling error bound, simplifying the tuning procedure.

Chapter 4

2 DoF controller structures

It is well known that the main advantage of Two-Degree-of-Freedom controllers (2DoF) over 1DoF, is that the first allow to tune the reference model for the closed-loop function and the reference model for the sensitivity at the same time. However, few work has been performed about tuning methods for 2DOF controllers via data-driven approaches, see e.g. Lecchini et al. (2002b); Previde et al. (2010).

4.1   Problem formulation

In this Section, the data-driven 2DoF controller design problem is formulated. It is proposed a scheme to avoid the requirement of the plant model $P(q^{-1})$ in the procedures for: (i) sensitivity tuning and, (ii) closed-loop reference model tuning.
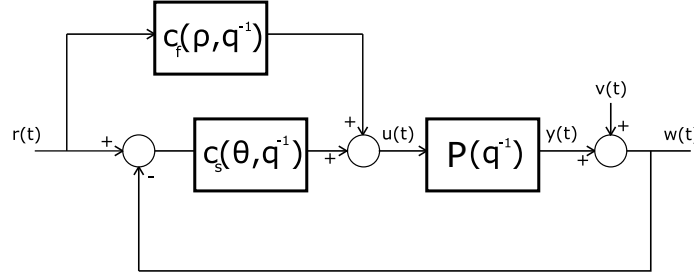
Figure 4.1: Two-Degree-of-Freedom feedback control system

Consider the discrete-time linear-time invariant (LTI) single-input single-output (SISO) 2DoF feedback control scheme, depicted in Figure 4.1, where q^{-1} denotes backward shift operator, $P(q^{-1})$ is the plant transfer function, $C_f(\rho, q^{-1})$ and $C_s(\theta, q^{-1})$ are feed-forward controller and main controller transfer functions respectively, ρ and θ are vectors of controllers parameters. For the system interconnection shown in Figure 4.1, the aim of the controller tuning procedure is to select optimal controllers C_f^o and C_s^o minimizing some performance criterion. For example, the following two optimization problems can be stated:

$$C_s^o(\theta, q^{-1}) = \text{argmin } J_1(\theta) \tag{4.1}$$

$$C_f^o(\rho, q^{-1}) = \text{argmin } J_2(\rho, \theta) \tag{4.2}$$

for the costs

$$J_1(\theta) = \left\| S(q^{-1}) - \frac{1}{1 + P(q^{-1})C_s(\theta, q^{-1})} \right\|_s \tag{4.3}$$

43

and

$$J_2(\rho, \theta) = \left\| M(q^{-1}) - \frac{P(q^{-1})(C_s(\theta, q^{-1}) + C_f(\rho, q^{-1}))}{1 + P(q^{-1})C_s(\theta, q^{-1})} \right\|_s \tag{4.4}$$

where s is a proper system norm, $M(q^{-1})$ is a model reference for the closed-loop function (I/O transfer function), and $S(q^{-1})$ is a reference model for the sensitivity function. Note that problems (4.1) and (4.2) should be solved sequentially. The solution of problem (4.1) corresponds to the controller $C_s(\theta)$. Then, when such controller is known, problem (4.2) can be solved in order to obtain controller $C_f(\rho)$.

If $P(q^{-1})$ is known, problems (4.1) and (4.2) can be seen as a loop-shaping problem and, for H_2, H_∞, and l_1 norms, known techniques exist to solve it under proper basis selection Zhou and Doyle (1998). However, when system $P(q^{-1})$ is unknown, such problems can not be solved directly.

Before to state the data-driven controller tuning problem, some definitions and remarks are presented.

Definition 7. Sensitivity matching error transfer function: *The sensitivity matching error transfer function $E_s(q^{-1})$ is defined as:*

$$E_s(q^{-1}) = S(q^{-1}) - \frac{1}{1 + P(q^{-1})C_s(\theta, q^{-1})} \tag{4.5}$$

Definition 8. Sensitivity matching error transfer function: *For any given sensitivity function $S(q^{-1})$, the ideal controller $C_s^*(\rho, q^{-1})$ is defined as the controller such that the condition*

$$E_s(q^{-1}) = 0 \tag{4.6}$$

is satisfied.
    Therefore, the ideal controller is

$$C_s^*(\theta, q^{-1}) = \frac{1 - S(q^{-1})}{P(q^{-1})S(q^{-1})} \tag{4.7}$$

It is worth noting that, $C_s^*(\rho, q^{-1})$ could be complex or, in the worst case, not physically realizable. However, the former definition plays a key role in our approach for data-driven controller tuning.

Definition 9. Model matching error transfer function:

$$E_m(q^{-1}) = M(q^{-1}) - \frac{P(q^{-1})(C_s(\theta, q^{-1}) + C_f(\rho, q^{-1}))}{1 + P(q^{-1})C_s(\theta, q^{-1})} \tag{4.8}$$

Definition 10. Ideal controller for model-reference tuning: *If we assume that ideal controller $C_s^*(\theta, q^{-1})$ is known, the ideal controller $C_f^*(\rho, q^{-1})$ is defined as the system such that the condition*

$$E_m(q^{-1}) = 0 \tag{4.9}$$

is satisfied.
    Therefore, the ideal controller is

$$C_f^*(\rho, q^{-1}) = \frac{P(q^{-1})C_s^*(\theta, q^{-1})[M(q^{-1}) - 1] + M(q^{-1})}{P(q^{-1})} \tag{4.10}$$

Evidently, $C_f^*(\rho, q^{-1})$ can also be complex and even not physically realizable.

As in the previous sections, the controllers to implement are parametrized as a linear combination of fixed basis functions, that is,

$$C_s(\theta, q^{-1}) = \sum_{i=1}^{m} \theta_i \beta_i(q^{-1})$$

$$C_f(\rho, q^{-1}) = \sum_{i=1}^{m_\rho} \rho_i \beta_i^\rho(q^{-1}) \tag{4.11}$$

Where m and m_ρ are designated as the controllers order.

Based on the Assumptions 1 and 3 and previous definitions, a new controllers tuning problem can be stated as follows:

Problem 3. Data-Driven Two-degree-of-freedom tuning: *Given a data set $\mathcal{D}$ generated as in Assumption 1, a noise bounded as Assumption 3, a reference closed loop model $M(q^{-1})$, a sensitivity model $S(q^{-1})$. Find vectors $\hat{\theta}$ and $\hat{\rho}$ that approximately solve problems stated in (4.1) and (4.2).*

As above mentioned, problems 4.1 and 4.2 can be sequentially solved, in order to solve the problem 3 . Results of the next two subsections allow to tackle the sub-problems involved. The technique proposed here is named Output Error Approach (OEA).

4.2 Sensitivity tuning via Set-membership

In order to pose the problem in a set-membership framework, the next lemma is proposed.

Lemma 3. *Given a data set $\mathcal{D}$ generated as in Assumption 1 affected by noise bounded as in Assumption 3. Then, any controller $C_s(\theta)$ satisfies the time-domain relation,*

$$e(\theta, t) = S^2 C_s(\theta) y(t) - S(1 - S) u(t) + d(t) \tag{4.12}$$

where $e(\theta, t)$ is the output of the model matching error sensitivity transfer function,

$$E_s(q^{-1}) = S(q^{-1}) - \frac{1}{1 + P(q^{-1})C_s(\theta, q^{-1})} \tag{4.13}$$

and the unknown signal $d(t)$ is bounded as

$$\|d(t)\|_{\ell_p} \leq \left\| S^2 C_s(\theta) \right\|_{\ell_p, \ell_p} \epsilon_p = \delta_p^{sens} \tag{4.14}$$

where $\ell_p \in [2, \infty]$ and $\left\| S^2 C_s(\theta) \right\|_{\ell_p, \ell_p}$ is the proper induced norm of the system relating $v(t)$ and $d(t)$.

Proof: From *Definition 7*, E_s can be rewritten as

$$E_s = \frac{1}{1 + PC_s^*(\theta)} - \frac{1}{1 + PC_s(\theta)} \tag{4.15}$$

since the Equation (4.7) indicates that $\frac{1}{1+PC_s^*(\theta)} = S$.
Note that, to simplify notation, we drop the backward shift operator q^{-1}. Now, the sensitivity matching error transfer function also is given by

$$E_s = \frac{(1 + PC_s(\theta)) - (1 + PC_s^*(\theta))}{(1 + PC_s^*(\theta))(1 + PC_s(\theta))}$$
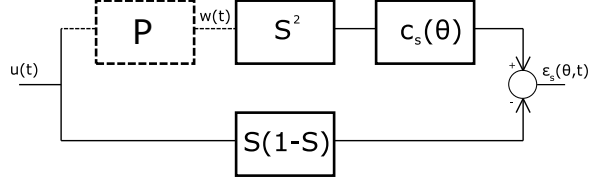
Figure 4.2: Block diagram for sensitivity tuning

and, if we introduce the following approximation

$$\frac{1}{1 + PC_s(\theta)} \approx \frac{1}{1 + PC_s^*(\theta)} = S, \tag{4.16}$$

then, E_s is given by

$$E_s \approx S[SC_s(\theta)P - SC_s^*(\theta)P].$$

Finally, using (4.7) to replace $C_s^*(\theta)$, the following expression is obtained,

$$E_s \approx S^2 C_s(\theta)P - S(1 - S). \tag{4.17}$$

Since the transfer function of the plant is unknown, we can multiply both sides of above equation by signal $u(t)$, in such way the following model-free equation is obtained:

$$e(\theta, t) = S^2 C_s(\theta)w(t) - S(1 - S)u(t) \tag{4.18}$$

Now, in order to avoid using the plant transfer function, the input signal $u(t)$ is applied to the system in eq. (4.18), as depicted in the block diagram of Fig. 4.2. In this case, the following model-free equation is obtained:

$$\begin{aligned}
\epsilon_s(\theta, t) &= S^2 C_s(\theta)w(t) - S(1 - S)u(t) \tag{4.19} \\
&= S^2 C_s(\theta)(y(t) + v(t)) - S(1 - S)u(t) \tag{4.20} \\
&= S^2 C_s(\theta)y(t) - S(1 - S)u(t) + d(t) \tag{4.21}
\end{aligned}$$

where $d(t) = S^2 C_s(\theta)v(t)$.

Finally, from Assumption 3, for any controller $C_s(\theta)$ guaranteeing an internally stable loop, the noise $d(t)$ can be bounded as,

$$\|d(t)\|_{\ell_p} \leq \left\|S^2 C_s(\theta)\right\|_{\ell_p, \ell_p} \epsilon_p = \delta_p^{sens}$$

Now, we are in position to define a Feasible Parameters Set (FPS_{C_s}) as the set of all parameters $\theta \in \Theta$ that are compatible with hypotheses and data, as follows,

Definition 11. Feasible parameters set to sensitivity tuning:

$$FPS_{C_s} = \{\theta \in \Theta : \left\|S^2 C_s(\theta)w(t) - S(1 - S)u(t)\right\|_{\ell_p} < \delta_p^{sens}\} \tag{4.22}$$

Theorem 5. *Given a dataset $\mathcal{D}$ as Assumption 1, a sensitivity model $S(q^{-1})$, a noise bounded as Assumption 3, and a set of basis functions $[\beta_1(q^{-1}), \ldots, \beta_m(q^{-1})]$. If $\delta_p \geq \delta_p^{sens*}$, for δ_p^{sens*} the solution to*

46

the convex optimization problem

$$\delta_p^{sens*} = \min_{\theta \in \Theta, \varepsilon \in \Re} \delta \tag{4.23}$$
$$s.t.$$
$$\left\| S^2 C_s(\theta) w(t) - S(1-S) u(t) \right\|_{\ell_p} < \delta$$
$$\delta \geq 0$$

Then, $FPS_{C_s} \neq \emptyset$.

Remark 5. *The Chebyshev center calculated using Theorem 2 can be employed to calculate the controller parameters, but this time using FPS_{C_s}.*

4.3 Closed-loop reference model tuning

In order to pose this problem in a set-membership framework, the next lemma is proposed.

Lemma 4. *Given a data set $\mathcal{D}$ generated as in Assumption 1 affected by noise bounded as in Assumption 3, and a controller $C_s(\hat{\theta}, q^{-1})$. Then, any controller $C_f(\rho, q^{-1})$ satisfy the time-domain relation*

$$e(\rho, \theta, t) = Mu(t) - S \left[C_s(\hat{\theta}) + C_f(\rho) \right] y(t) + d(t) \tag{4.24}$$

where $e(\rho, t)$ is the output of the model matching error transfer function,

$$E_m(q^{-1}) = M(q^{-1}) - \frac{P(q^{-1})(C_s(\hat{\theta}, q^{-1}) + C_f(\rho, q^{-1}))}{1 + P(q^{-1})C_s(\hat{\theta}, q^{-1})} \tag{4.25}$$

and the unknown signal $d(t)$ is bounded as

$$\|d(t)\|_{\ell_p} \leq \left\| S(C_s(\hat{\theta}) + C_f(\rho)) \right\|_{\ell_p, \ell_p} \epsilon_p = \delta_p^M \tag{4.26}$$

Proof: From *Definition 9*, E_m can be rewritten as

$$E_m(q^{-1}) = M(q^{-1}) - \frac{P(q^{-1})(C_s(\hat{\theta}, q^{-1}) + C_f(\rho, q^{-1}))}{1 + P(q^{-1})C_s(\hat{\theta}, q^{-1})} \tag{4.27}$$

Now, taking into account that that $\frac{1}{1+PC_s^*(\theta)} = S \approx \frac{1}{1+PC_s(\theta)}$, then Eq. 4.27 can be rewritten as follows

$$E_m(q^{-1}) \approx M(q^{-1}) - S(C_s(\hat{\theta}, q^{-1}) + C_f(\rho, q^{-1}))P(q^{-1}) \tag{4.28}$$
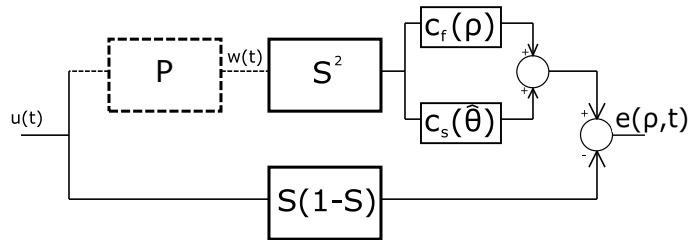
Figure 4.3: Block diagram for closed-loop model reference tuning

Since the transfer function of the plant is unknown, we can multiply both sides of above equation by signal $u(t)$ as is depicted in Figure 4.3, in such way the following model-free equation is obtained:

$$e(\rho, t) \quad = \quad Mu(t) - S\left[C_s(\hat{\theta}) + C_f(\rho)\right] w(t) \tag{4.29}$$

$$= \quad Mu(t) - S\left[C_s(\hat{\theta}) + C_f(\rho)\right](y(t) + v(t)) \tag{4.30}$$

$$= \quad Mu(t) - S\left[C_s(\hat{\theta}) + C_f(\rho)\right] y(t) + d(t) \tag{4.31}$$

where it is easy to deduce that $d(t) = S\left[C_s(\hat{\theta}) + C_f(\rho)\right] v(t)$.

Finally, from Assumption 3, and given a controller $C_s(\hat{\theta})$ that guarantees an internally stable loop, the noise $d(t)$ can be bounded as,

$$\|d(t)\|_{\ell_p} \leq \left\|S(C_s(\hat{\theta})) + C_f(\rho))\right\|_{\ell_p, \ell_p} \epsilon_p = \delta_p^M$$

Remark 6. *Under the assumption that $C_s(\hat{\theta}))$ is a stabilizing controller, an easy way to guarantee that $d(t)$ is bounded is selecting $C_f(\rho)$ controller as $C_f(\rho) \in \mathcal{H}_\infty$*

Now, it is possible to define a Feasible Parameters Set (FPS_{C_f}) as the set of all parameters $\rho \in \mathbf{P}$ that are compatible with hypotheses and data, as follows,

Definition 12. Feasible parameters set to closed-loop model reference tuning:

$$FPS_{C_f} = \{\rho \in \mathbf{P} : \left\|Mu(t) - S\left[C_s(\hat{\theta})) + C_f(\rho)\right] w(t)\right\|_{\ell_p} < \delta_p^M\} \tag{4.32}$$

Theorem 6. *Given a $C_s(\hat{\theta})$, a dataset $\mathcal{D}$ as Assumption 1, a reference model $M(q^{-1})$, a noise bounded as Assumption 3, and a set of basis functions $[\beta_1^\rho(q^{-1}), \ldots, \beta_{m\rho}^\rho(q^{-1})]$. If $\delta_p \geq \delta_p^{M*}$, for δ_p^{M*} the solution to the convex optimization problem*

$$\delta_p^{M*} = \min_{\rho \in \mathbf{P}, \varepsilon \in \Re} \delta \tag{4.33}$$
$$s.t.$$
$$\left\|Mu(t) - S(C_s(\hat{\theta}) + C_f(\rho))w(t)\right\|_{\ell_p} < \delta$$
$$\delta \geq 0$$

Then, $FPS_{C_f} \neq \emptyset$.

Remark 7. *The Chebyshev center calculated using Theorem 2 can be employed to calculate the controller parameters, but this time using FPS_{C_f}.*

4.4 Illustrative examples

4.4.1 Comparison Set-membership approaches

In this Section a numeric example is used to compare our approach (OEA) against Errors in Variables approach, which has been proposed in Cerone et al. (2017) for 1DoF controller tuning problem. In this work such method has been adapted to 2DoF controller tuning problem. Details can be found in Annex A.3.

Consider the LTI stable system

$$P(q^{-1}) = \frac{q^{-1}}{1 - 0.6q^{-1}} \tag{4.34}$$

This system has been employed in Campi et al. (2002) for controller design from data with VRFT approach.

The goal is to find the controllers $C_s(q^{-1})$ and $C_f(q^{-1})$ such that the sensitivity function and I/O transfer function behave as

$$S(q^{-1}) = \frac{1 - q^{-1}}{1 - 0.4q^{-1}} \tag{4.35}$$

$$M(q^{-1}) = \frac{0.8q^{-1} - 1.04q^{-2} + 0.336q^{-3}}{1 - 1.6q^{-1} + 0.84q^{-2} - 0.144q^{-3}} \tag{4.36}$$

If system $P(q^{-1})$ is known, simple algebra leads to the following controllers:

$$C_s(q^{-1}) = \frac{0.6 - 0.36q^{-1}}{1 - q^{-1}}, C_f(q^{-1}) = 0.2 \tag{4.37}$$

The system is excited by a random input sequence $u(t)$ uniformly distributed in the range $[-3, 3]$. To compare the effect of the data set size, experiments with $N = 100$, $N = 200$ and $N = 300$ are considered. The plant output sequence $y(t)$ is corrupted by random additive noise $v(t)$. In this work two different cases are investigated, the first with a $SNR \approx 20dB$ (moderate noise) and the second with $SNR \approx 30dB$ (small noise).

If we fix the value of $a_1^{C_s} = 1$, in order to ensure integral action, and $a_1^{C_f} = 0$ to ensure a class of proportional controllers for C_f, then the parameters $\theta^* = [b_0^{C_s}, b_1^{C_s}] = [0.6, -0.36]$ and $\rho^* = [b_0^{C_f}] = [0.2]$ must be found.

4.4.1.1 Computational solution

For the OEA solution, we select $p = 2$, noise bounded in 2-norm. For all cases of N and SNR, $\delta_2 = 3$ is selected, since preliminary testing indicates that lower values produce unfeasible results (i.e $FPS = \varnothing$). The CVX Matlab toolbox is used to solve problems (2.18) and (2.19).

For the EiVA Δ_v is known. However, it is worth noting that some tests led to infeasible results, therefore choosing larger Δ_v (+3%) is necessary. Problems (A.14) and (A.15) are solved by means of a convex relaxation approach, as proposed in Cerone et al. (2012). Matlab implementation of the sparse semidefinite programming (SDP) relaxation method proposed in Waki et al. (2008) has been used to relax the polynomial optimization problems, for a relaxation order $\delta = 2$.

Both frameworks are executed in Windows environment, on a Personal computer with Intel core i7-6700T (2.8 GHz) processor.

4.4.1.2 Result analysis

The estimated parameters obtained via OEA and EiVA for different N and SNR values are shown in Tables 4.1 and 4.2. The average computation time required to estimate one parameter, for both settings, is reported in Table 4.3. Considering that the most challenging setting is with $N = 100$ and $SNR = 20dB$, the frequency response of the required M and S and the estimates via both approaches are shown in Figures 4.4a and 4.4b.

According to Table 4.1, in the case of moderate noise, the mean estimation error for the OEA is near to 2%, and the worst case is 4%, while for EiVA the mean estimation error is near to 1% and the worst

case is 8%. On the other hand, in the case of small noise, Table 4.2 indicates that for the OEA the mean estimation error is near to 1%, and the worst case is 2%, while for EiVA the mean estimation error is near to 2% and the worst case is 4%. It can be seen that the EiVA obtains better estimates for the C_s parameters, while the OEA gives better approximations for the C_f parameters. When the noise is low, OEA offers better performance for all the data set sizes.

Table 4.3 illustrates that OEA is clearly faster than EiVA. The execution time is 100 times lower for the OEA. Moreover, for the EiVA the computational cost increases more than linearly as N increases, on the other hand, for the OEA it remains stable.

Table 4.1: Parameters estimated via both approaches for $SNR = 20dB$

Method	Parameter	N=100 Estimate (Error %)	N=200 Estimate (Error %)	N=300 Estimate (Error %)
OEA	$b_0^{C_s} = 0.6$	0.586 (2%)	0.589 (2%)	0.587 (2%)
	$b_1^{C_s} = -0.36$	-0.349 (3%)	-0.355 (2%)	-0.347 (4%)
	$b_0^{C_f} = 0.2$	0.197 (1%)	0.197 (1%)	0.199 (1%)
EiVA	$b_0^{C_s} = 0.6$	0.593 (1%)	0.582 (3%)	0.607 (1%)
	$b_1^{C_s} = -0.36$	-0.357 (1%)	-0.360 (0%)	-0.358 (1%)
	$b_0^{C_f} = 0.2$	0.216 (8%)	0.221 (2%)	0.201 (1%)

Table 4.2: Parameters estimated via both approaches for $SNR = 30dB$

Method	Parameter	N=100 Estimate (Error %)	N=200 Estimate (Error %)	N=300 Estimate (Error %)
OEA	$b_0^{C_s} = 0.6$	0.593 (1%)	0.601 (0%)	0.596 (1%)
	$b_1^{C_s} = -0.36$	-0.354 (2%)	-0.36 (0%)	-0.357 (1%)
	$b_0^{C_f} = 0.2$	0.197 (1%)	0.199 (0%)	0.2 (0%)
EiVA	$b_0^{C_s} = 0.6$	0.590 (2%)	0.587 (2%)	0.601 (0%)
	$b_1^{C_s} = -0.36$	-0.369 (2%)	-0.347 (4%)	-0.362 (0%)
	$b_0^{C_f} = 0.2$	0.192 (4%)	0.198 (1%)	0.202 (1%)

Table 4.3: Average computation time for both approaches

Method	Average time [seconds]		
	N=100	N=200	N=300
OEA	0.42	0.44	0.45
EiVA	43	165	218
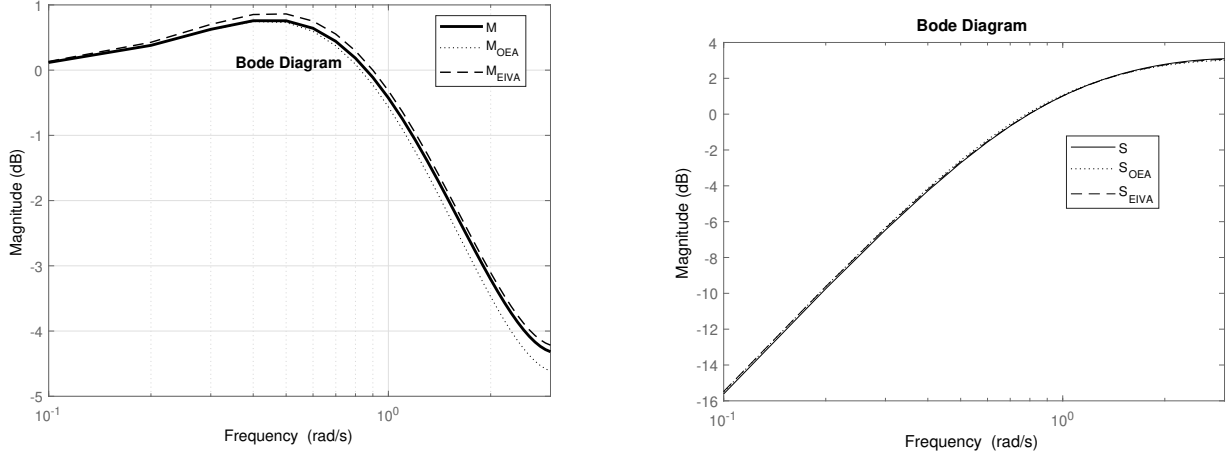
(a) Comparison of frequency responses obtained for (I/O) trans-(b) Comparison of frequency responses for sensitivity function
fer function

Figure 4.4: Bode plot results.

4.4.2   Comparison against VRFT

In Lecchini et al. (2002a) the VRFT technique was adapted for 2DoF controllers tuning. In this Section, our approach is tested against VRFT by means of an example shown in the mentioned paper.

Consider the LTI stable system

$$P(q^{-1}) = \frac{0.1622q^{-1} - 0.01622z^{-2}}{1 - 1.7q^{-1} + 0.8825z^{-2}} \tag{4.38}$$

The goal is to find the controllers $C_s(q^{-1})$ and $C_f(q^{-1})$ such that the sensitivity function and I/O transfer function behave as

$$S(q^{-1}) = 1 - \frac{(1 - \beta)q^{-1}}{1 - \beta q^{-1}}, \beta = 0.8 \tag{4.39}$$

$$M(q^{-1}) = \frac{(1 - \alpha)q^{-1}}{1 - \alpha q^{-1}}, \alpha = 0.4 \tag{4.40}$$

The magnitude bode plots from P, M and S can be observed in Figure 4.5
The system is excited by a random input PRBS sequence $u(t)$ in the range $[-2, 2]$ with $N = 512$. The output of the plant if affected by an additive stochastic disturbance signal $d(t)$ having the following form:

$$v(t) = \frac{0.3}{1 - 0.7q^{-1}} \varepsilon(t) \tag{4.41}$$

where $\varepsilon(t)$ is selected such that $SNR = 20dB$. In order to compare our results against VRFT methodology, we employ the controllers reported in Lecchini et al. (2002a). Note that, we can't compare directly the parameters because the 2DoF structures are different, that is the reason why we only compare the performance regarding to sensitivity and reference model achieved, as is shown in the Figures 4.6a, 4.6b, 4.7a and 4.7b. Results indicate a better performance with our approach to sensitivity shaping, however, better reference model tracking is attained via VRFT. It is worth noting that VRFT requires two experiments to deal with noisy measurements, while our approach only requires one experiment.

51
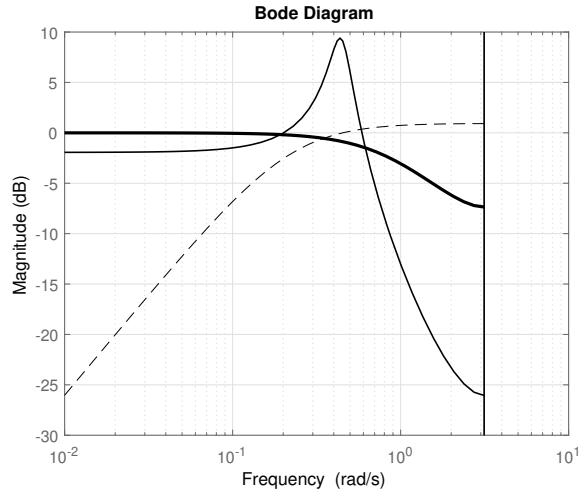
Figure 4.5: Magnitude Bode plots: The plant (continuous line), the reference-model M (bold line) and the reference sensitivity model S (dotted line

4.5 Conclusions

Taking into account the method proposed in Chapter 2, one novel method to solve the 2DoF data-driven controller tuning problem has been proposed, such has been named called Output-error approach (OEA). In order to validate our approach, the Errors-in-Variables approach proposed in Cerone et al. (2017) for 1DoF has been adapted to solve the 2DoF problem. Both methods are developed within a Set Membership framework. The methods allow to handle Unknown but Bounded noises, without any statistical hypothesis. The approaches allows shaping the sensitivity and I/O transfer functions, without requiring
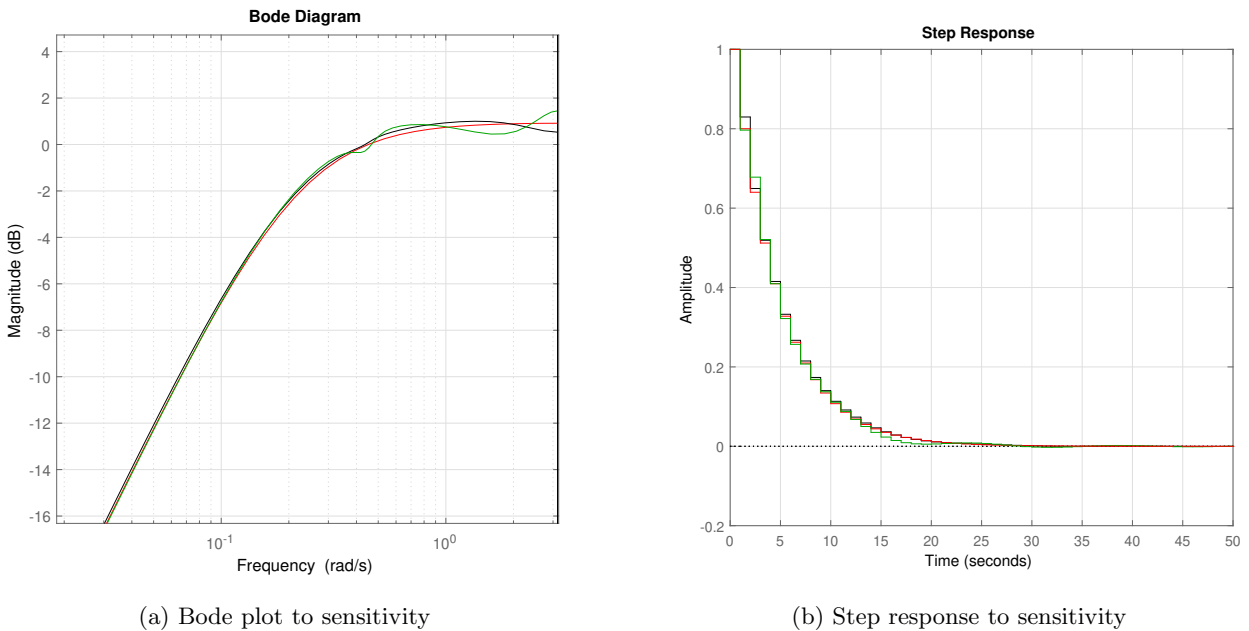
(a) Bode plot to sensitivity

(b) Step response to sensitivity

Figure 4.6: Sentitivity ideal S (red line), sensitivity achieved via OEA (black line), sensitivity achieved via VRFT (green line)
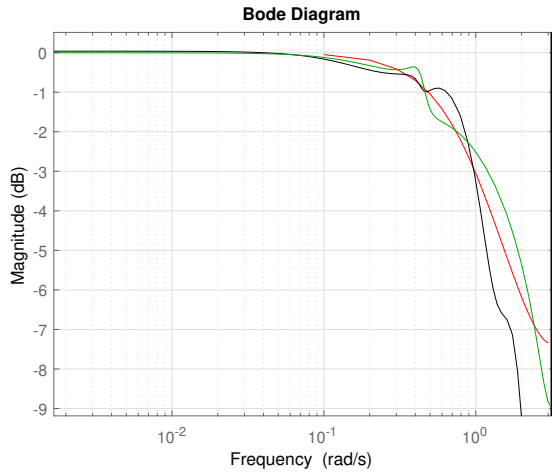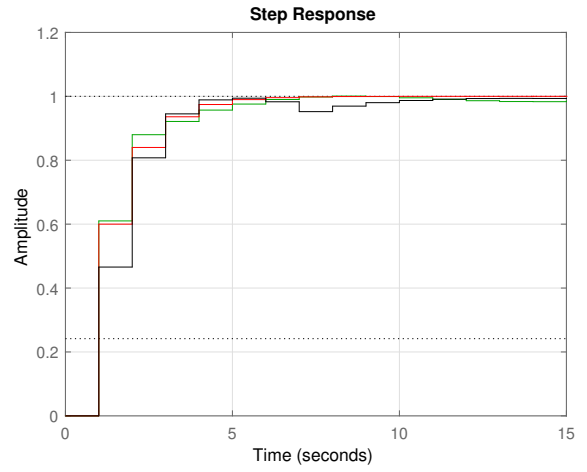
(a) Bode plot M (b) Step response M

Figure 4.7: Reference model ideal M (red line), Tracking achieved via OEA (black line), tracking achieved via VRFT (green line)

a model of the plant.

Results indicate that the computational cost, in terms of execution time of Errors-In-Variables approach is higher than the our setting, even three hundred times bigger. It can be concluded that similar estimation errors are presented in both approaches. It is a highlighted that our approach achieves better results for the feed-forward controller, which is estimated in a second step after the estimation of the feedback controller parameters.

A disadvantage of the Output-Error approach is the controller must be linearly-parametrized, while for Errors-in-Variables approach the controller class allows to estimate the poles of the transfer function. Further research is required to test the methods in a realistic setting.

Chapter 5

A Youla-Kucera Parametrization for Data-driven Controllers Tuning

One of the main challenges in the context of DDC methods is guaranteeing stability. Considering that no plant model is available in this framework, a precise stability test cannot be performed. A possibility is to test the controller before actual implementation, van Heusden et al. (2009) (i.e. a-posteriori tests). In Kammer et al. (2000) some a-posteriori stability estimators are proposed for an iterative DDC tuning scheme. In Sala and Esparza (2005) an invalidation test step, based on the available data, is employed for a non-iterative DDC scheme, in order to detect if the controller may led to unstable closed-loops. This test requires the accurate identification of a possibly unstable system in an errors-in-variables problem.

Some attempts to incorporate a stability constraint at the design step in non-iterative DDC can be found in Lanzon et al. (2006) and Van Heusden et al. (2011a). Both methods consider an extended PID controller structure leading to convex optimization problems. However, such methods do not offer acceptable performances when the desired reference model is not achievable employing the selected controller structure. In Battistelli et al. (2018), the unfalsified control theory is employed to derive relations between the choice of the performance criterion to be optimized and the closed-loop stability conditions. However, the controller is non-linearly parametrized, leading to non-convex optimization problems.

The Youla-Kucera parametrization is a fundamental result in system theory that allows to parametrize all the controllers that stabilize a given plant. It has been extensively applied in optimal and robust control when designing model-based controllers, see e.g. Doyle et al. (1991). However, in its original form it is not applicable when the plant model is not available.

In this paper, Youla-Kucera parametrization is employed to solve the problem of controllers design without requiring a process model. The proposed controller structure allows to reach more stringent reference models than those proposed previously in the literature, maintaining a convex optimization problem to tune the controller parameters. The approach is a non-iterative solution that exploits the CbT formulation. Thus, the controller tuning procedure does not require iterations or multiple experiments.

The outline of the chapter is as follows. In Section 5.1, the problem formulation is presented. In Section 5.2, a stabilizing controller structure is comprehensively formulated. In section 5.3, employing the structure proposed, a tuning scheme inspired by the CbT approach is developed. In Section 5.4 the proposed solution is applied to two simulated controller design problems, comparing it with the standard CbT scheme. Finally, in Section 5.5 the solution is extended to the MIMO case. The conclusions end the chapter in Section 5.6.

5.1 Statement of the problem

In this section, the data-driven controller (DDC) tuning problem is formulated. Consider again a discrete-time linear-time invariant (LTI) single-input single-output (SISO) feedback control scheme, as depicted in Fig. 2.1, where q^{-1} denotes the backward shift operator, $P(q^{-1})$ is a stable plant transfer function, $C(\theta, q^{-1})$ is the controller transfer function, θ is a vector of controller parameters, $r(t)$ is the reference signal, $v(t)$ is output noise/disturbance, $u(t)$ and $w(t)$ are the plant input and output signals, respectively.

For the system interconnection in Fig. 2.1, the aim of the controller tuning procedure is to select an optimal controller $C^o(\theta^o)$ minimizing some performance criterion and guaranteeing internal stability. For example, an optimization problem can be stated as:

$$C^o(\theta, q^{-1}) \qquad = \qquad \mathrm{argmin} J_{MR}(\theta) \qquad\qquad (5.1)$$
$$s.t.$$
$$\text{Loop internally stable}$$

For the cost function

$$J_{MR}(\theta) = \left\| M(q^{-1}) - \frac{P(q^{-1})C(\theta, q^{-1})}{1 + P(q^{-1})C(\theta, q^{-1})} \right\|_2^2 \qquad\qquad (5.2)$$

Being $M(q^{-1})$ a strictly proper reference model for the closed-loop system (i.e. $M \neq 1$), where performance specifications are embedded. Now, considering the Assumption 1 about availability of experimental data, a data-driven stabilizing controllers tuning problem can be stated as follows:

Problem 4. Data-Driven Stabilizing Controller Tuning: *Given a dataset $\mathcal{D}$ generated as in Assumption 1 and a reference model $M(q^{-1})$. Find a controller $\hat{C}(\theta)$ that solves (5.1).*

5.2 A stabilizing controller structure

Let us recall that the set of all the stabilizing controllers $C(\theta, q^{-1})$ for the loop in Fig. 2.1, given a stable plant $P(q^{-1})$ can be expressed as

$$\mathcal{C}^{sta} = \left\{ C(\theta, q^{-1}) = \frac{Q(\theta, q^{-1})}{1 - P(q^{-1})Q(\theta, q^{-1})} : Q(q^{-1}) \in \mathcal{H}_\infty \right\} \qquad\qquad (5.3)$$

where $Q(\theta, q^{-1})$ is any stable and proper transfer function. The previous result is known as the Youla-Kucera parametrization for a stable plant Doyle et al. (1991).
When the *Youla-Kucera* parametrization is adopted to find an optimal controller solving (5.1), the cost function (5.2) can be rewritten as

$$J_{MR}(\theta) = J_Q(\theta) = \left\| M(q^{-1}) - Q(\theta, q^{-1})P(q^{-1}) \right\|_2^2 \qquad\qquad (5.4)$$

That is, the complementary sensitivity function of the loop becomes $Q(\theta, q^{-1})P(q^{-1})$.

Assumption 6. *For the given closed-loop reference model $M(q^{-1})$, there exist an optimal filter $Q^*(\theta^*, q^{-1})$ such that,*

$$M(q^{-1}) = Q^*(\theta^*, q^{-1})P(q^{-1}) \qquad\qquad (5.5)$$

Remark 8. *From the previous assumption, the optimal controller $C^*(\theta^*, q^{-1})$, which solves Problem 4 is,*

$$C^*(\theta^*, q^{-1}) = Q^*(\theta^*, q^{-1})(1 - M(q^{-1}))^{-1} \tag{5.6}$$

It is worth noting that only the term $Q^*(\theta^*, q^{-1})$ is unknown, since $M(q^{-1})$ is proposed by the user.

Given the previous analysis, from now on we focus in the problem to estimate $Q^*(\theta^*, q^{-1})$, such that the cost function (5.4) is minimized.

5.2.1 A structure for Q.

Several structures can be assumed to design the filter $Q(\theta, q^{-1})$. For example, recursive polynomial structures such as ARX, ARMAX or OE, can be employed. The only requirement is that $Q(\theta, q^{-1}) \in \mathcal{H}_\infty$. However, imposing stability constraints in autoregressive structures, such as AR or ARMAX, leads to complex non-linear constraints, turning the tuning problem into a highly non-convex optimization program, see e.g. Ljung (1999). On the other hand, Finite Impulse Response (FIR) models guarantee stability without additional constraints. Therefore, a FIR structure is adopted for $Q(q^{-1}$ as follows,

$$Q(\theta, q^{-1}) = \sum_{i=1}^{m_q} \theta_i q^{-(i-1)}, \tag{5.7}$$

where m_q is the filter impulse response length.
Then, the controller design problem becomes a parametric estimation problem, where the filter parameters are selected from the set:

$$\mathcal{Q} = \left\{ Q(\theta, q^{-1}) : \theta \in \Theta \subseteq \mathcal{R}^{m_q} \right\}$$

5.2.2 The Q filter in terms of data.

Notice that to estimate a filter $\hat{Q}(\theta, q^{-1})$ minimizing (5.4) it is required the knowledge of the plant $P(q^{-1})$. But, under the assumptions of the framework, the plant is unknown. The following Lemma allows to relate the model-based cost function with a data-based error signal.

Lemma 5. *Given an asymptotically stable system $P(q^{-1})$ and a data set $\mathcal{D}$ generated as in Assumption 1, any stable filter $Q(\theta, q^{-1}) \in \mathcal{Q}$ satisfies the time-domain relation:*

$$e(\theta, t) = Mu(t) - Q(\theta)(w(t) - v(t)) \tag{5.8}$$

where $e(\theta, t)$ is the output of the model matching error transfer function (i.e., the argument of cost function in Eq. 5.2),

$$E_m(q^{-1}) = M(q^{-1}) - \frac{P(q^{-1})C(\theta, q^{-1})}{1 + P(q^{-1})C(\theta, q^{-1})}. \tag{5.9}$$

Moreover, if the reference model $M(q^{-1})$ satisfies Assumption 6, there exist an optimal filter $Q(\theta^*, q^{-1})$ such that:

$$e(\theta^*, t) = 0$$

then

$$Mu(t) = Q(\theta^*)(w(t) - v(t)) \tag{5.10}$$

Remark 9. *In most previous approaches to DDC tuning (i.e. CbT,VRFT,..) it has been considered the approximation $1/(1 + P(q^{-1})C^0(\theta, q^{-1})) \approx 1/(1 + P(q^{-1})C(\theta, q^{-1}))$ to obtain a time expression which approximates the cost function (5.2). Note that such approximation is not required in our approach.*

From the previous development, we are able to cast the problem to tune a filter $Q(\theta, q^{-1})$ into an identification problem as follows:

Problem 5. *Given the signals*

$$y_q(t) = M(q^{-1})u(t), \ u_q(t) = w(t)$$

Estimate from data an optimal filter $Q(\theta^*, q^{-1})$ that satisfies the relation:

$$y_q(t) = Q(\theta^*, q^{-1})u_q(t) \tag{5.11}$$

Note that the previous estimation problem is a system identification problem for system Q where the output $y_q(t)$ is measured without noise and the input $u_q(t)$ is noisy (see Figure 5.1).
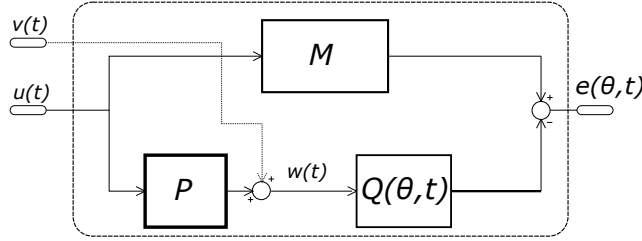
Figure 5.1: Block diagram for Q tuning problem

5.3 $\hat{Q}$ tuning scheme

In Problem 5 the estimation of Q has been posed as an identification problem where the input $u_q(t)$ is noisy and the output $y_q(t)$ is free of noise, i.e., an Errors In Variables (EIV) problem. In this work, we assume that $v(t)$ is i.i.d noise, however, is possible to adapt the formulation to deal with Unknown but Bounded noises, following Set-Membership identification methods, such as Cerone et al. (2017).

The instrumentals Variables (IV) method is a well know procedure to deal with EIV identification problems, Soderstrom and Stoica (1983). A proper selection of the IV vector is a key point to obtain good results. In the framework of DDC design three alternatives to select the IV have been proposed. Campi et al. (2002) proposes two alternatives, in the first one a second experiment with the same input is required to define the IV, and the second one consist into estimate a model $\hat{P}$ of the plant. The former option is difficult to achieve in realistic applications, and the last one does not make sense in the DDC framework. A third option to select the IV has been proposed in Karimi et al. (2007). In the following, we adapt such method to our framework, since it does not require a second experiment neither the plant identification.

5.3.1 Correlation approach to tune $\hat{Q}$

Let the correlation function be defined as follows

$$f(\theta) = \lim_{N \to \infty} \frac{1}{N} \sum_{t=1}^{N} E\left\{\zeta_w(t)e(\theta, t)\right\} \tag{5.12}$$

Where $E\{\cdot\}$ indicates the mathematical expectation. $\zeta_w(t)$ is a vector of instrumental variables well correlated with $u(t)$ and uncorrelated with $v(t)$ given by,

$$\zeta_w(t) = [u_w(t+l), u_w(t+l-1), \cdots u_w(t),$$
$$u_w(t-1), \cdots, u_w(t-l)]^T \tag{5.13}$$

where $u_w(t)$ is generated as a filtered version of the plant input, $u_w(t) = W(q^{-1})u(t)$, l is an proper integer and $e(\theta, t)$ is the data matching error defined in (5.8). Details for the selection of l can be found in Karimi et al. (2007).

For the cost function

$$J_c(\theta) = f^T(\theta)f(\theta) \tag{5.14}$$

The optimal parameters defining filter Q are selected as

$$\hat{\theta} = arg \min_{\theta} f^T(\theta)f(\theta) = \sum_{\tau=-l}^{l} R_{eu_w}^2(\tau) \tag{5.15}$$

where $R_{eu_w}(\tau)$ is the cross-correlation function between $e(\theta, t)$ and $u_w(t)$, that is

$$R_{eu_w}(\tau) = \lim_{N \to \infty} \frac{1}{N} \sum_{t=1}^{N} E\{e(\theta, t)u_w(t-\tau)\}$$

From (5.8), the previous equation can be rewritten as

$$R_{eu_w}(\tau) = \lim_{N \to \infty} \frac{1}{N} \sum_{t=1}^{N} E\{[M - PQ(\theta)]u(t)Wu(t-\tau)\}$$

Then, the cost function can also be represented in frequency domain by means of applying the Parseval's theorem, as follows:

$$\lim_{l \to \infty} J_c(\theta) = \frac{1}{2\pi} \int_{-\pi}^{\pi} |[M - PQ(\theta)]W|^2 \, \Phi_u^2(w)dw \tag{5.16}$$

where $\Phi_u^2(w)$ is the spectrum of the input signal. Finally, it is easy to note that $W(q^{-1}) = 1/\Phi_u(w)$ is required for criteria (5.4) and (5.16) being equal. In this way, $\lim_{l \to \infty} J_c(\theta)$ is a good approximation of $J_{MR}(\theta)$.

Remark 10. *Note that our main aim is minimizing the model matching error in (5.4) and in turn (5.9). But in order to apply the correlation method to tune the parameters of Q, a data error expression is required (i.e. $e(\theta, t)$ in (5.12)).Therefore, we have considered that the model matching error in (5.4) can be represented by means of a time expression in (5.8), this theoretical assumption can be approximated in practice when a signal $u(t)$ persistently exciting is employed, it means that its spectrum is rich enough to excite the dynamics of M.*

5.3.2   Selecting a proper number of parameters

In order to choose a proper filter impulse response length m_q, now we analyze the set of equations that define the filter impulse response. From Equation (5.4) the impulse response error can be expressed as:

$$e_h(\theta, k) = h^M(k) - h^P(k) * h^Q(\theta, k) \tag{5.17}$$

where $h^M(k)$, $h^P(k)$ and $h^Q(\theta, k)$ are the reference model, plant and Q impulse response correspondingly.

Let us recall that we have assumed M is a stable and strictly proper, therefore, its impulse response h^M is such that $\left|h^M(k)\right| \le L\rho^k$ for $k = 0, 1, 2, \dots$ given a finite bound $L > 0$ and decay rate $\rho \in (0,1)$, that is, $h^M(k)$ decays exponentially. Therefore one may assume that the impulse response of M is negligible for $k \ge L_M$, for a L_M reasonable value.

Now, given that P is stable, Q is FIR and $h^M(t)$ is selected by the user, a necessary condition to achieve $e_h(\theta, k) \approx 0$ is that $m_q \ge L_M$.

Remark 11. *Reference models with small values of L_M (i.e impulse response energy is concentrated in the first coefficients) are strongly recommended because they lead to low-complexity controllers. In other cases, a controller order reduction step is advisable.*

5.3.3   Procedure to tune $\hat{Q}$

Given a data set generated as in Assumption 1, a reference model M and a filter length m_q, properly selected. The following procedure leads to a controller that approximately minimizes (5.2).
Given the structure for Q, it can be said that

$$Q(\theta, q^{-1}) = \beta^T(q^{-1})\theta \tag{5.18}$$

where

$$\beta(q^{-1}) = \left[1, q^{-1}, \cdots, q^{-(m_q-1)}\right] \tag{5.19}$$

Now, define the regressor as

$$\phi(t) = \beta(q^{-1})u_q(t) \tag{5.20}$$

Then, note that the error signal $e(\theta, t)$ can be expressed as

$$e(\theta, t) = y_q(t) - \phi(t)\theta \tag{5.21}$$

In terms of data, the Equation 5.15 for $W = 1$ is estimated as

$$f_N(\theta) = \frac{1}{N}\sum_{t=1}^{N} \zeta_w(t)\left[y_q(t) - \phi(t)\theta\right] \tag{5.22}$$

Recalling that $\zeta_w(t)$ is defined in Equation (5.13), it is possible to estimate the parameters of Q minimizing the criterion

$$J_N(\theta) = f_N^T(\theta)f_N(\theta). \tag{5.23}$$

the Least squares solution is:

$$\hat{\theta} = (X^T X)^{-1} X^T Z \tag{5.24}$$

where

$$X = \frac{1}{N}\sum_{t=1}^{N} \zeta_w(t)\phi^T(t), \tag{5.25}$$

$$Z = \frac{1}{N}\sum_{t=1}^{N} \zeta_w(t)y_q(t) \tag{5.26}$$

Finally, the controller to implement is given by

$$C(\hat{\theta}, q^{-1}) = Q(\hat{\theta}, q^{-1})(1 - M(q^{-1}))^{-1} \tag{5.27}$$

5.3.4 Stability margin estimation

Once a controller has been estimated by the previous procedure, it is necessary to estimate whether it guarantees an internally stable loop. A stability margin can be determined using the Small Gain Theorem, Doyle et al. (1991), considering the uncertainty associated to the estimated controller. The loop in Fig. 2.1 can be reformulated as shown in Fig. 5.2. From this scheme, the Small Gain Theorem leads to the following condition:

The controller given by

$$C(\hat{\theta}, q^{-1}) = Q(\hat{\theta}, q^{-1})(1 - M(q^{-1}))^{-1} \tag{5.28}$$

achieves a robustly stable loop if

$$\delta_Q(\theta) = \|\Delta_\theta\|_\infty = \|M(q^{-1}) - P(q^{-1})Q(\hat{\theta}, q^{-1})\|_\infty < 1 \tag{5.29}$$
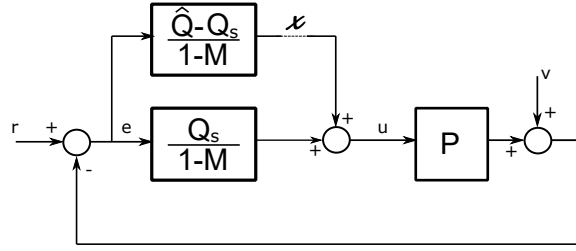

Figure 5.2: Closed-loop with representation of the controller error $\frac{\hat{Q}-Q_s}{1-M}$

Eq. 5.29 is a tool to determine the stability of the loop, the approach in van Heusden et al. (2007) can be employed as it requires one data batch to estimate the norm, as in Assumption 1. However, data-driven methods only allow to estimate lower bounds of the system H_∞ norm, converging to the actual norm for infinite data lengths. In practice, a finite number of data is available, thereby only an under estimate of the stability condition is available. Moreover, the small gain theorem provides an stability condition for any unstructured uncertainty with norm less than 1. Therefore, the estimated condition in (5.29) can be employed as a guide only. The stability condition of a controller that leads to an estimated norm lower than 1 can be invalidated by new data, while a controller that leads to a norm larger than 1 can produce a stable loop for the particular structure of the uncertainty. In conclusion, $\delta_Q(\theta)$ values near to zero, indicate a lower risk that the controller led to stable closed loops.

From now on, our method will be called Youla-Kucera data driven controllers tuning (YK-DDC).

5.4 Numerical examples

In this Section, the Youla-Kucera data driven controllers tuning (YK-DDC) method proposed in the previous sections is evaluated in simulation. The performance of the solution is compared with the Correlation-based Tuning (CbT) method presented in Van Heusden et al. (2011a).

5.4.1 Flexible transmission

Consider the flexible transmission system introduced as a benchmark for digital control design by Landau et al. (1995). The plant is

$$P(q^{-1}) = \frac{0.28261q^{-3} + 0.50666q^{-4}}{1 - 0.418q^{-1} + 1.589q^{-2} - 1.316q^{-3} + 0.886q^{-4}}$$

The control objective is given in terms of model-reference specifications. Two classes of reference models are tested,

$$M_1(q^{-1}) = \frac{(1-\alpha)^2 \, q^{-3}}{(1-\alpha q^{-1})^2}, \; M_2(q^{-1}) = \frac{0.6q^{-5}}{1 - 0.75q^{-1} + 0.35q^{-2}}$$

considering under and over-damped required closed-loop behaviors.

The Correlation-based Tuning (CbT) method, presented in Van Heusden et al. (2011a), is employed in order to evaluate the performance of our approach. In CbT approach, the controller is parametrized as:

$$C(\theta, q^{-1}) = \sum_{i=1}^{m} \frac{\theta_i q^{-(i-1)}}{1 - q^{-1}} \tag{5.30}$$

Case I: Reference Model M_1.

In this case, α indicates the location of the poles defining the desired loop speed and bandwidth (See Figure 5.3). As the first step, data set is generated using a PRBS signal with $N = 512$ samples as plant input. We assume $\Phi_u(\omega) \approx 1$. White noise is added to the plant output. The noise variance is selected such that the Signal to Noise Ratio (SNR) is approximately $20dB$. The SNR is calculated as

$$SNR = 10 log \frac{\sum_{t=1}^{N} y(t)^2}{\sum_{t=1}^{N} v(t)^2}.$$
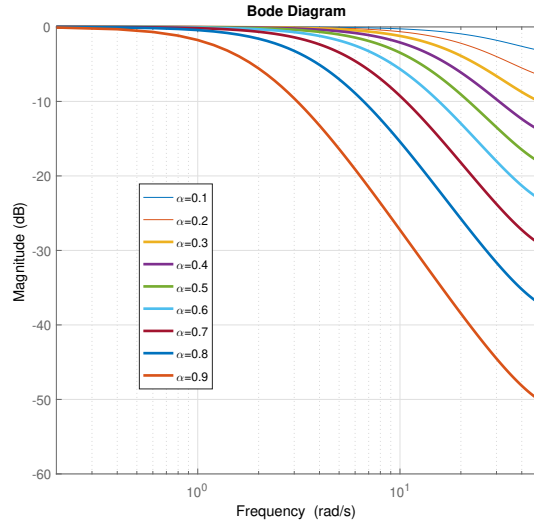
Figure 5.3: Reference models M_1 class for diferrent α values

Before applying both methods to tune the controllers (i.e. YK-DDC and CbT) we analyze the realizability of the different reference models employing our controller structure. To achieve this, we have evaluated the cost function J_N in eq. (5.23) for different α and m_q values. The obtained results are shown in Figure 5.4. It can be observed that J_N decreases as α increases, that means better results are obtained for slow reference models (i.e low bandwidth), however, it is necessary to select high values of m_q. On the other hand, for the references model with high bandwidth fewer parameters are necessary, but results in terms of tracking the reference model worsen. We choose the case of $\alpha = 0.5$ (see Figure 5.5), therefore, m_q must be greater than 8. We select $m_q = 11$ taking into account the step response of M (see Subsection 5.3.2).

A Monte-Carlo simulation is carried out, therefore, 1000 reference signals $u(t)$ are generated and applied to the plant P, maintaining $N = 512$. The set of output signals $y(t)$ is corrupted by noise $v(t)$ maintaining

Figure 5.4: Cost function for reference models M_1, evaluated for different α and m_q parameters.
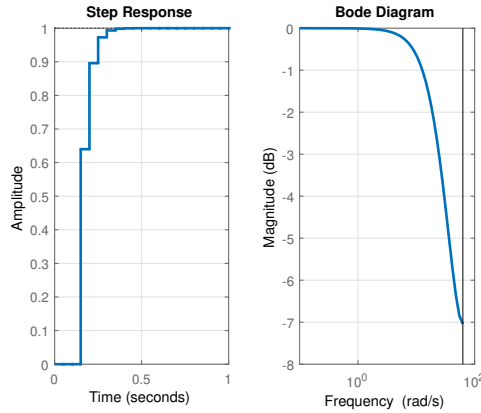
Figure 5.5: Step response and bode plot of reference model M_1 for $\alpha = 0.5$

a $SNR \approx 20dB$, leading to 1000 data sets $\mathcal{D}$. For each data set, a set of controllers has been tuned via the procedure in subsection 5.3.3 employing $l = 20$, then the controllers are tested in closed-loop with the actual model of the plant P. For the CbT algorithm, it has been assumed $m = 6$ and also $l = 20$ as the instrumental variables length, the same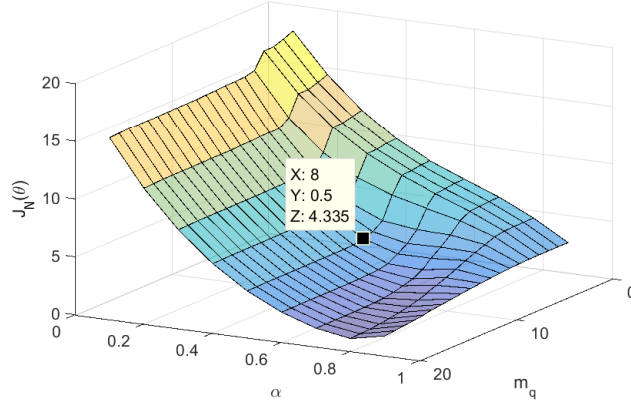 values are assumed in Van Heusden et al. (2011a). Results, in terms of step response, are depicted in Figure 5.6 for both methods.

For all controllers tuned via both approaches $\hat{\delta}(\theta)$ is estimated via the method in van Heusden et al. (2007), employing proper signals $e(\theta, t)$ for each approach. In CbT approach 16 controllers led to $\hat{\delta}(\theta) \geq 1$, while in our approach all controllers led to $\hat{\delta}(\theta) \leq 1$. Results for stability criterion are reported in Table 5.1. Nevertheless, none of the controllers obtained via both approaches leads to unstable loops. It is worth noting that, according to Figure 5.6, the tracking of the reference model is better for the controllers obtained by means of our approach. The quality of the control action is measured employing the maximum error E_{MAX} and the root mean squared error E_{RMS} of the closed-loop step response, the results are reported in Table 5.2.

Now, in order to validate the Q filter estimation procedure, our Q filters are compared with the optimal Q^* filter in terms of frequency response, such results are depicted in Figure 5.7. Note that, in this case, P is known, therefore the optimal Q filter is known, that is $Q^* = M_1 P^{-1}$.

Now, as an example, one of the 1000 controllers $C(\theta, q^{-1})$ is reported in Equation (5.31).
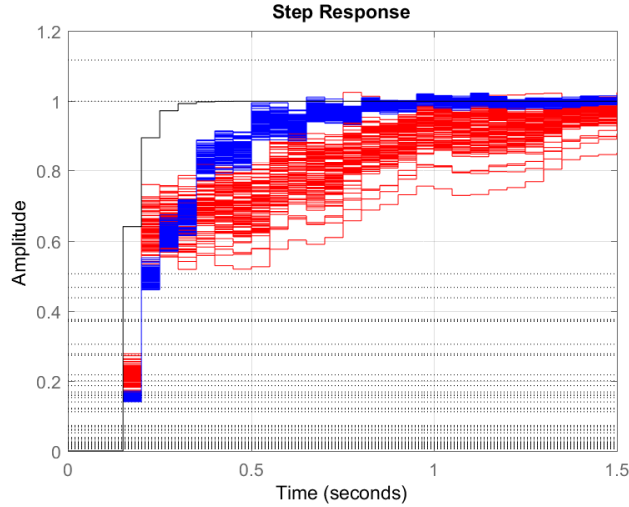
Figure 5.6: Step response of M_1 (black line), results for 1000 controllers tuning via our approach (continuous blue lines) and results for 1000 controllers tuning via CbT (dashed red lines)

.

| | Employed | $\hat{\delta}(\theta)$ | | |
	Method	Max	Min	Mean
Case I	CbT	1.433	0.193	0.393
	YK-DDC	0.531	0.179	0.241
Case II	CbT	2.610	0.970	1.101
	YK-DDC	0.510	0.171	0.261

Table 5.1: Stability results for infinity norm criterion for both approaches.
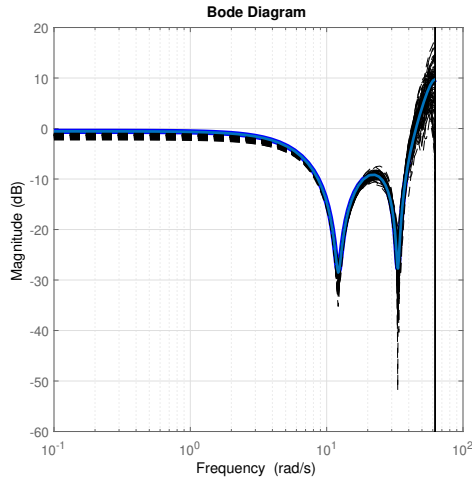
Figure 5.7: Magnitude Bode plots of Q^* (continuous blue line), and for 1000 Q filters tuning by procedure in subsection 5.3.3 (dashed black lines)

	Employed	Quality measures	
	Method	E_{MAX}	E_{RMS}
Case I	CbT	0.1819	0.0563
	YK-DDC	0.1489	0.0413
Case II	CbT	0.5184	0.1415
	YK-DDC	0.1091	0.0298

Table 5.2: Quality control results for both approaches in both cases.

$$C(\theta, q^{-1}) = \sum_{i=1}^{11} \theta_i q^{-(i-1)}(1 - M_1(q^{-1}))^{-1} \tag{5.31}$$

where the vector $\theta = [0.54, -0.66, 1.01, -0.97, 1.01, -0.6, ... \ 0.7, -0.43, 0.37, -0.16, 0.07]$
Finally, replacing M_1 the resulting controller is

$$C(\rho, q^{-1}) = \frac{\sum_{i=1}^{13} \rho_i q^{-(i-1)}}{1 - q^{-1} + 0.25q^{-2} - 0.25q^{-3}} \tag{5.32}$$

where the vector $\rho = [0.54, -1.21, 1.81, -2.59, 2.24, -1.86, ... \ 1.56, -1.29, 0.98, -0.64, 0.32, -0.11, 0.02]$

Case II: Reference Model M_2.
In this case, a more stringent reference model with underdamped behavior is imposed. The aim is to evaluate the robustness of the design procedure when the reference model can produce unstable loops. The step response and bode plot of M_2 are shown in Figure 5.8.
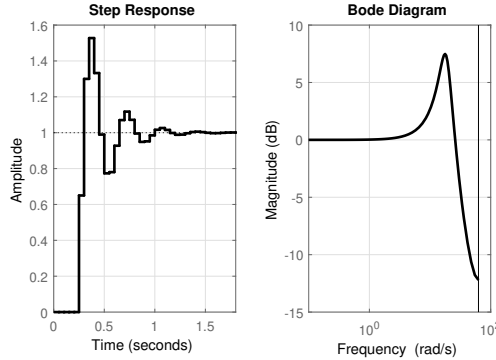
Figure 5.8: Step response and bode plot of reference model M_2

In order to select a proper m_q, the cost function J_N is evaluated. Results are depicted in Figure 5.9. As the first case, a data set with $N = 512$ and $SNR \approx 20dB$.(SNR) is generated. A Monte-Carlo experiment with 1000 data sets is performed. $m_q = 13$ is employed based on the step response in Figure 5.8. The same parameters as in the case I are selected for the CbT approach. The resulting closed-loop step responses are depicted in Figure 5.10. As can be observed, the performance obtained with the YK-DDC controllers (blue lines) is better than with CbT controllers.
For all controllers tuned via both methods $\hat{\delta}(\theta)$ is estimated via the method in van Heusden et al. (2007). For the CbT approach, 77% of the controllers led to $\hat{\delta}(\theta) \geq 1$, while with the YK-DDC approach, all the controllers led to $\hat{\delta}(\theta) < 1$. Results for stability criterion are reported in Table 5.1. Nevertheless, when evaluated on the actual plant, only 7 of the controllers obtained via CbT lead to unstable loops and all the controllers obtained via YK-DDC yield stable loops.
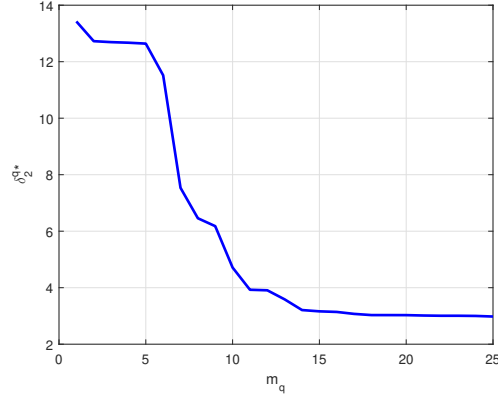
Figure 5.9: Cost function for reference model M_2 for different m_q values.

Figure 5.10: Step response of M_2 (black line), results for 1000 controllers tuning via our approach (continuous blue lines) and results for 1000 controllers tuning via CbT (dashed red lines)

.

5.4.2 Non-minimum phase plant equipped with integrator

In order to test the approach on an demanding condition, we take the next example from Battistelli et al. (2018). Consider the problem of controlling an unknown system with continuous-time transfer function given by

$$P(s) = \frac{s - 0.5}{s(s^2 + 2s + 1)}$$

The case of unstable (marginally stable) plants must be deal with employing an initial stabilizing controller. Although such a controller guarantees stability, it does not achieve the required performance.

The control requirements are given by the reference model:

$$M(s) = \frac{1}{w_n^2 * (s^2 + 2\zeta s/w_n + 1/w_n^2)}$$

where, $w_n = 4.5$ and $\zeta = 0.4$.

The proportional controller $C_s = -0.35$ is connected in closed loop with the plant, in order to assure stability and allowing to collect the data set $\mathcal{D}$. Now, the feedback interconnection of $P(s)$ and C_s is considered as the new plant $\mathcal{P}$ to be controlled (see Figure 5.11), with input $u(t)$ and output $w(t) = y(t)+v(t)$.

A Monte-Carlo experiment is performed on the new plant, 100 realizations of $u(t)$ are generated and applied to the plant, each one elapsing 1280 s and using $T_s = 2.5$ s, thus $N = 512$.

The set of output signals $y(t)$ is corrupted by noise $v(t)$ maintaining a $SNR \approx 20dB$. The reference model is discretized by means of the zero-order hold method with sampling time T_s. Taking into account the step response of the reference model M, $m_q = 12$ is selected. The same parameters as in the previous example are selected for the CbT approach. The performance in terms of frequency response obtained for the 100 controllers is illustrated in the Figure 5.12. The architecture of the closed-loop implemented is presented in Figure 5.11.
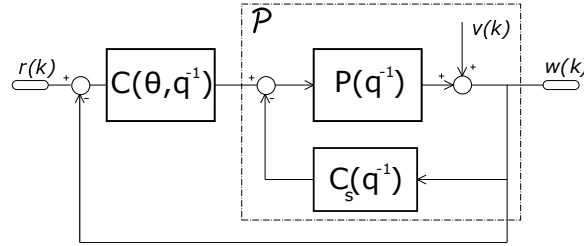
Figure 5.11: Cascade control for the non-minimum phase plant

.

As in the previous example, for all controllers tuned via both methods $\hat{\delta}(\theta)$ is estimated, employing the proper signals $e(\theta, t)$ for each approach. In CbT approach, the worst case for $\hat{\delta}(\theta)$ was 0.99 (i.e. there exist a bigger risk that the controller led to unstable loop) and the mean was 0.54, while in our approach, the worst case was 0.61 and the mean was 0.37.

5.5   Extension to MIMO case

In this section, the Youla-Kucera Parametrization for Data-driven Controllers Tuning is adapted to the MIMO case.

Consider now a plant $\boldsymbol{P}(q^{-1})$ with n inputs $\boldsymbol{u}(t)$ and n outputs $\boldsymbol{w}(t)$, a controller transfer matrix $\boldsymbol{C}(\theta, q^{-1})$, and a reference model matrix $\boldsymbol{M}(q^{-1})$ for the closed-loop system. Consider also the Assumption about the availability of experimental data:

Assumption 7. $\boldsymbol{P}(q^{-1})$ *is unknown. The available information on* $\boldsymbol{P}(q^{-1})$ *is a set of input-output data generated by* $\boldsymbol{P}(q^{-1})$, *initially at rest,*

$$\mathcal{D} = \{\boldsymbol{w}(t), \boldsymbol{u}(t), t = 1, 2, ..., N\} \tag{5.33}$$

Where

$$\boldsymbol{w}(t) = \sum_{j=0}^{t} \boldsymbol{h}_j \boldsymbol{u}(t - j) + \boldsymbol{v}(t),$$

where $\boldsymbol{h}_j$ *are the impulse response coefficients matrix of* $\boldsymbol{P}(q^{-1})$, $\boldsymbol{y}(t) = \sum_{j=0}^{t} \boldsymbol{h}_j u(t - j)$ *is the noise-free output vector, and* $\boldsymbol{v}(t)$ *is the plant output noise/disturbance vector.*
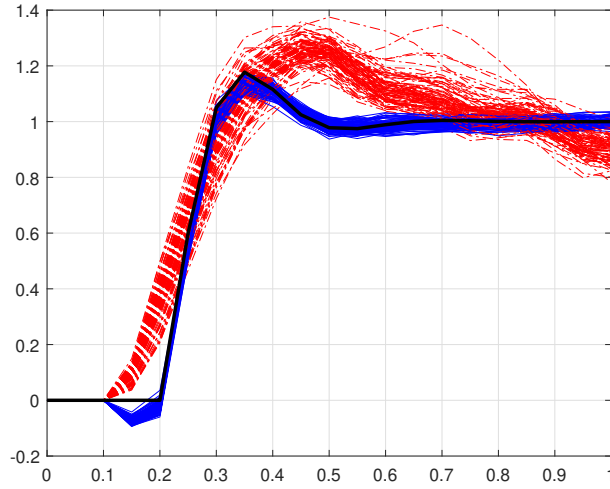
66
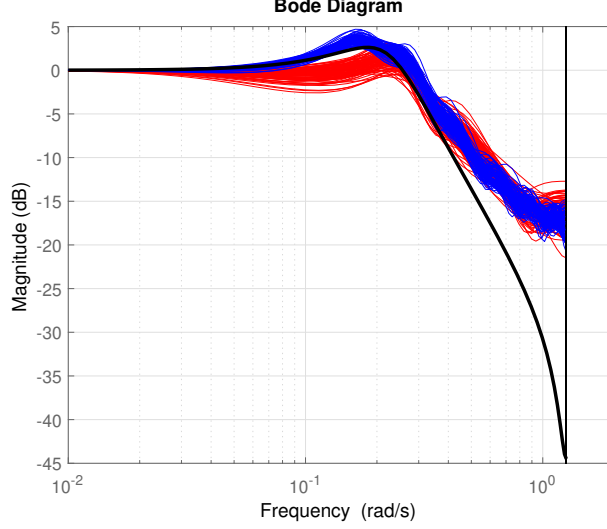
Figure 5.12: Magnitude Bode plots of M (black line), results for 100 controllers tuning via our approach (continuous blue lines) and results for 100 controllers tuning via CbT (dashed red lines)

.

Following the same analysis performed in the SISO case, when the *Youla-Kucera* parametrization is adopted the optimal controller $\boldsymbol{C}^*(\theta^*, q^{-1})$ is,

$$\boldsymbol{C}^*(\theta^*, q^{-1}) = \boldsymbol{Q}^*(\theta^*, q^{-1})(I - \boldsymbol{M}(q^{-1}))^{-1} \tag{5.34}$$

As in the SISO case, we select Finite Impulse Response (FIR) models for $\boldsymbol{Q}^*(\theta^*, q^{-1})$ filter, since such guarantee stability without additional constraints. For $n = 2$ the filter parametrization is:

$$\boldsymbol{Q}_{2x2}(\theta, q^{-1}) = \begin{bmatrix} \sum_{i=1}^{m_q} \theta_i q^{-(i-1)} & \sum_{i=1}^{m_q} \theta_{m_q+i} q^{-(i-1)} \\ \sum_{i=1}^{m_q} \theta_{2m_q+i} q^{-(i-1)} & \sum_{i=1}^{m_q} \theta_{3m_q+i} q^{-(i-1)} \end{bmatrix} \tag{5.35}$$

Now, given an asymptotically stable system $\boldsymbol{P}(q^{-1})$ and a data set $\mathcal{D}$ generated as in Assumption 7, any stable filter $\boldsymbol{Q}(\theta, q^{-1}$ satisfies the time-domain relation:

$$e(\theta, t) = \boldsymbol{M}\boldsymbol{u}(t) - \boldsymbol{Q}(\theta)(\boldsymbol{w}(t) - \boldsymbol{v}(t)) \tag{5.36}$$

which is useful to cast the problem to tune a matrix filter $\boldsymbol{Q}(q^{-1})$ into an identification problem as follows:

Problem 6. *Given the signals*

$$\boldsymbol{y}_q(t) = \boldsymbol{M}(q^{-1})\boldsymbol{u}(t), \ \boldsymbol{u_q}(t) = \boldsymbol{w}(t)$$

Estimate from data an optimal filter $\boldsymbol{Q}(\theta^*, q^{-1})$ that satisfies the relation:

$$\boldsymbol{y_q}(t) = \boldsymbol{Q}(\theta^*, q^{-1})\boldsymbol{u_q}(t) \tag{5.37}$$

As in the SISO case, the previous estimation problem is a system identification problem for system $\boldsymbol{Q}$ where the output $\boldsymbol{y_q}(t)$ is measured without noise and the input $\boldsymbol{u_q(t)}$ is noisy.

5.5.1 $\hat{Q}$ tuning scheme in the MIMO case

In Problem 6 the estimation of $\boldsymbol{Q}$ has been posed as an identification problem. In this case, we have neglected the effect of $\boldsymbol{v}(t)$. As future work, a set-membership or correlation-based framework can be employed to deal with noise measurements.

Given a data set generated as in Assumption 7, a reference model $\boldsymbol{M}$ and a filter length m_q, properly selected. The following procedure leads to a controller that approximately minimizes reference model criterion.

Given the structure for Q, it can be said that

$$\boldsymbol{Q}(\theta, q^{-1}) = \beta^T(q^{-1})\boldsymbol{\theta} \tag{5.38}$$

where

$$\beta(q^{-1}) = \left[1, q^{-1}, \cdots, q^{-(m_q-1)}\right] \tag{5.39}$$

and $\boldsymbol{\theta}$ must be organized conveniently according to $\boldsymbol{Q}$ structure. In case of $n = 2$ see Equation (5.35). Now, define the regressor as

$$\boldsymbol{\phi}(t) = \beta(q^{-1})\boldsymbol{u_q}(t) \tag{5.40}$$

Then, note that the error signal $\boldsymbol{e}(\theta, t)$ can be expressed as

$$\boldsymbol{e}(\theta, t) = \boldsymbol{y_q}(t) - \boldsymbol{\phi}(t)\boldsymbol{\theta} \tag{5.41}$$

Now, considering that the part of $\boldsymbol{e}(t)$ produced by $v(t)$ is white noise, the least-squares criterion is proposed to tune $\boldsymbol{Q}$. Let us define the following cost function.

$$J_N(\theta) = \frac{1}{N} \sum_{t=1}^{N} (\boldsymbol{y_q}(t) - \boldsymbol{\phi}(t)\theta) \tag{5.42}$$

the Least squares solution is:

$$\hat{\theta} = \left[\sum_{t=1}^{N} \boldsymbol{\phi}(t)\boldsymbol{\phi}(t)^T\right]^{-1} \sum_{t=1}^{N} \boldsymbol{\phi}(t)\boldsymbol{y_q}(t) \tag{5.43}$$

Finally, the controller to implement is given by

$$\boldsymbol{C}(\hat{\theta}, q^{-1}) = \boldsymbol{Q}(\hat{\theta}, q^{-1})(I - \boldsymbol{M}(q^{-1}))^{-1} \tag{5.44}$$

Remark 12. *In practice, M is diagonal because uncoupled loops are desirable. Therefore, the inverse exists as long as each element of the matrix M be invertible.*

5.5.2 2-DOF helicopter case study

The 2-DOF helicopter is an important model from the control engineering point of view due to its wide non-linear characteristics, highly cross-coupling effects, and instability in open loop (Patel and Mehta, 2019). The 2-DOF helicopter model (fixed base) with two propellers driven by DC motors is shown in Figure 5.13. The elevation of the nose over the pitch axis is controlled by the front propeller and the rotational motion around the yaw axis is controlled by the back propeller.

Figure 5.13: 2-DOF helicopter system. Courtesy : Quanser Inc.

5.5.2.1 Controller tuning problem

In this section a tracking problem is posed [1], the aim is to follow a given yaw and pitch displacement. The system has two inputs and two outputs (i.e. $n = 2$), the voltage v_p (Voltage for pitch axis) and v_y (Voltage for yaw axis) are the manipulated variables (u), measured in Volts. The outputs are y_a and p_i, these are yaw and pitch angles respectively, measured in deg. The loop performance specifications are defined as a reference model matrix that allows uncoupling the dynamics of the two degrees of freedom, as follows

$$\boldsymbol{M}(q^{-1}) = \begin{bmatrix} M_{11} & 0 \\ 0 & M_{22} \end{bmatrix} \tag{5.45}$$

and, to select M_{11} and M_{22} next loop specifications are keeping in mind

$$Pitch = \left\{ \begin{array}{c} Steady\ state\ error = 0 \\ Settling\ time \leq 3[s] \\ Rise\ time \leq 2[s] \\ Maximum\ overshoot \leq 10\% \end{array} \right\}, Yaw = \left\{ \begin{array}{c} Steady\ state\ error = 0 \\ Settling\ time \leq 7[s] \\ Rise\ time \leq 3[s] \\ Maximum\ overshoot \leq 10\% \end{array} \right\} \tag{5.46}$$

The reference models M_{11} and M_{22} can be selected of any order. In practice, several combinations has been tested employing first and second order models. To this report, the reference model of the Equation (5.47) is selected.

$$\boldsymbol{M} = \begin{bmatrix} \frac{10}{3s+10} & 0 \\ 0 & \frac{2.5^2}{s^2+2*0.592*2.5s+2.5^2} \end{bmatrix} \tag{5.47}$$

5.5.2.2 Experiment design

As mentioned in the previous chapter, the case of unstable plants must be deal with employing an initial stabilizing controller. In this case, a state-space feedback controller is connected in closed-loop with the plant, in order to assure stability and allowing to collect the data set $\mathcal{D}$, as shown in Figure 5.14. It must be highlighted that the initial controller allows stabilizing the closed-loop, but it does not guarantee the loop specifications mentioned above.

---

[1] These results are extracted from the master thesis project developed by Lenin Samuel Marin. Maestría en ingeniería electrónica, Pontificia Universidad Javeriana 2019.
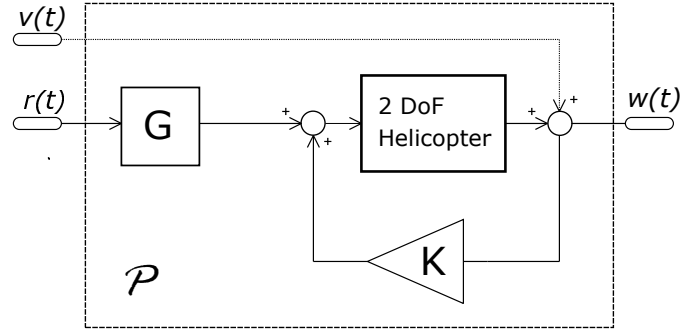
Figure 5.14: 2-DOF helicopter system connected with the stabilizing controller.

The controller K and the G filter employed are in Equations (5.48) and (5.49) respectively.

$$K = \begin{bmatrix} 21.11 & 1.99 & 10.98 & 1.38 \\ -1.99 & 21.11 & -0.39 & 11.99 \end{bmatrix} \tag{5.48}$$

$$G = \left[C(BK - A)^{-1}B \right]^{-1} \tag{5.49}$$

where A, B and C are taken from the model provided by Quanser Inc. A PRBS signal with $N = 14000$ is used as input (v_y, v_p), $Fs = 80[Hz]$ is employed . Outputs y and p obtained are depicted in Figures 5.15b and 5.15a respectively.
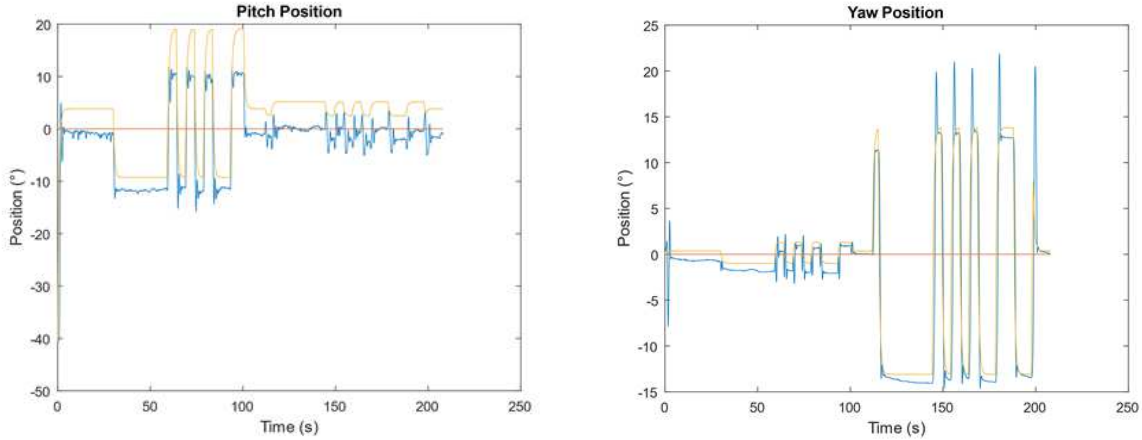
(a) Pitch position obtained for PRBS input, blue line   (b) Yaw position obtained for PRBS input, blue line

Figure 5.15: Pitch and Yaw signals obtained for PRBS input

Given the sampling frequency $Fs = 80[Hz]$, the reference corresponding reference model is

$$M(q^{-1}) = \begin{bmatrix} \frac{0.06050q^{-1}}{1-0.9394q^{-1}} & 0 \\ 0 & \frac{0.0006928q^{-1}+0.000682q^{-2}}{1-1.955q^{-1}+0.9566q^{-2}} \end{bmatrix} \tag{5.50}$$

5.5.2.3   Results

To estimate the controller $m_q = 15$ is selected, taking into account the analysis in subsection 5.3.2. With all ingredients defined, the $\hat{Q}$ tuning procedure of subsection 5.5.1 is performed.The controller resulting is

70

$$\boldsymbol{C}(q^{-1}) = \begin{bmatrix} \frac{\sum_{i=1}^{16} A_i q^{-(i-1)}}{1-q^{-1}} & \frac{\sum_{i=1}^{17} B_i q^{-(i-1)}}{1-q^{-1}} \\ \frac{\sum_{i=1}^{16} C_i q^{-(i-1)}}{1-1.95q^{-1}+0.95q^{-2}} & \frac{\sum_{i=1}^{16} D_i q^{-(i-1)}}{1-1.95q^{-1}+0.95q^{-2}} \end{bmatrix} \tag{5.51}$$

where,

$$A = [4.54, -3.52, -1.42, -0.63, -0.17, 0.03, 0.005, 0.41, 0.34, 0.10, 0.38, 0.33, 0.15, -0.03, -0.07, -0.42] \tag{5.52}$$
$$B = [-2.165, 1.736, 1.261, 0.366, -0.079, -0.244, -0.165, -0.582, -0.514, 0.162, -0.354, -0.393, 0.324, 0.559, 0.863, -0.779] \tag{5.53}$$
$$C = [-2.39, 4.91, -1.60, -0.70, -0.38, -0.22, 0.43, -0.72, 0.33, -0.04, -0.21, 0.56, -0.12, 0.99, 2.23, -5.61, 2.54] \tag{5.54}$$
$$D = [12.85, -25.20, 9.21, 1.94, 1.26, 0.95, -0.46, 0.30, 0.45, -0.89, 0.48, -0.60, 0.19, -1.57, -0.57, 2.53, -0.85] \tag{5.55}$$

The final controller architecture for our approach is the same as in the case of non-minimum phase plants (see Figure 5.17). Now, in order to validate our controller (YK-DDC), the LQR+I controller provided by Quanser Inc. is used to perform a comparison. The experimental results are summarized in Table 5.3 and depicted in Figure 5.16.

Table 5.3: Results for YK-DDC and LQR+I controller in the case of 2DOF helicopter

	Pitch position (p)			Yaw position(y)		
	YK-DDC	LQR+I	M	YK-DDC	LQR+I	M
Reference model class	Over-damped			Under-damped		
Maximum overshoot	N/A	N/A	N/A	5%	11.8%	10%
Rise time	0.78 [s]	0.66 [s]	0.25 [s]	1.75 [s]	1.22 [s]	0.6 [s]
Settling time	2.22 [s]	6.07 [s]	1[s]	2.3 [s]	14.4 [s]	2 [s]
Steady state error	0%	0%	0%	0%	0%	0%
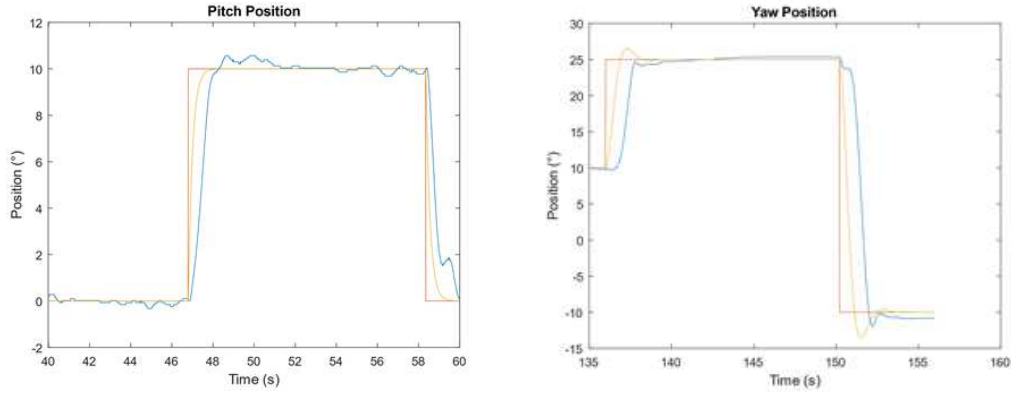
(a) Pitch position with YK-DDC controller (blue line), output of reference model (orange line)

(b) Yaw position with YK-DDC controller(blue line), output of reference model (orange line)

Figure 5.16: Pitch and Yaw positions via YK-DDC controller

According to the results in Table 5.3, in the case of the pitch position, the rise time achieved is comparable for both controllers, however, the settling time achieves via the YK-DDC controller is near to three times smaller than the LQR+I controller. For the yaw position, the settling time for the YK-DDC controller is near to seven times smaller than the LQR+I controller, the rise time for both controllers is comparable and the maximum overshoot for the YK-DDC is half of the obtained for the LQR+I controller.
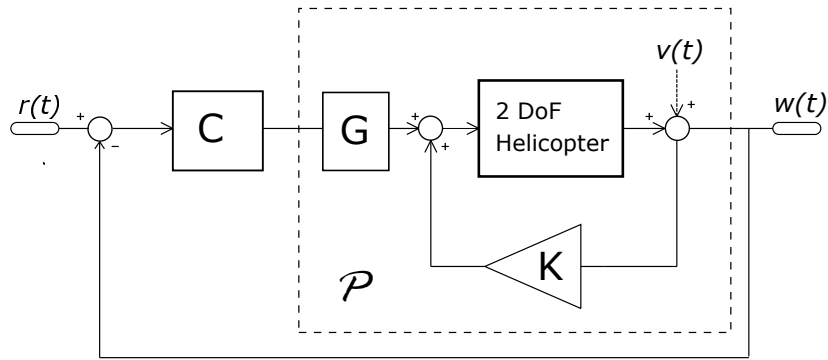
Figure 5.17: Cascade controller for the 2DOF helicopter

5.6 Conclusions

In this chapter, in the SISO case, we have presented a solution to the controller design from data problem, based on a Youla-Kucera parametrization of the controller. Departing from a set of input-output data measured from an stable, linear, time-invariant, SISO system, we have proposed a procedure to estimate a Finite Impulse Response filter that parametrizes an stabilizing controller, without requiring the plant model. The presented method translates the controller design process into an errors-in-variables identification problem and the solution is obtained by least-squares estimation. An *a-posteriori* stability estimation procedure has been derived, allowing to estimate from data the possible failure of the stability requirement (in the SISO case). The performance of the solution has been illustrated by means of Monte-Carlo simulations. Further research is required to state a robust stability test.

The approach of the SISO case has been extended to the MIMO case. A procedure to tune the controller is proposed employing the least-squares method. This extension is experimentally evaluated on a 2-DoF Helicopter. Our approach achieves better results compared with the LQR+I controller proposed by the system manufacturer since the former meets the control requirement with smaller settling time and smaller maximum overshoot. However, given that the 2DOF helicopter is unstable an initial stabilizing controller is required to collect the dataset and to construct a cascade control strategy. Further research is required to deal with noise in the data-driven approach to the MIMO case proposed here.

Chapter 6

Application in essential oil extraction processes

6.1 Introduction

Essential Oil (EO) is an agro product which has great prospect to be developed (Kusuma et al., 2018). The essential oils market accounted for USD 4.46 Billion in 2016, according to the Observatory of Economic Complexity (Simoes, 2018), and it is projected to reach USD 11.19 Billion by 2022. The top exporters of EO are India (14%) and the United States (14%), while the main importers are the United Sates (24%), France (8.8%), Germany (8.2%) and the United Kingdom (6.6%). EO from aromatic plants and spices are highly prized in the pharmaceutical, food, and cosmetic industries, due to their fragrance, antioxidant and anti-microbial properties (Burt, 2004). Lavender oil is one example of EO obtained form aromatic plants. The annual production of lavender essential oil es estimated in more than 1.300 tonnes, being France and Bulgaria the main producers (Krausz, 2014). According to Stashenko (2009), in Colombia (Cundinamarca, Boyacá and Eje cafetero) there is good experience in the cultivation and commercialization of aromatic plants for fresh sale, however, it is not so for the essential oils; in Colombia, most relevant works in this sense have been carried out in the CENIVAM research center of the Universidad Industrial de Santander.

The commercialization of essential oils depends largely on their quality, which depends on several factors that can be classified into two groups: The first group is related to the pre-harvest stage, factors such as origin and harvesting time are part of this group. It is worth mentioning that this group of factors is beyond the scope of this project; the second group is related to the extraction process, we can say that the factors related to quality are: processing temperature, pressure, batch-time and in some cases extraction technology used.

Essential oils (EO) are complex mixtures of volatile compounds extracted from a large number of plants. In general they represent a small fraction of plant composition (less than 5% of the vegetable dry matter) and comprise mainly hydrocarbon terpenes (isoprenes) and terpenoids (Asbahani et al., 2015). Antimicrobial or other biological activities of EO are directly correlated to the presence of bioactive volatile components. Chemically, the EO consist of terpene compounds (mono-, sesqui-, and diterpenes), alcohols, acids, esters, epoxides, aldehydes, ketones, amines, and sulfides) (Calo et al., 2015). Some terpenes are potent drugs against diseases such as cancer (Ebada et al., 2010). The functional role of aromatic plants, spices, and constituents is an important research topic (Loizzo et al., 2009).

Essential oil is stored in different parts of plants, for example in leaves, flowers, stems, roots, etc. The location depends on the plant variety (Vargas A, 2008) and, according to Sovová (2005), EO is deposited in

various types of cavities (vacuoles, glands, and others). In aromatic plants, the EO is stored in glandular trichomes on the outer surface of flowers and leaves, develop from epidermal cells. They are characteristic of the Lamiaceae family (Turner et al., 2000). There are many types of glandular trichomes: sessile and stalked trichomes. The latter can be of three types: peltate, capitate or digitiform trichomes (Asbahani et al., 2015).

There exist multiple essential oil extraction techniques for aromatic plants (Stashenko, 2009). The most employed ones are hydro-distillation, steam distillation and steam-water distillation. Some new techniques have been proposed, such as supercritical fluids extraction (SFE), microwave assisted hydrodistillation (MWD), and ohmic-assisted hydrodistillation (OAHD). The new techniques offer advantages such as higher extraction speeds, lower operation temperature or avoidance of organic solvents usage (which are potentially harmful in terms of environmental impact) (Arranz et al., 2015; Hashemi et al., 2017). However, in industrial scale implementations it is preferred to use steam distillers because those imply lower initial installation costs, lower operating and maintenance costs (Masango, 2005). One drawback of steam-distillation and hydrodistillation methods is the thermolability of the essential oil constituents, which undergo chemical degradation due to the high applied temperatures (Arranz et al., 2015).

This part of dissertation is organized as follows. In the first section, an optimal control approach to steam distillation is posed, developed and tested in simulation. In the second section, the ohmic-assisted hydrodistillation process is explained, and the design of a lab-scale ohmic distiller is showed. The third section describes some experimental tests for different input power trajectories in the OAHD process. Finally, in section 4 two data-driven techniques are employed to tune temperature controllers in the OAHD process.

6.2 An optimal control approach to steam distillation of essential oils from aromatic plants

6.2.1 Extraction process model

The model employed in this section is taken from Cerpa et al. (2008). Details of the model are reported in this chapter as a necessary background to discuss the dynamic optimization solution. Before describing the model, it is important to give an brief explanation of the extraction process

6.2.1.1 Process description

Figure 6.1 shows the diagram of an steam distiller. In this equipment, water is heated in a boiler to produce superheated steam, which is transported through a pipe to the vessel, steam helps to release the molecules of essential oil from the plant, by increasing temperature and pressure. The oil molecules released from the plant then mix with the steam. That mixture rises through the distiller and reaches the condenser, this device allows the mixture to cool and change to liquid phase. Finally, the liquid mixture reaches the florentine, in which oil and water are separated. Such water is known as hydrolate or hydrosol and is valuable in several industries.

6.2.1.2 Model description

It is a phenomenological model able to reproduce the essential oil recovery from process variables. The following assumptions were used to derive the model:

1. The system is isothermal and isobaric.

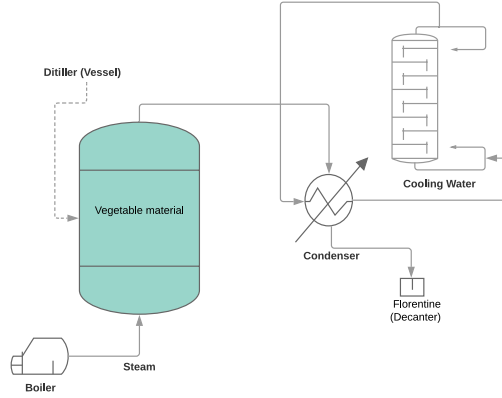2. The bed of leaves and stems is considered as a batch.

Figure 6.1: Steam distiller

3. The porous bed formed by the plant is stable. No changes in form or disposition take place during the process.

4. Vapor phase inside the distillation vessel is considered perfectly mixed, with constant flow rate. Oil accumulation in the vapor phase is neglected.

5. All oil inside trichomes is extracted during the process.

6. Four-phase system: oil inside the trichome, condensed water, free-oil outside the trichome, and vapor phase.

7. Essential oil is considered as a mixture of 10 components. Oil composition inside trichomes $(w_i^t r)$ agrees with distilled essential oil collected during the entire process. Composition is determined by GC/MS.

8. Condensed water and essential oil are completely immiscible.

9. The steam stream fed to the distillation vessel is oil-free $(C_{in} = 0))$.

10. Fixed bed porosity.

The model considers three stages in the oil obtaining process: (i) thermal oil exudation from the glandular trichomes, (ii) vapor liquid equilibrium at the interface, and (iii) vapor phase oil mass transfer.

The following three equations represent the dynamics of the three stages:

$$\dot{m}^{tr \to os} = -\frac{d(GW)}{dt} = K_{tr}GW \tag{6.1}$$

$$\frac{dM^{os}}{dt} = K_{tr}GW - \frac{K_g M^{os}}{h\rho_{eo}}(C^* - C) \tag{6.2}$$

$$\frac{dM^{sd}}{dt} = \dot{m}^{os \to vp} = QC \tag{6.3}$$

where C is the essential oil mass concentration in the vapor-phase, the model parameters are defined in Table 6.1 and the rest of the variables will be defined when used. In this work, the essential oil is considered as a single constituent, that is, the model generates the same extraction dynamics for each

essential oil constituent.

In order to obtain a state space representation of the process for the formulation of the optimal control problem, the state vector (x) and the manipulated input (u) are defined as follows:

$$x = [x_1, x_2, x_3]^T = \left[G, M^{os}, M^{sd} \right]^T, u = Q \tag{6.4}$$

Where $x_1 = G$ is the oil mass inside trichomes per mass of fresh plant $[g/g]$ (stage I), $x_2 = M^{os}$ is the oil mass in aqueous layer $[g]$ (stage II), $x_3 = M^{sd}$ is the oil mass collected $[g]$ (stage III), and $u = Q$ is steam volumetric flow, $[cm^3/min]$. Using the above definitions, and the auxiliary equation

$$\frac{dM^{sd}}{dt} = \frac{K_g M^{os} Q}{(Qh\rho_{eo} + K_g M^{os})} C^*, \tag{6.5}$$

it is possible to obtain the state space representation shown in (6.6).

$$
\begin{aligned}
\dot{x}_1 &= -K_{tr} W x_1 \\
\dot{x}_2 &= K_{tr} W x_1 - \frac{K_g C^* x_2}{h\rho_{eo}} \left[1 - \left(\frac{K_g x_2}{uh\rho_{eo} + K_g x_2} \right) \right] \\
\dot{x}_3 &= \frac{K_g u C^* x_2}{(uh\rho_{eo} + K_g x_2)}
\end{aligned}
\tag{6.6}
$$

Table 6.1 shows the model parameters. According to (Cerpa et al., 2008), all parameters of the above model are constant except the mass transfer coefficient K_g, which varies with Q. From the reported experimental data, it is observed that K_g exhibits an affine relation with Q, approximated by the following expression:

$$K_g = 4.7 * 10^4 (Q - 74400) + 31.4 \tag{6.7}$$

From the available data, relation (6.7) is valid for $21100 < Q < 100000 [cm^3/min]$, which are the minimum and maximum flow rates evaluated.

6.2.1.3 Model analysis

A next step is to simulate the model (6.6), in order to analyze the dynamic behavior. It is important to mention that there exists a filling time t_{fill} required to warm up the distiller, and the model equations are valid from t_{fill}. Without loss of generality we assume $t_{fill} = 0$

Equations (6.6) are solved with an implicit fixed-step numerical method in Simulink (ODE14x). Simulation parameters used are shown in Table 6.1. A constant steam flow $Q = 30[Kcm^3/min]$ is assumed.

The evolution of the three states is shown in Figure 6.2. As expected, x_1 has an exponentially decreasing behavior as proposed in Benyoussef et al. (2002). Note that W is constant. State x_3 increases quickly over the first time interval (first 20 minutes) but at the final interval it increases slowly. That means that most of the oil is collected during first time interval. Finally, the most interesting dynamic corresponds to state x_2, since the aqueous layer is a bridge that allows the transportation of oil from trichomes toward the vapor phase. Note that an important amount of oil essential is stored in such layer at the initial time interval of the process (i.e the 20 first minutes), and this effect is undesirable. To reduce energy consumption, oil should go through directly from the trichomes towards vapor phase.
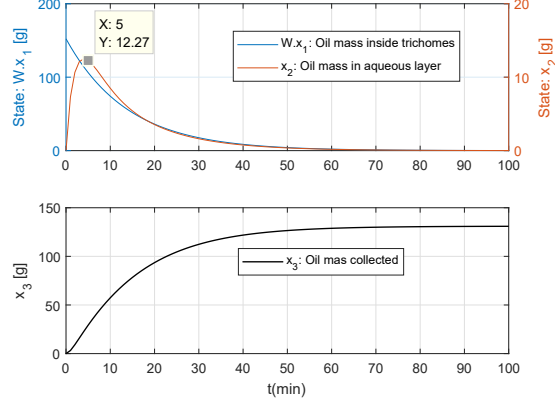
Figure 6.2: Model analysis

Table 6.1: Model parameters and initial conditions

Name	Description	Value
W	Fresh plant mass	$2175[g]$
K_{tr}	Exudation kinetic constant	$0.072 min^{-1}$
C^*	Oil mass concentration-equilibrium	$0.001[g/cm^3]$
h	Oil spots average thickness	$115 * 10^{-4}[cms]$
ρ_{eo}	Essential oil liquid density	$1[g/cm^3]$
$x_1(0)$	Initial oil mass fraction inside trichomes	$0.07[g/g]$
$x_2(0)$	Initial oil mass in aqueous layer	$0[g]$
$x_3(0)$	Initial oil mass collected	$0[g]$

6.2.2 Optimal oil extraction control problem

In an industrial essential oil extraction distiller plant, the main purpose is to maximize the yield of extraction and, at the same time, minimize the energy consumption.

Extraction yield (Y) is defined, at any given time t, as

$$Y_t = 100\frac{M_t^{sd}}{W} = 100\frac{x_3(t)}{W} \tag{6.8}$$

Energy consumption in a steam distillation plant can be measured as the volume of steam used during the extraction process. Therefore the energy consumption for a batch of length t_f is

$$E = \int_{t=0}^{t_f} Q(t)dt = \int_{t=0}^{t_f} u(t)dt. \tag{6.9}$$

6.2.2.1 Optimal control problem

From the previous discussion, the optimal operation of the extraction process has two objectives: maximization of yield and minimization of steam. A multi-objective control problem is formulated as a weighting sum of (6.8) and (6.9), as follows:

$$\begin{aligned}
\min_{u(t)} \quad & J = \int_{t=0}^{t_f} \left(-\bar{x}_3(t) + \gamma\bar{u}(t)\right) dt \\
\text{s.t.} \quad & \dot{x}(t) = f(x,u) \\
& U_{min} < u(t) < U_{max}
\end{aligned} \tag{6.10}$$

77

Where the dynamic constraint $\dot{x}(t) = f(x, u)$ is given by (6.6), $\bar{x}_3(t) = x_3(t)/max(x_3(t))$ and $\bar{u}(t) = u(t)/max(u(t))$. γ is a weighting factor that allows the user to balance the trade-off between yield and energy savings, and the effect is studied in next section.

Note that problem (6.10) is nonlinear and the structure is not input-affine. Therefore, an analytic solution by means of necessary conditions (Pontryagin's maximum principle) is not an easy task. The resulting Hamiltonian, Eq. (6.11), does not allow separation of the Lagrange multipliers (λ) from the manipulated variable (u).

$$
\begin{aligned}
H(x, t, \lambda) = & -x_3(t) + \gamma u(t) - \lambda_1(t) K_{tr} W x_1(t) \\
& + \lambda_2(t) \left[K_{tr} W x_1(t) - \frac{K_g C^* x_2(t)}{h \rho_{eo}} \left[1 - \left(\frac{K_g x_2(t)}{u(t) h \rho_{eo} + K_g x_2(t)} \right) \right] \right] \\
& + \lambda_3(t) \left[\frac{K_g u(t) C^* x_2(t)}{(u(t) h \rho_{eo} + K_g x_2(t))} \right]
\end{aligned}
\tag{6.11}
$$

A numerical optimization tool is employed to solve the problem, whose model is represented by Differential Algebraic Equations (DAE). *APMonitor* has been selected as the optimization tool. This software has been previously used in similar applications, see e.g. (Hedengren et al., 2014; Safdarnejad et al., 2015b),(Safdarnejad et al., 2015a) and (Afram and Janabi-Sharifi, 2017). Internally, *APMonitor* converts the DAE system into a nonlinear programming form (NLP) by means of a technique known as orthogonal collocation on finite elements. It is possible to select different solvers, like active set solver (APOPT), reported in Jacobsen et al. (2013) or an interior point method (IPOPT), Wächter and Biegler (2006).

6.2.3 Results & discussion

Different solutions to problem (6.10) are presented and discussed in this section. Consider the process described by Eq. (6.6), with parameters in Table 6.1 and steam flow rates limits defined in the modeling section. Several optimal input trajectories can be found by varying the weighting factor γ. Without loss of generality, $t_f = 100[min]$ is fixed as the batch length.

6.2.3.1 Case I: Maximizing yield

A first approach is to neglect energy consumption (i.e volume of steam), that is, to solve problem (6.10) with $\gamma = 0$. The results are shown in Figure 6.3. Notice that the optimal $u(t)$ trajectory starts at the lowest permitted flow and quickly saturates at the upper flow limit. The steam flow is kept low at the beginning because at that time there is no oil available in the aqueous layer (i.e $x_2 = 0$). This is an interesting result, because in any static optimization solution, $u(t)$ is fixed during the whole extraction process, producing a waste of water and energy for little additional separation.

6.2.3.2 Case II: Minimizing energy

A second test is performed, minimizing volume of steam only. In order to obtain such effect $\gamma = 100$ is selected (it should be ∞). The trivial solution is to completely curtail steam flow at every time. However, the lower bound on stem flow, fixed in (6.10), does not allow to fix a flow lower than U_{min}. The resulting trajectories are reported in Figure 6.4. The numerical solution is $u(t) = U_{min}$ at every time, as expected, although the yield obtained at the final time is low when compared with the yield in case I. At $t = t_f$ more than 12% of the available oil has not been extracted.
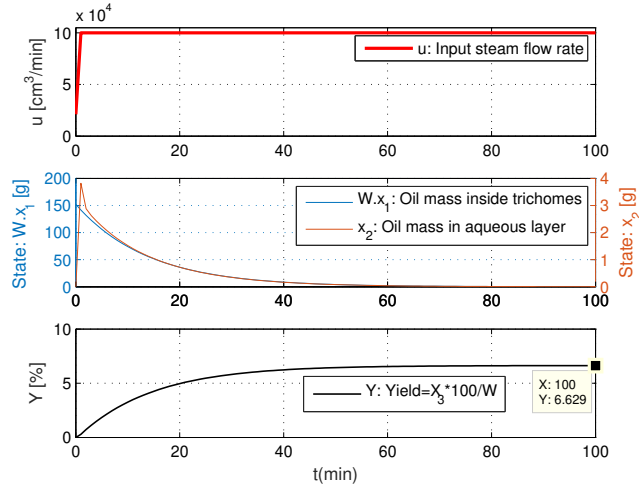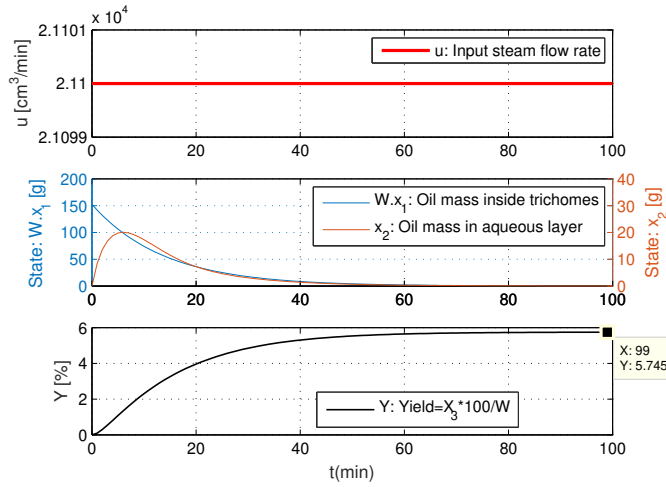
Figure 6.3: Results in case I

Figure 6.4: Results in case II

6.2.3.3 Case III: Trade-off between yield and energy

To obtain a balance between yield of extraction and energy consumption, γ was varied within the interval [0.01 0.9]. Results are summarized in Table 6.2. Energy savings (W_{sv}) and yield reduction (Yo) are evaluated with respect to a batch with constant maximum steam flow.

Figure 6.5 presents the optimal solution for $\gamma = 0.02$. Steam flow trajectories obtained by means of different γ values are depicted in Figure 6.6a. Note that as the weighting parameter is reduced, the optimal strategy maintains the maximum steam flow during more time. However, there is always a point where flow is reduced, minimizing energy consumption.

Figure 6.6b shows the Pareto front of the multi-objective problem. Notice that from $\gamma \geq 0.02$ the yield of extraction decreases quickly below 99%, while the saving in steam consumption are more than 60%. This is an important finding for industrial applications.

In the following, the weighting parameter is fixed as $\gamma = 0.02$. Table 6.3 summarizes the results for three cases studied. The following remarks can be highlighted:
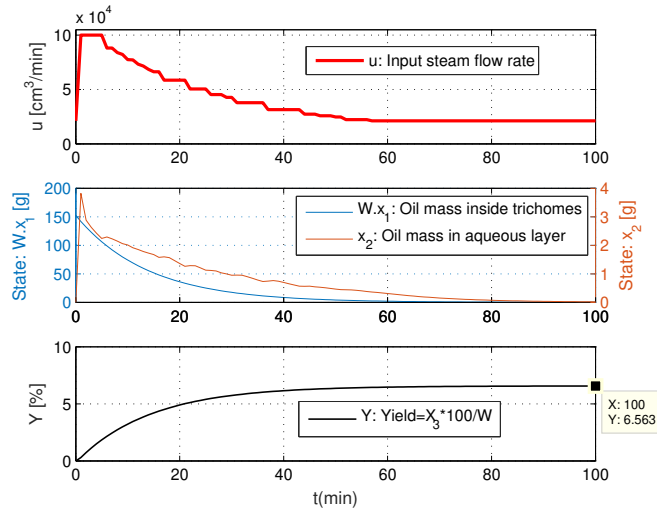
Figure 6.5: Results in case III

(a) Effect of gamma on u trajectories

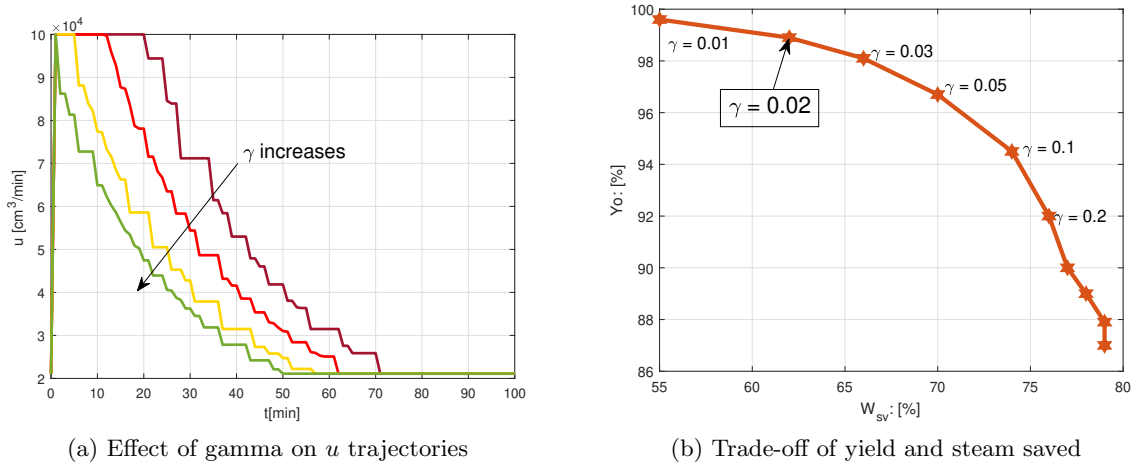(b) Trade-off of yield and steam saved

Figure 6.6: Effect of gamma and Pareto front

1. When maximizing yield only (case I), it is not necessary to apply maximum steam flow while there is not oil in the aqueous layer (i.e $x_2 = 0$).

2. In order to save energy, it is desirable to maintain mass in the aqueous layer x_2 as small as possible, this fact is confirmed if the results of cases I and III are compared with case II; note that the maximum x_2 value in the case II is near to $20[g]$ when $t \approx 7[min]$, that means, at such time there is an important amount of oil stored in the aqueous layer. Meanwhile in case I and III, the maximum x_2 value is nearly $3[g]$.

6.2.3.4 Sensitivity analysis

According to Cerpa et al. (2008), parameters K_{tr} and h do not depend on operating conditions, but vary with the aromatic plant. However, in industrial applications, it is desirable to obtain operating conditions that perform well for several aromatic plants, i.e the optimal input should not change significantly if parameters K_{tr} and h are modified. Likewise, energy savings should be maintained and yield not reduced.

Table 6.2: Results for different γ values

γ	Steam volume cm^3	Steam saved (W_{sv})	Yield %	Yo
0.01	4.45M	55%	6.61	99.6%
0.02	3.75M	62%	6.56	98.9%
0.03	3.36M	66%	6.50	98.1%
0.05	2.97M	70%	6.41	96.7%
0.1	2.60M	74%	6.26	94.5%
0.2	2.35M	76%	6.10	92.0%
0.3	2.26M	77%	6.01	90.0%
0.5	2.18M	78%	5.90	89.0%
0.7	2.14M	79%	5.83	87.9%
0.9	2.12M	79%	5.78	87.0%

Table 6.3: Results for different weighting factors

Experiment	Steam volume $[cm^3]$	Yield of extraction [%]
Case I ($\gamma = 0$)	9.96 M	6.62
Case II ($\gamma = 100$)	2.11 M	5.74
Case III ($\gamma = 0.02$)	3.75 M	6.56

In order to evaluate the dependence of the optimal conditions on the aromatic plant parameters, a sensitivity analysis is performed, considering variations within $\pm 10\%$ of nominal values, maintaining $\gamma = 0.02$. Results are shown in Table 6.4. Yield is maintained at 99% of maximum extraction for all conditions, while energy savings are 59% in the worst case. Figure 6.7 reports the steam flow trajectories obtained when considering the parameters in Table 6.4. Note that solutions are concentrated around the nominal optimal condition. Product variations do not cause important losses in yield or increments in energy requirements. Table 6.4 also shows that when plants present higher K_{tr} and h parameters, greater energy savings can be achieved.
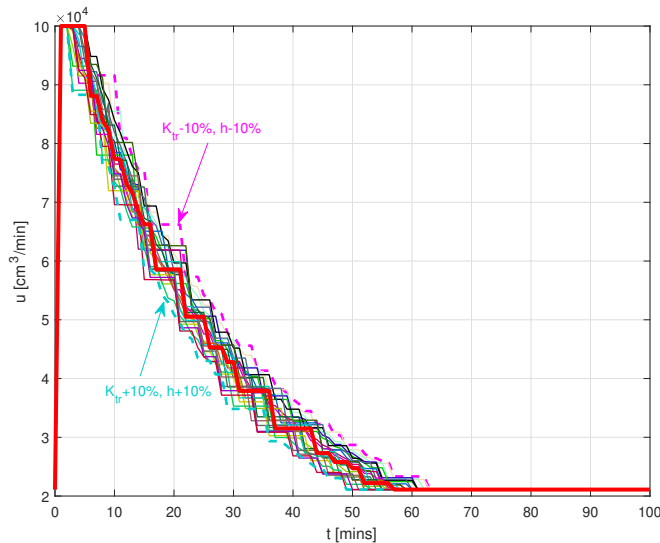

Figure 6.7: Effect on input trajectory produced by variations of K_{tr} and h parameters, red is the nominal case
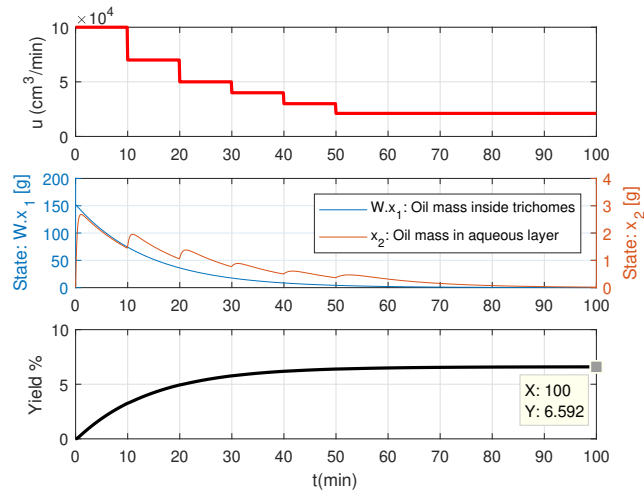
Figure 6.8: Optimal trajectory for non-automated plants

Table 6.4: Sensitivity analysis ($\gamma = 0.02$): Effect on saved energy

Saved energy [%]	$h - 10\%$	$h - 5\%$	$\mathbf{h}$	$h + 5\%$	$h + 10\%$
$K_{tr} - 10\%$	59	60	61	61	62
$K_{tr} - 5\%$	60	61	62	62	63
K_{tr}	61	62	62	63	63
$K_{tr} + 5\%$	62	63	63	64	64
$K_{tr} + 10\%$	63	63	64	64	65

6.2.3.5   Applicability discussion

The optimal trajectories obtained as solution to problem (10) imply changes in steam flow at each sample time. In this case, every minute. Such changes are not a problem in automated plants. However, in manual or semi-automatic plants, operators should adjust the manipulated variable constantly, making this approach difficult to run in practice.

A possible alternative to this drawback is proposed now. In order to reduce the number of flow adjustments, the optimal trajectory is sampled at a lower rate that the control problem solution and the flow level is averaged for any given interval. Figure 6.8 shows the resulting extraction when the number of changes is reduced to 10 moves during the batch. It can be seen that the yield increases 0.6% with respect to the optimal solution shown in Table 6.3, and the energy consumption increases 3%. Although it does not offer an optimal performance, energy saving is high and the reduced amount of flow changes makes this approach easier to implement in non-automated plants.

6.3   Ohmic-assisted hydrodistillation (OAHD)

6.3.1   Process description

As mentioned above, there exist multiple essential oil extraction techniques. The OAHD method is part of the modern techniques of essential oil extraction. According to Seidi Damyeh et al. (2016) its main advantage over conventional distillation is that, for the OAHD method, shorter extraction times and lower energy consumption are obtained, thereby, it is environmentally friendly. In OAHD the short extraction

time is due to the rapid increase in temperature as a result of internal heating and electroporation[1], produced by electrical current passing through the material (Damyeh and Niakousari, 2016).

The ohmic heating (OH) technology is employed in OAHD method. OH is defined as a process wherein electric current is passed through materials with the primary purpose of heating them (Knirsch et al., 2010). In OH there is no need to transfer heat through solid-liquid interfaces or inside solid particles once the energy is dissipated directly into the material to heat. A large number of existing and potential applications have been proposed for OH, including blanching, evaporation, dehydration, fermentation, extraction, sterilization, pasteurization and heating of foods to serving temperature, including military or long-duration space missions (Knirsch et al., 2010). OAHD is one way of using ohmic heating in an extraction process where the material is a water-vegetal mixture.

The extraction process in OAHD is similar to the steam distillation process described in Subsection 6.2.1, but the heating method is different. Figure 6.9 shows the main parts of the OAHD plant constructed for this research project. In this equipment, a mixture of water-salt-plants is heated in an ohmic-heater camera by electric current. Salt is required since in general, the conductivity of a plant is not enough to allow electrons to flow. Essentially, the camera is a vessel equipped with two electrodes. The mixture temperature is increased in order to bring it to the boil point (during this stage the voltage can also produce electroporation (Seidi Damyeh et al., 2016; Gavahian et al., 2019)). At this point, steam is produced, this steam drags the oil molecules that are released from the plant. That mixture rises through the camera and reaches the condenser, this device allows the mixture to cool and change to liquid phase. Finally, the liquid mixture reaches the Clevenger apparatus, in which oil and water are separated. The Clevenger allows refilling the OH camera with water, in order to maintain the water level into the camera.
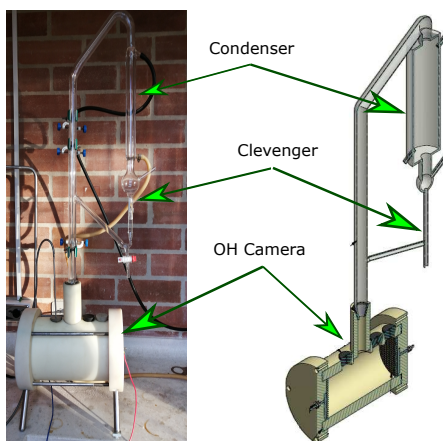

Figure 6.9: Left: Ohmic heating system constructed. Right: Ohmic heating designed

6.3.2 Ohmic heating distiller design

As a starting point to design an ohmic distiller, we can select the aromatic herb and the mass to be processed. In literature, the maximum capacity reported is 20 [g] of vegetal mass (Hashemi et al., 2017) in the case of the extraction of essential oil from oregano. In this work, we opt to work with essential oil from Eucalyptus since the high yield facilitates the measure of its extraction kinetic. For the Eucalyptus, the yields obtained and reported in the literature are between 0.8% and 5%. Considering the minimum yield and 100 [g] of Eucalyptus, then 0.8 [mL] of essential oil can be expected. Such volume is measurable

---

[1] A non-thermal effect, which may facilitate the extraction of essential oil via the breakdown of cell membranes through the electric energy which cause the cell walls and membranes become permeable

without additional process, that is why we have set out to construct a distiller for 100 [g] of vegetal mass. In Gavahian et al. (2012) the plants-water recommended ratio is (10% [w/v]) therefore, 1 [L] of water is required. Finally, assuming that an AC power supply of 120 V [rms] at 60 [Hz] is available, and taking into account that 8 [A] is the maximum current reported (Gavahian et al., 2012, 2018), we have selected an extraction maximum power of 1 [kW], avoiding an oversized condenser.

The previous discussion indicates that the design of a distiller for OAHD is mainly composed of two parts: (i) camera,(ii) condenser. As above mentioned we have set out to design a camera with the capacity for 100 [g] of vegetal mass. Once the camera measures are defined, the condenser is designed taking into account the maximum extraction power, which in this case is assumed of 1 [kW]. We also assume that an AC power supply of 120 [Vrms] at 60 [Hz] is available.

6.3.2.1 Camera design

All cameras reported in the literature are designed with a cylindrical shape in order to achieve uniformly heated material (i.e. avoiding cool points). Assuming such shape in our design, the direction of the electric field remains as a design parameter, since it can be axial or radial. As a part of this Ph.D. thesis in (Valderrama, 2018) we have showed that the radial direction is not proper for commercial AC power supplies (i.e. 120-240 [Vrms]), because such an option leads to camera dimensions where it would not be possible connecting sensors and to charge the mixture. Now, assuming a cylindrical camera with axial electric field, as depicted in Fig. 6.10, the parameters to design are: L the gap between the electrodes and A is the surface area of each electrode. Taking into account that the material put into an Ohmic heater behaves as an electrical resistance (R) (Sakr and Liu, 2014). The relation between such variables is:

$$R = \frac{L}{A\sigma} \tag{6.12}$$

where σ is the mixture conductivity. Considering that the plant conductivity is negligible, then the conductivity will be produced mainly by the mixture salt-water (distilled water). In Gavahian et al. (2012) it has been recommended salted water (1% NaCl, [w/v]). Now, considering that in ambient temperature the seawater conductivity is 5 [s/m] and its salt concentration is (3.5% NaCl, [w/v]) and, the conductivity of distilled water is negligible, therefore, the conductivity of our mixture can be estimated as 1 [s/m] approximately.

Given an AC power supply of $120[V]$ and $P_{max} = 1[kW]$, is true that $I_{max} = 8.3[A]$ therefore the next expression can be stated:

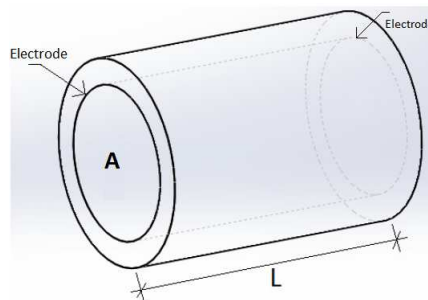$$P_{max} = I^2 R = 1000 = 8.3^2 \frac{L}{A * 4} \tag{6.13}$$

Figure 6.10: Ohmic heating camera with axial electric field

Where $\sigma = 4$ is assumed because the conductivity increases with temperature. Recalling that the capacity assumed is $100[g]$, and taking into account the plants-water recommended (10% [w/v]), then the water volume is $1[L]$ (i.e. The minimum camera volume is $1[L]$),consequently, given the cylindrical shape the next expression for the camera volume must be fulfilled.

$$V_{min} = 1 = L * A \tag{6.14}$$

Equations (6.13) and (6.14) lead to $L = 24[cm]$ and the area of the electrode $A = 41[cm^2]$. Finally, in order to avoid steam contact with the electrodes, we opt for a cylindrical camera and semi-circular electrodes, as can be seen in Fig. 6.11.

The selection of the cover material of the camera also is an important design decision, because such material must be electrical insulate, moreover, a low thermal conductivity is desirable in order to maintain the temperature into the camera. The Teflon is considered ideal for this application, because it has low thermal conductivity ($\approx 0.2[W/m.K]$) and a high electrical resistivity ($> 10^{18} ohm - cm$). In this work, we propose to use Nylon 66, which has high electrical resistivity($> 10^{10} ohm - cm$) and its thermal conductivity is ($\approx 0.25[W/m.K]$) while allowing a price reduction of 70% with respect to Teflon. The camera contains a steam outlet and three holes for sensors and material feeding, moreover, in order to avoid the contact of vegetal mass with the electrodes two nylon grooved discs were set up.
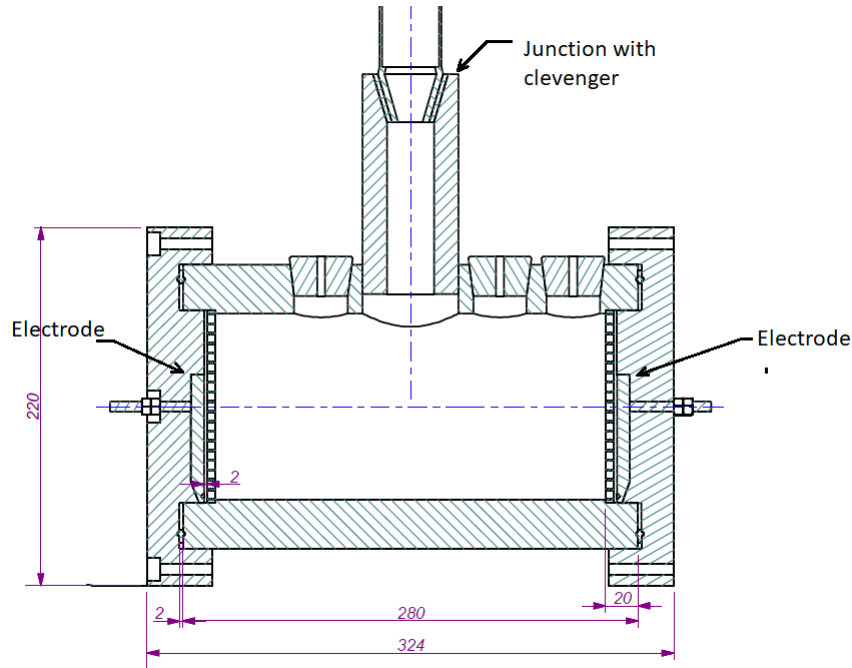

Figure 6.11: Ohmic heating camera- Measures in [mm]

6.3.2.2 Condenser designing

Once the camera has been designed for an extraction power of 1 [kW], we are in a position to design the condenser, which must be able to allow the mixture (i.e. water steam and essential oil steam) cooling and change to the liquid phase. We opt for a conventional vertical cylindrical glass condenser. The heat needed in the condenser is given by,

$$\dot{Q} = -\lambda.F \tag{6.15}$$

where $\dot{Q}$ is heat flow in $[kJ/h]$, λ is the latent heat of steam in $[kJ/kg]$ and F is the steam flow rate in $[kg/h]$. According to (Howell, 1992), assuming that steam is composed of water only, for pressure of 1 [atm], it is known that $\lambda \approx 2275[kJ/kg]$ when temperature is $92.5[^0C]$ (i.e. saturated steam), and when the power is 1[kW] the steam flow rate expected is $F \approx 1.75[kg/h]$. Therefore, the heat needed in the condenser is $\dot{Q} = -3981[kJ/h]$. Now, according to Thompson (1987) for a condenser is true that,

$$\dot{Q} = U.A_c.\Delta T_{LM} \tag{6.16}$$

where U is the heat transfer coefficient in $[kJ/(m^2.h.^\circ C)]$, A_c is the condenser area in $[m^2]$ and ΔT_{LM} is the temperature difference in a logarithmic scale. The latter is employed since the temperature gradient varies with the position of the mixture in the condenser.

$$\Delta T_{LM} = \frac{\Delta T_1 - \Delta T_2}{ln\left(\frac{\Delta T_1}{\Delta T_2}\right)} \tag{6.17}$$

where $\Delta T_1 = T_1 - t_2$, and $\Delta T_2 = T_2 - t_1$. T_1 is input steam temperature, t_2 input cold water temperature. T_2 is output steam temperature, t_2 output warm water temperature. According to the conditions of the laboratory the next values are assumed: $T_1 = 93^\circ C$, $t_2 = 17^\circ C$, $T_2 = 70^\circ C$, and $t_1 = 50^\circ C$. Therefore $\Delta T_{LM} = 42^\circ C$.

Now, for steam water the heat transfer coefficient can be assumed as $U = 7650[kJ/(m^2.h.^\circ C)]$ (Howell, 1992). Given all parameters, Equation 6.16 allows to estimate the condenser area, as

$$A_c = \frac{\dot{Q}}{U.\Delta T_{LM}} = 0.012[m^2] \tag{6.18}$$

Finally, considering a conventional vertical cylindrical glass condenser, its area is given by,

$$A_c = 2\pi r h \tag{6.19}$$

where r is radius and h is height. Assuming $r = 1.28[cm]$, applying Equation 6.19 $h = 15[cm]$ is obtained. To assure total steam to liquid change $h = 25[cm]$ is selected, avoiding essential oil steam leakage. As mentioned above, in the lab-scale, a distiller for OAHD must be equipped with a Clevenger apparatus that is required to separate oil and water. The designed pair condenser-Clevenger is depicted in Figure 6.12.

6.4 Experimental tests for input power trajectories in OAHD process

In the section 6.2, an optimal control problem has been formulated in order to save energy during the extraction process while maintaining the yield of extraction for the steam distillation case. The availability of the kinetic model in Cerpa et al. (2008) allowed solve of the optimal control problem, unfortunately, in literature, as far as the author knows, no kinetic model for OAHD have been proposed, useful to optimize the operation, however, notice that the steam is the common oil transport medium for OAHD and steam distillation. Moreover, in both processes, it has been observed that the rate of essential oil accumulation decreases as the time passes, in spite of that, in all literature consulted, the steam flow rate for steam distillation is maintained constant during the period of extraction (see e.g. Gawde et al. (2014); Cerpa et al. (2008); Cassel et al. (2009)), the same happens in OAHD, the extraction power is maintained constant during the period of extraction (see e.g. in Roohi and Hashemi (2019); Gavahian et al. (2015, 2018)).
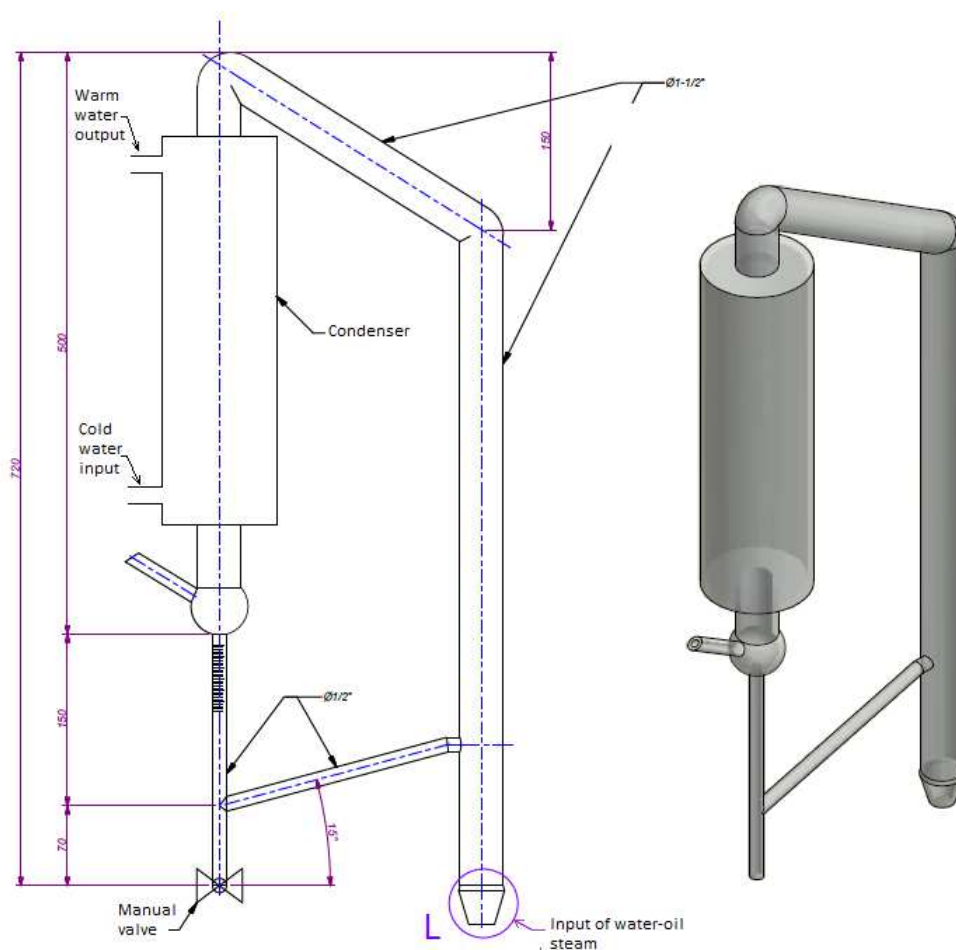
Figure 6.12: Condenser-clevenger designed. Linear measures in [mm]

Therefore one can formulate the hypothesis that the reduction of the rate of extraction is due to the less essential oil availability to drag.

The above analysis allows formulating the next hypothesis. *In order to save energy during the extraction process while maintaining the yield of extraction in an OAHD process, the input power trajectory is not necessarily constant, moreover, it can be reduced during the extraction period.*

From now on in this chapter, all of our efforts are aimed to work on such a hypothesis.

6.4.1 Materials and methods

6.4.1.1 Vegetal mass

As above mentioned, there exist several aromatic plants susceptible to extract their EO, however, the yields reported in the literature are generally low. For the Eucalyptus, the yields obtained and reported in literature are between 0.8% and 5%. The eucalyptus globulus leaves were collected at Duitama, Boyacá. It is worth noting that the leaves were taken from the same plant and processed in a fresh condition.

6.4.1.2 The mixture

For each extraction batch, $100[g]$ of fresh leaves are processed. The plants:water ratio used for the extraction process was 1:10 as proposed in the Ohmic-heating distiller design section (i.e. 10% [w/v]); thereby 1 [L] of water was required for each batch. The employed salt-water ratio was 1% NaCl [w/v], so 10 [g] of NaCl were added for each batch.

6.4.1.3 Experimental setup

The distiller for OAHD designed and constructed as was described in the previous section is employed to perform the extraction experiments. Its main characteristics are (i) Volumetric capacity 1 [L] for the mixture plants:water, and 1 [L] for produced steam. (ii) Maximum working power 1 [kW] to guarantee the efficiency of the condenser. To vary the extraction power a digitally controlled dimmer regulated by LabView is employed. Such a dimmer module also includes a wattmeter. An electrically isolated thermocouple is employed to register the temperature of the mixture (TC2198JG120A120 fabricated by MINCO). Its signal is acquired by the NI9210 acquisition module constructed by National Instruments. Notice that, during the extraction process the mixture is electrically charged, then any conventional thermocouple could not work properly. Figure 6.13 illustrates the experimental setup.
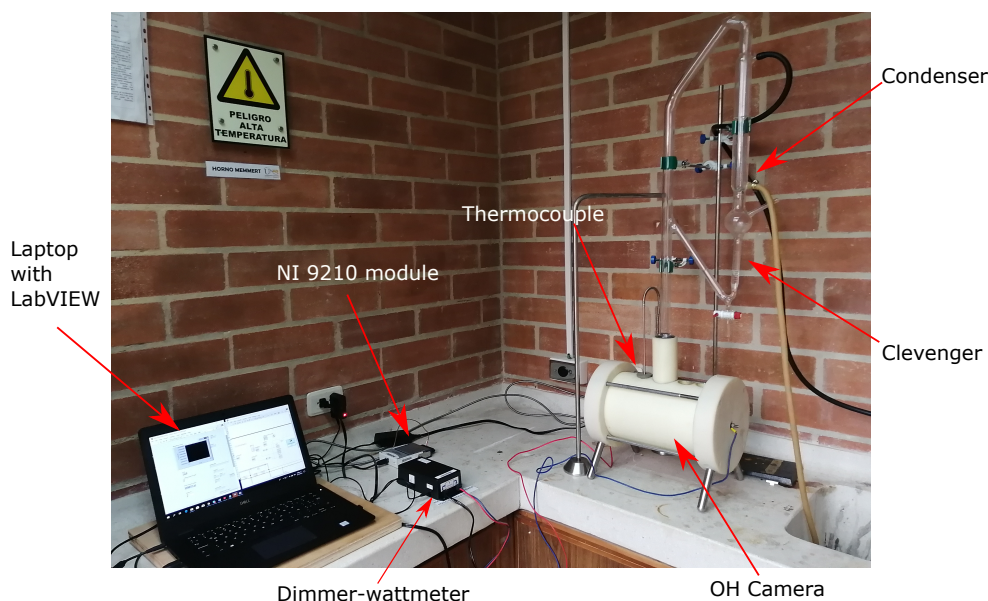

Figure 6.13: Experimental setup

6.4.1.4 Experiment description

Each batch extraction experiment can be divided into two time periods, the first one is the time required by the mixture plants-water to reach the boiling point (t_b)(i.e. *heating period*), and the last one is the *extraction period* (t_e), that is, the time measured from t_b and required to extract as much essential oil as possible. Preliminary tests led to select $t_e = 37[min]$, because after such time no measurable essential oil was extracted. The aim is to evaluate the hypothesis about the extraction period. To do that, two input power trajectories are tested, the first one maintains a constant power during all the extraction period, and the second one is a decreasing input power trajectory inspired by the results in the previous chapter. An open-loop control structure is employed to vary the input power. The dimmer employs a PWM signal as the manipulated variable, and the duty cycle (d) is sent from LabVIEW.

6.4.2 Experiments performed

6.4.2.1 Scenario I: Constant input power trajectory

Five batch extraction experiments with constant input power were performed. The dimmer is connected to a power source of 120 [VRMS] and the duty cycle employed to this experiments is 100%. As an example, an input power trajectory and the variation of the temperature profile are depicted in Figure 6.14. As expected, during the heating time period the input power is not constant, due to the electrical resistance associated with the temperature, however, after the boiling point is reached (i.e. extraction time period), the input power remains almost constant and near to $700[W]$.
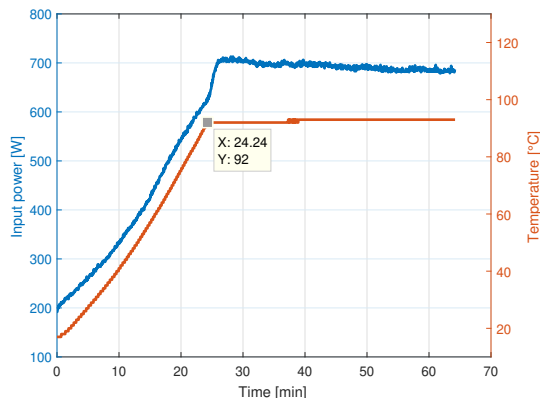

Figure 6.14: Example for constant input power trajectory

The kinetic of extraction resulting in the five experiments is depicted in Figure 6.16. An example of the essential oil accumulated in the Clevenger is shown in Figure 6.15.

Figure 6.15: Essential oil accumulated in the Clevenger

6.4.2.2 Scenario II: Decreasing input power trajectory

As mentioned, in this part of the book, the similarities between steam distillation and OAHD will be exploited in order to propose an input power trajectory for OAHD, such that it allows saving energy maintaining the yield of extraction. As the first step to pose an input power trajectory, the maximum and minimum input power values are proposed. The maximum input power level is limited for the actuator, in this case, it corresponds to the maximum duty cycle (100%) which produces $\approx 700[W]$. The
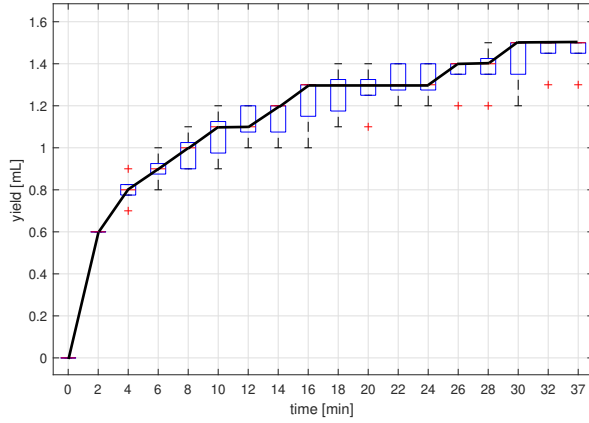
Figure 6.16: Yield obtained in five experiments with constant input power trajectory. The mean values are represented with black continuous line

minimum input power level is detected by means of preliminary tests to maintain the boiling point in the camera, $250[W]$ input power achieves such a goal.

Results from subsection 6.2.3.3 shown that several input flow trajectories $(u(t))$ allow saving energy, and the energy-saving depends on the γ parameter value. We propose employing the input flow trajectory resulting from $\gamma = 0.02$ (see Figure. 6.17a) to find an analogous input power trajectory for OAHD. Notice that selecting $\gamma = 0.02$ it can be expected 62% of energy savings according to Table 6.2. Finally, considering four input power adjustments, the previous analysis and that the extraction time employed in steam distillation case is $t_e = 100[min]$ but for OAHD is $t_e = 37[min]$ (i.e. The same time employed in scenario I), the analogous input power trajectory for $\gamma = 0.02$ in OAHD case is depicted in Figure 6.17b.
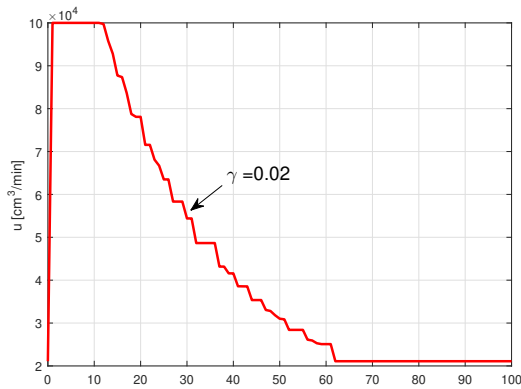
(a) Optimal input steam flow for $\gamma = 0.01$
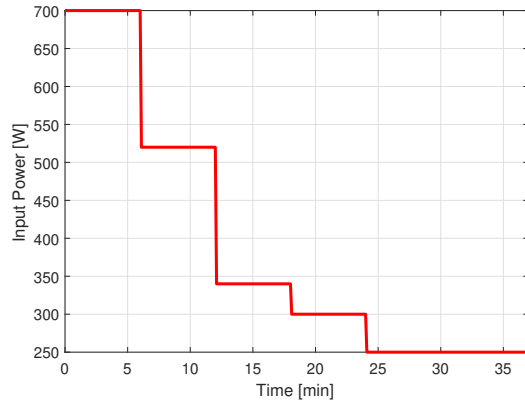
(b) Input decreasing power trajectory proposed employing 4 adjustments during extraction

Figure 6.17: Analogous trajectories for steam distillation (a) and OAHD (b)

Five batch extraction experiments with decreasing input power were performed. The dimmer is connected to a power source of 120 [VRMS] rms and the input power is manipulated in such way to obtain a decreasing input power as proposed. As an example, an input trajectory and the temperature profile resulting are reported in Figure 6.18. Notice that, in order to do a fair comparison, the extraction time

Table 6.5: Energy consumption in two different trajectories

	Energy consumption [Wh]				
Procedure	Exp 1	Exp 2	Exp 3	Exp 4	Exp 5
Constant input power	464.8	450.2	469.8	426.4	466.0
Decreasing input power	259.4	249.7	257.9	257.5	250.4

employed is the same as constant input power experiments. The kinetic of extraction resulting in the five experiments is depicted in Figure 6.19.
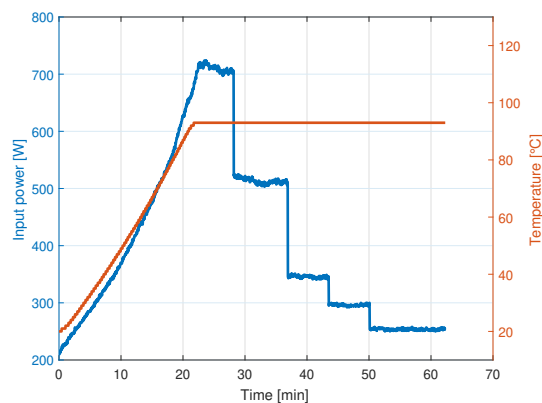

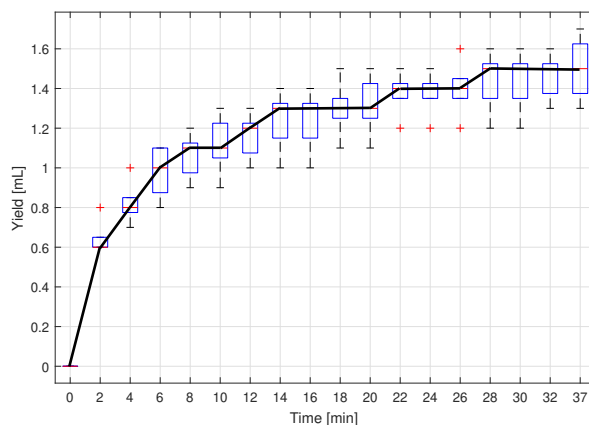Figure 6.18: Example for decreasing input power trajectory

Figure 6.19: Yield obtained in five experiments with decreasing input power trajectory. The mean values are represented with black continuous line

6.4.3 Analysis and comparison

As mentioned above, we are interested in saving energy during the extraction process while maintaining the yield of extraction in an OAHD process. Now, we compare the results with respect to saved energy. Energy consumption has been calculated during the extraction period ($t_e = 37[min]$) and the results for the two trajectories are reported in Table 6.5. Results indicate that employing a decreasing input power trajectory allows 44% of energy savings on average.

Table 6.6: Yield obtained in the experiments

Procedure	Total yield in experiment [mL]				
	Exp 1	Exp 2	Exp 3	Exp 4	Exp 5
Maximum constant power	1.5	1.3	1.5	1.5	1.5
Decreasing power	1.4	1.4	1.7	1.5	1.6

The T-student test allows to establish the differences between the means of the two samples. We use such a test to prove that the total yield obtained for both scenarios is the same.

Defining X_1 as yield obtained via maximum constant power, and X_2 as yield obtained via decreasing power, and considering that X_1 and X_2 comes from normal distributions, from data in Table 6.6, $\bar{x}_1 = 1.46$, $\bar{x}_2 = 1.52$, $s_1 = 0.09$, $s_2 = 0.13$, and $n1 = n2 = 5$. Assuming the variance is the same, in order to probe the null hypothesis (i.e. $\mu_1 - \mu_2 = 0$) for a level significance of $\alpha = 0.05$, the next values are calculated.

$$S_p^2 = \frac{(n_1 - 1)s_1^2 + (n_2 - 1)s_2^2}{n_1 + n_2 + 2} = 0.008$$

therefore,

$$T_0 = \frac{\bar{x}_2 - \bar{x}_1}{S_p\sqrt{\frac{1}{n_1} + \frac{1}{n_2}}} = 1.03$$

Now, since $g.d.l = 2 * n_1 - 2$ (degree of freedom) then in this case $g.d.l = 8$, according to the critical values of a T-student distribution $T = 2.306$, in conclusion $T_0 = 1.03 < T$ indicates that the null hypothesis cannot be rejected. Thereby, we conclude that the mean yield obtained via both procedures is statistically the same.

6.5 Controlling the heating curve

Several authors have indicated that in OAHD process there exists a nonthermal effect known as electroporation, which may facilitate the extraction of essential oil via the breakdown of cell membranes through the electric field which causes the cell walls and membranes to become permeable. However, in literature, such an effect has not been quantified. An estimation of the electroporation effect can be useful in order to obtain a dynamic model for the OAHD process. To quantify the electroporation impact isolated from of the temperature effect is required, therefore, a possible way to quantify such a effect can be by controlling the temperature of the mixture into the camera during the *heating time period*, employing different input AC voltages, for later evaluating the resulting kinetic of extraction. To avoid model identification step, in this section, two data-driven controller tuning strategies are evaluated experimentally using the Ohmic heating distiller previously described in this chapter. The first strategy is the Youla-Kucera parametrizing data-driven controllers tuning (YK-DDC), comprehensively explained in chapter 5, and the second strategy is Correlation-based tuning (CbT) proposed by Karimi et al. (2007). The latter is selected in order to do a fair comparison since both strategies employ the same input information.

6.5.1 Controller design tuning problem

A tracking problem is posed, where the aim is to follow a given temperature trajectory. The duty cycle (provided by the dimmer) is the manipulated variable (u), measured in percentage, and the output variable is the temperature, measured in ($^\circ C$). The reaction curve for $u = 100\%$ is shown in Figure 6.20.

The loop performance specifications are defined as a first-order reference model M, as shown in (6.20), its rise time (t_r) is selected considering the slope of the reaction curve in Figure 6.20, notice that employing
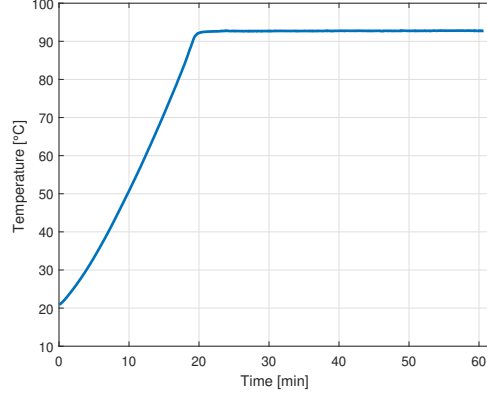
Figure 6.20: Reaction curve in OAHD for $u = 100\%$

100% of the duty cycle, to increase temperature $1°C$, 15 seconds are required. That is why $t_r = 20$ is chosen for the reference model. Step response of reference model is shown in Figure 6.21.
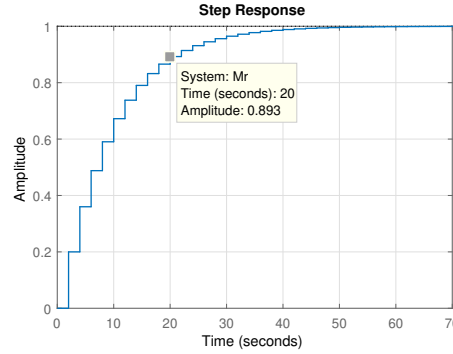
$$M = \frac{0.2z^{-1}}{1 - 0.8z^{-1}} \tag{6.20}$$

Figure 6.21: Reference model for temperature control in OAHD process

6.5.2 Tuning procedure

In this case, $T = 90°C$ is selected as operating point. Therefore, datasets $\mathcal{D}$ required for both strategies are obtained as follows: employing $Ts = 2[s]$, a PRBS signal with $N = 512$ samples is used as input u and temperature is measured, both signals are depicted in Figure 6.22. Notice that the temperature range is around the operating point previously selected.

The first step in the tuning procedure is to define the number of basis to be employed. For CbT $m = 6$ basis is selected, while for YK-DDC $m_q = 5$, the latter is selected taking into account the impulse response length of the reference model M. Employing the dataset from figure 6.22 both methods are applied. The resulting controller for CbT method is reported in Equation (6.21), while the YK-DDC controller is shown in Equation (6.22).

$$K_{cbt} = \frac{130.9 - 154z^{-1} + 26.82z^{-2} - 8.87z^{-3} + 4z^{-4} + 3.17z^{-5}}{1 - z^{-1}} \tag{6.21}$$
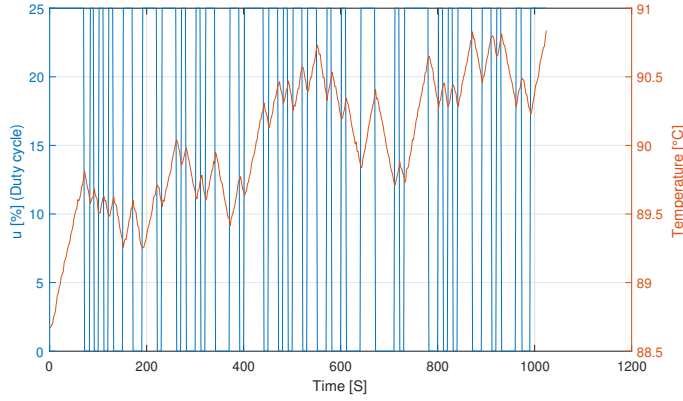
Figure 6.22: Dataset used for both strategies in temperature control for OAHD process

$$K_{yk} = \frac{219.6 - 372.5z^{-1} + 222.8z^{-2} - 63.85z^{-3} - 21z^{-4} + 22z^{-5}}{1 - z^{-1}} \qquad (6.22)$$

Each controller is tested with an experiment in closed-loop employing different temperature references. The results for CbT are depicted in Figure 6.23, and the results for YK-DDC are shown in Figure 6.24. In both figures, the duty cycle (u) is shown also.

Figure 6.23: Tracking results for CbT controller in OAHD process.Reference is the black line, the temperature is green dashed line and, duty cycle is the orange continuous line.

The closed-loop step-response achieved by the controllers are depicted in Figure 6.25. It must be highlighted that in the case of YK-DDC controller the rise time $t_r = 35[s]$ and in the case of the CbT controller $t_r > 100[s]$. The results indicate that the performance obtained via the YK-DDC method is better than the achieved with the CbT approach,even though the same controller structure is implemented.
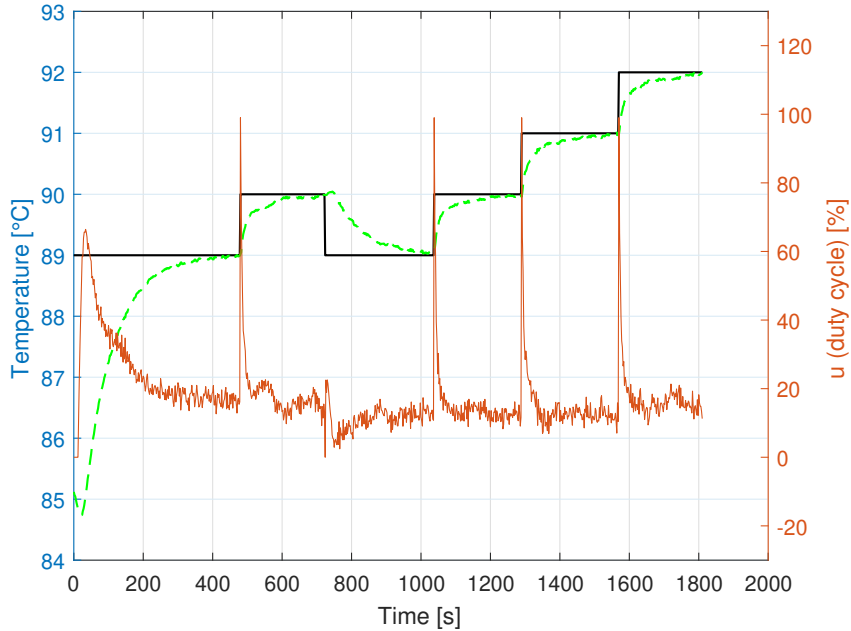
94
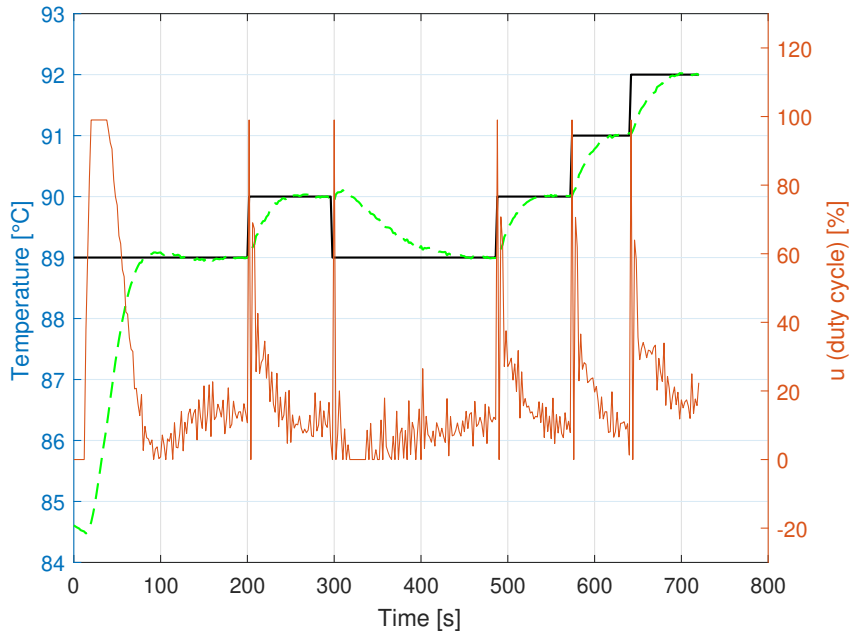
Figure 6.24: Tracking results for YK-DDC controller in OAHD process.Reference is the black line, the temperature is green dashed line and, duty cycle is the orange continuous line.
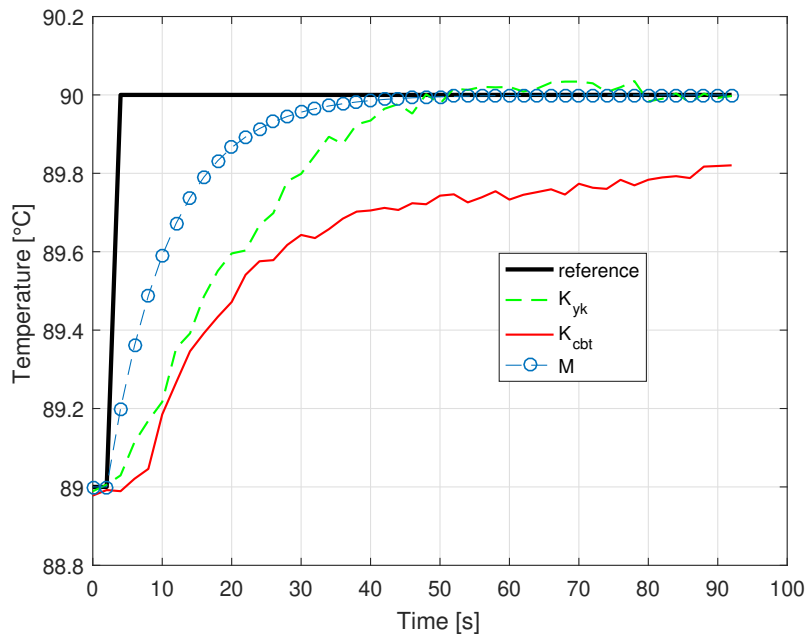
Figure 6.25: Tracking results for YK-DDC controller green dashed line. CbT controller red continuous line. Reference model (M) in blue line. Reference is black line

6.6   Conclusions

In this chapter, optimal operating conditions for the extraction of essential oils by steam distillation has been proposed. Starting from an existing kinetic model of the process, an optimal control problem has been formulated in order to save energy during the extraction process while maintaining the yield of ex-

traction. A linear relationship between mass transfer coefficient (K_g) and steam flow rate (u) has been obtained from experimental data previously reported in literature. Based on that relation, a non-linear state space model has been derived and employed in the solution of the optimal control problem. Numerical solutions to the problem were obtained using the software APMonitor. The results give insight into the efficient operation of essential oils extraction for the industry. The solutions show that optimal steam flow trajectories are not necessarily constant, as previously mentioned in the literature. The trade-off between yield and energy savings is an important finding of the proposed framework. A Pareto front guides the selection of the best-operating conditions. In an industrial environment, this selection would require better costs analysis, specifically the costs implied in steam production and the value of essential oil. Results of the sensitivity analysis indicate that the optimal conditions do not suffer strong changes with parameters of the vegetable material. For 10% variations in critical parameters, yields above 99% of the maximum are obtained, while energy savings are between 59% and 65%.

A lab-scale ohmic distiller able to extract EO from $100[g]$ of vegetal mass (aromatic herb), employing $1[L]$ of salted water, and a maximum input power of $1[kW]$, has been designed and constructed. The selected characteristics of the distiller allowed to obtain measurable essential oil quantity from Eucalyptus, in order to obtain kinetic extraction curves.

Given some phenomenological similarities between steam distillation and OAHD, the optimal input trajectories found to the former were extended to OAHD during the *extraction time period*. In order to save energy, the experimental results for OAHD indicate that the optimal input power is not necessarily constant. Numerical results indicate that employing a decreasing input power trajectory allows 44% of energy savings on average, maintaining the yield statistically equal to the yield with a constant input power.

The DDC method proposed in Chapter 5 is employed to control the temperature in the camera of the ohmic distiller. In order to evaluate the performance of our method, the CbT method is used. Both approaches allowed tuning controllers with the same structure; however, in light of results, our controller offers better tracking results than CbT controller, specifically, the rise time is three times lesser, maintaining null overshot and null steady-state error. Future experimental work to quantify the electroporation effect in OAHD by employing the controllers designed is required.

Chapter 7

Conclusions

In this dissertation are proposed new methods for the design of controllers from data for linear systems, useful when the plant model is unavailable, two frameworks have been considered using set-membership techniques (SMT) and the Youla-Kucera parametrization (YK-DDC). The developed methods have been extensively evaluated in simulation and experimental settings.

In the SMT approach proposed, the UBB noise hypothesis leads to a novel overbound formulation, which derives linear constraints resulting in a convex problem. In the set-membership framework, only one oriented work to controller design from data is known by the author, where polynomial optimization constraints are stated, which result in a non-convex problem. Two SMT extensions have been proposed, the first one allows to design limited-complexity controllers using sparse identification methods, to meet this aim, this is the first attempt in the literature that employs Set-Membership techniques. The proposed algorithm avoids solving big combinatorial problems that arise when the dimension of the vector parametrizing the candidate controllers is large and the number of desired parameters is much lower, moreover, when comparing with literature, our method has just one parameter to be adjusting and it has a direct interpretation as modeling error bound, simplifying the tuning procedure. The second extension proposes a procedure to estimate controllers capable of approaching a given closed-loop reference model and a sensitivity transfer function. To do this, an efficient solution based on convex optimization is proposed, in literature, this the first attempt at employs set-membership to meet this aim. On the other hand, Youla-Kucera parametrization is employed to solve the problem of controllers design without requiring a process model. The proposed controller structure allows reaching more stringent reference models than those proposed previously in the literature, maintaining a convex formulation and a procedure to estimate the closed-loop stability. In addition, the YK-DDC approach has been extended to the MIMO case and it has been experimentally evaluated.

The proposed SMT approach has been experimentally validated on an active suspension system via a Monte-Carlo experiment using one hundred controllers estimated with the SMT algorithm, and it has been compared with VRFT methodology. Results have shown that using the same information about the plant to be controlled, the VRFT controllers are strongly affected by the size of the dataset while the SMT controllers exhibit good performances, even when they are estimated from reduced datasets. The proposed YK-DDC extension to the MIMO case has been experimentally validated on a 2-DoF Helicopter. This is an important model from the control engineering point of view due to its wide non-linear characteristics, highly cross-coupling effects, and instability in open-loop. Experimental results showed that our approach achieves better results compared with the LQR+I controller proposed by the system manufacturer since the former meets the control requirement with lower settling time and smaller maximum overshoot. However, given that the 2DOF helicopter is unstable an initial stabilizing controller is required to collect the dataset and to construct a cascade control strategy.

Regarding essential oil extraction processes, a lab-scale ohmic distiller able to extract EO from $100[g]$ of vegetal mass (aromatic herb), employing $1[L]$ of salted water, and a maximum input power of $1[kW]$, has been designed and constructed by the author. The selected characteristics of the distiller allowed to obtain measurable essential oil quantity from Eucalyptus, in order to obtain the kinetic extraction curves. In steam distillation, an optimal control problem has been formulated and solved in order to save energy during the extraction process while maintaining the yield of extraction. The results give insight into the efficient operation of essential oil extraction for the industry. Our solutions show that optimal steam flow trajectories are not necessarily constant, as previously mentioned in the literature. Given some phenomenological similarities between steam distillation and Ohmic assisted hydrodistillation (OAHD), the optimal input trajectories found to the former were extended to OAHD during the *extraction time period*. Experimental results indicate that our input trajectories allow 44% of energy savings on average, maintaining the yield statistically equal to the yield with a constant input. In addition, the proposed YK-DDC approach is applied for the regulation of temperature in an ohmic-heater, where experimental results show that our controller offers better tracking results than a procedure extracted from recent literature.

As future work, in both proposed data-driven techniques, further research is required to state a stability test that guarantees closed-loop stability. Current results lead to think that the key point is in the controller structure, which must be consistent with the plant structure, this would require certain assumptions about plant prior to the estimation of controller parameters. In the proposed YK-DDC approach for the MIMO case, further research is required to deal with noise. The constructed lab-scale ohmic distiller, its instrumentation and control equipment are constituted as a new experimentation platform. Employing a proper set of experiments, our platform could be used to state an OAHD model in order to quantify the electroporation impact, this would permit to design optimal input trajectories that include the *heating time period* in order to save energy and/or to get better extraction yields. Finally, it is highlighted that our platform allows extracting essential oil from any aromatic herb, therefore, several future works can be carried out to investigate the kinetic curves for different vegetal mass.

Appendix A

Annexes

A.1 Annex I: VRFT

VRFT is a well-known method for tuning controllers avoiding to build a model of the plant. Such method is deeply explained in Lecchini et al. (2002b), notwithstanding, for the sake of completeness in this section the main features of the method are explained. In this framework, as in the Set Membership case, the aim is to modify Problem (2.1) avoiding the requirement of the knowledge of the plant model.

The solution is to build a virtual reference signal $r_v(t)$ from the reference model and the available output measurements in $\mathcal{D}$, i.e.,

$$r_v(t) = M^{-1}(q^{-1})y(t),$$

From this signal, the virtual error can be obtained as

$$e_v(t) = r_v(t) - y(t).$$

Fig. A.1 shows the resulting scheme. Note that $e_v(t)$ and $u(t)$ are the input and output of the controller to be identified. The model based cost function in (3.2), for the case of a $\mathcal{H}_2$ norm, is replaced by the signal based cost function

$$J_l(\theta) = \frac{1}{N} \sum_{t=1}^{N} \left(u_l(t) - C(\theta, q^{-1})e_l(t) \right)^2, \tag{A.1}$$

following a PEM (Prediction Error identification Method) approach, see e.g., Ljung (1999). The subscript l indicates that signals $e_v(t)$ and $u(t)$ are filtered by the system

$$L(q^{-1}) = (1 - M(q^{-1}))M(q^{-1}) \tag{A.2}$$

i.e., $e_l(t) = L(q^{-1})e_v(t)$ and $u_l(t) = L(q^{-1})u(t)$. It is shown in Lecchini et al. (2002b) that this filter guarantees an asymptotic convergence of the argument that minimizes (A.1) to the minimizer of (2.1).

When measurement noise $v(t)$ is considered, the minimizer of (A.1) becomes a biased estimate. In order to get unbiased results, it is necessary to perform a second experiment using the same input (repeated experiment) or to obtain a model of the plant (system identification). These approaches are not evaluated in the case study because they require more information than the Set Membership approach.

The following algorithm summarizes the VRFT method.
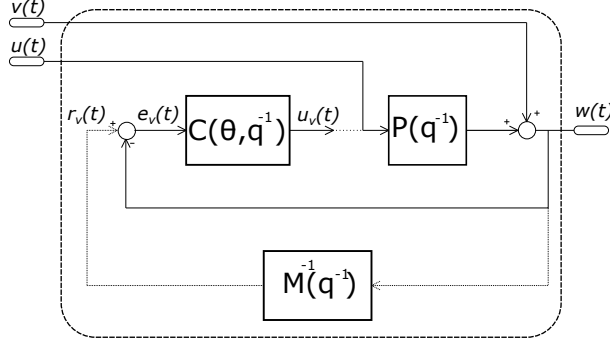
Algorithm 3. VRFT Algorithm

Figure A.1: VRFT tuning problem block diagram

1. *Collect a dataset $\mathcal{D}$ performing an experiment starting with plant at rest. A low noise condition should be guaranteed in order to avoid biased results.*

2. *Select a proper reference model $M(q^{-1})$ and basis functions $\beta_i(q^{-1})$.*

3. *Obtain the virtual reference and error signals*

$$r_v(t) = M^{-1}y(t)$$

and

$$e_v(t) = y(t) - r_v(t).$$

4. *Filter the virtual error $e_v(t)$ and plant input $u(t)$ as*

$$e_l(t) = L(q^{-1})e(t), u_l = L(q^{-1})u(t)$$

with the system in (A.2).

5. *Solve the least-squares problem*

$$\theta^{VR} = \arg \min_{\theta \in \Re^m} \frac{1}{N} \sum_{t=1}^{N} \left(u_l(t) - \sum_{i=1}^{m} \theta_i \beta_i(q^{-1})e_l(t) \right)^2. \tag{A.3}$$

6. *Select as controller the system*

$$C^{VR}(\theta^{VR}, q^{-1}) = \sum_{i=1}^{m} \theta_i^{VR} \beta_i(q^{-1})$$

A.2   Annex II: sparse-CbT algorithm

In this section, some aspects of sparse-CbT are briefly explained. As the first step to solve the Problem 2, the cost function in Eq. (3.2) that depends on the process model is transformed to the model-free equation:

$$e(\theta, t) = Mu(t) - C(\theta)(1 - M)y(t). \tag{A.4}$$

When data are collected in a noisy environment, the method resorts to the correlation approach to identify the controller. Specifically, an extended instrumental variable $\xi(t)$ correlated with $u(t)$ and uncorrelated with $v(t)$ is introduced to decorrelate the error signal $e(\theta, t)$ and $u(t)$. $\xi(t)$ is defined as

$$\xi(t) = \{u(t+l), ..., u(t), ..., u(t-l)\}$$

where l is an integer sufficiently large. The correlation function is

$$f_{N,l}(\theta) = \frac{1}{N} \sum_{t=1}^{N} \xi(t) e(\theta, t)$$

and the correlation criterion function is

$$J_{N,l}(\theta) = f_{N,l}^T(\theta) f_{N,l}(\theta) \tag{A.5}$$

As a second step to solve Problem 2, it is proposed using ℓ_1 *regularization* to deal with the sparsity problem. In order to force to zero some elements of the parameter vector θ, a regularization term is added to the cost function:

$$\tilde{J}_{N,l}(\theta) = J_{N,l}(\theta) + \lambda \left\| \theta \right\|_0, \ \lambda \in \mathbb{R}^+ \tag{A.6}$$

Finally, the ℓ_1 norm is used instead of ℓ_0 quasi-norm to obtain a convex relaxation of (A.6), leading to the algorithm shown below:

Algorithm 4. *Sparse Correlation Based Tuning (SCbT)*

1. *Set m_{max}, $\epsilon > 0$ and the maximum number of iterations allowed j_{max}.*

2. *Set the iteration counter $j = 0$ and the weighting diagonal matrix $W(0)$ equal to the identity matrix.*

3. *Solve the mixed $\ell_1 - \ell_2$ weighted minimization problem*

$$\hat{\theta}^{(j)} = \arg \min_{\theta} \left[J_{N,l}(\theta) + \lambda \left\| W^{(j)} \theta \right\|_1 \right] \tag{A.7}$$

4. *Update the diagonal elements w_i of the weighting matrix W as*

$$w_i^{(j+1)} = \frac{1}{\left| \theta_i^{(j)} \right| + \epsilon}, i = 1, ..., m_{max};$$

5. *Terminate the iterations on convergence or when $j = j_{max}$. Otherwise, go to step 3.*

A.3   Annex III: Errors in Variables to 2DoF controller tuning problem

In this Annex, the approach in Cerone et al. (2017) is used to cast the 2DoF controller tuning problem into an Errors-In-Variables identification problem.

From the model-free eq. (4.18), we define the Feasible Controller Set (FCS) for the sensitivity tuning problem as:

$$\mathfrak{D}_{c_s} = \{ C_s(\theta) \in \mathbf{C} : C_s(\theta) S^2 \left[y(t) + v(t) \right] - S(1 - S) u(t) = 0$$
$$|v(t))| \leq \Delta v, \forall t = 1, ...N\} \tag{A.8}$$

Where the noise sequence $v(t)$ affects the system input. In this work, the class $\mathbf{C}$ includes all the linear time-invariant (LTI) controllers of order at most $max(na, nb)$, i.e.,

$$(C_s(\theta) \in \mathbf{C}) \Leftrightarrow C_s(\theta) = \frac{b_0 + b_1 q^{-1} + ... b_{n_b} q^{-n_b}}{1 + a_1 q^{-1} + ... a_{n_a} q^{-n_a}}, \theta = [a1, a2, ..., a_{n_a}, b_0, b_1, ..., b_{n_b}], \theta \in \mathbb{R}^{n_\theta} \tag{A.9}$$

In the same way, from eq. (4.28), it is possible to define the FCS for the model reference tuning problem as:

$$\begin{aligned} \mathfrak{D}_{c_f} = \{ & C_f(\rho) \in \mathbf{C} : Mu(t) - S\left[C_s(\theta) + C_f(\rho) \right](y(t) + v(t)) = 0 \\ & |v(t))| \leq \Delta v, \forall t = 1, ...N \} \end{aligned} \tag{A.10}$$

where the same class $\mathbf{C}$ in eq. (A.9) is considered.

Result. The Feasible controller sets (A.8) and (A.10) are defined by the following set of equalities

$$\begin{aligned} \mathfrak{D}_{c_s} = \{ & (\theta, v) \in \mathbb{R}^{N+n_\theta} : \\ & m(t) + \sum_{i=1}^{n_a} a_i m(t-i) = \sum_{i=o}^{n_b} b_j(y(t-j) - v(t-j)), \\ & |v(t)| \leqslant \Delta v, \forall t = n_a + 1, ...N \} \end{aligned} \tag{A.11}$$

$$\begin{aligned} \mathfrak{D}_{c_f} = \{ & (\rho, v) \in \mathbb{R}^{N+n_\rho} : \\ & f(t) + \sum_{i=1}^{n_a} a_i f(t-i) = \sum_{i=o}^{n_b} b_j(y(t-j) - v(t-j)), \\ & |v(t)| \leqslant \Delta v, \forall t = n_a + 1, ...N \} \end{aligned} \tag{A.12}$$

Where

$$m(t) = \frac{1 - S(q^{-1})}{S(q^{-1})} u(t), \ \ f(t) = \frac{M(q^{-1})}{S(q^{-1})} u(t) \tag{A.13}$$

Note that for a controller to belong to $\mathfrak{D}_{c_s}$ or $\mathfrak{D}_{c_f}$, it is necessary to find a noise sequence $v(t)$, satisfying Assumption 3, such that equality (A.12) and (A.11) are satisfied for all the available data samples.

The structure of the equations defining the FCS in (A.11) and (A.12) is similar to the identification problem reported in Cerone et al. (2012). It can be concluded that the data-driven controller (i.e for 2DoF) tuning problem is equivalent to a set-membership errors-in-variables identification problem, in the specific case where the output noise is identically zero, and only the input data are corrupted by noise. This result was remarked in Cerone et al. (2017) for a 1DoF problem.

Theorem 2 allows to obtain central estimates for the EiVA setting a $\theta^c = (\overline{\theta} + \underline{\theta})/2$ and $\rho^c = (\overline{\rho} + \underline{\rho})/2$, where,

$$\overline{\theta}_j = \max_{(\theta, v) \in \mathfrak{D}_{C_s}} \theta_j, \quad \underline{\theta}_j = \min_{(\theta, v) \in \mathfrak{D}_{C_s}} \theta_j, \tag{A.14}$$

$$\overline{\rho}_j = \max_{(\rho, v) \in \mathfrak{D}_{C_f}} \rho_j, \quad \underline{\rho}_j = \min_{(\rho, v) \in \mathfrak{D}_{C_f}} \rho_j, \tag{A.15}$$

Optimization problems in (A.14) and (A.15) are non-convex because there are nonlinear constraints in the equalities defining the sets $\mathfrak{D}_{C_s}$ and $\mathfrak{D}_{C_f}$. Moreover, they are semialgebraic problems where the

number of optimization variables is $N + n_\theta$ or $N + n_\rho$ respectively. It can be seen that the constraints include bilinear terms (products between noise samples and unknown parameters), so they are polynomial problems. Furthermore, such problems have a sparse structure when the objective function and each constraint defining the feasible region involve a small subset of variables Piga (2009).

Bibliography

Afram, A., Janabi-Sharifi, F., 2017. Supervisory model predictive controller (mpc) for residential hvac systems: Implementation and experimentation on archetype sustainable house in toronto. Energy and Buildings 154, 268 – 282. doi:https://doi.org/10.1016/j.enbuild.2017.08.060.

Anderson, B.D.O., Liu, Y., 1989. Controller reduction: concepts and approaches. IEEE Transactions on Automatic Control 34, 802–812. doi:10.1109/9.29422.

Arranz, E., Jaime, L., López de las Hazas, M.C., Reglero, G., Santoyo, S., 2015. Supercritical fluid extraction as an alternative process to obtain essential oils with anti-inflammatory properties from marjoram and sweet basil. Industrial Crops and Products 67, 121–129. doi:10.1016/j.indcrop.2015.01.012.

Asbahani, A.E., Miladi, K., Badri, W., Sala, M., Addi, E.H., Casabianca, H., Mousadik, A.E., Hartmann, D., Jilale, A., Renaud, F.N., Elaissari, A., 2015. Essential oils: From extraction to encapsulation. Int. J. Pharm. 483, 220–243. URL: http://dx.doi.org/10.1016/j.ijpharm.2014.12.069, doi:10.1016/j.ijpharm.2014.12.069.

Battistelli, G., Mari, D., Selvi, D., Tesi, P., 2018. Direct control design via controller unfalsification. International Journal of Robust and Nonlinear Control 28, 3694–3712. URL: https://onlinelibrary.wiley.com/doi/abs/10.1002/rnc.3778, doi:10.1002/rnc.3778, arXiv:https://onlinelibrary.wiley.com/doi/pdf/10.1002/rnc.3778.

Benyoussef, E.H., Hasni, S., Belabbes, R., Bessiere, J.M., 2002. Modelisation du transfert de matiere lors de l'extraction de l'huile essentielle des fruits de coriandre. Chemical Engineering Journal 85, 1 – 5. doi:https://doi.org/10.1016/S1385-8947(01)00134-6.

Burt, S., 2004. Essential oils: their antibacterial properties and potential applications in foods. A review. Int. J. Food Microbiol. 94, 223–253. doi:10.1016/j.ijfoodmicro.2004.03.022.

Calo, J.R., Crandall, P.G., O'Bryan, C.A., Ricke, S.C., 2015. Essential oils as antimicrobials in food systems - A review. Food Control 54, 111–119. URL: http://dx.doi.org/10.1016/j.foodcont.2014.12.040, doi:10.1016/j.foodcont.2014.12.040.

Campestrini, L., Eckhard, D., Chía, L.A., Boeira, E., 2016. Unbiased MIMO VRFT with application to process control. Journal of Process Control 39, 35–49. URL: http://dx.doi.org/10.1016/j.jprocont.2015.12.010, doi:10.1016/j.jprocont.2015.12.010.

Campi, M., Lecchini, a., Savaresi, S., 2002. Virtual reference feedback tuning: a direct method for the design of feedback controllers. Automatica 38, 1337–1346. doi:10.1016/S0005-1098(02)00032-8.

Cassel, E., Vargas, R., Martinez, N., Lorenzo, D., Dellacassa, E., 2009. Steam distillation modeling for essential oil extraction process. Industrial Crops and Products 29, 171 – 176. URL: http://www.sciencedirect.com/science/article/pii/S0926669008000861, doi:https://doi.org/10.1016/j.indcrop.2008.04.017.

Cerone, V., Piga, D., Regruto, D., 2012. Set-membership error-in-variables identification through convex relaxation techniques. IEEE Transactions on Automatic Control 57, 517–522. doi:10.1109/TAC.2011.2168073.

Cerone, V., Regruto, D., Abuabiah, M., 2017. Direct data-driven control design through set-membership errors-in-variables identification techniques, in: Proceedings of the American Control Conference, pp. 388–393. doi:10.23919/ACC.2017.7962984.

Cerpa, M.G., Mato, R.B., JosÃ© Cocero, M., 2008. Modeling steam distillation of essential oils: Application to lavandin super oil. AIChE Journal 54, 909–917. URL: http://dx.doi.org/10.1002/aic.11438, doi:10.1002/aic.11438.

Damyeh, M.S., Niakousari, M., 2016. Impact of ohmic-assisted hydrodistillation on kinetics data, physicochemical and biological properties of prangos ferulacea lindle. essential oil: Comparison with conventional hydrodistillation. Innovative Food Science & Emerging Technologies 33, 387 – 396. URL: http://www.sciencedirect.com/science/article/pii/S1466856415002659, doi:https://doi.org/10.1016/j.ifset.2015.12.009.

Donoho, D.L., Elad, M., Temlyakov, V.N., 2006. Stable recovery of sparse overcomplete representations in the presence of noise. IEEE Transactions on Information Theory 52, 6–18. doi:10.1109/TIT.2005.860430.

Doyle, J.C., Francis, B.A., Tannenbaum, A.R., 1991. Feedback Control Theory. Prentice Hall Professional Technical Reference.

Ebada, S.S., Lin, W.H., Proksch, P., 2010. Bioactive sesterterpenes and triterpenes from marine sponges: Occurrence and pharmacological significance. Mar. Drugs 8, 313–346. doi:10.3390/md8020313.

Formentin, S., van Heusden, K., Karimi, A., 2014. A comparison of model-based and data-driven controller tuning. International Journal of Adaptive Control and Signal Processing 28, 882–897. URL: https://onlinelibrary.wiley.com/doi/abs/10.1002/acs.2415, doi:10.1002/acs.2415, arXiv:https://onlinelibrary.wiley.com/doi/pdf/10.1002/acs.2415.

Formentin, S., Karimi, A., 2013. Direct data-driven design of sparse controllers, in: 2013 American Control Conference, pp. 3099–3104. doi:10.1109/ACC.2013.6580307.

Formentin, S., Savaresi, S.M., 2011. Virtual Reference Feedback Tuning for nonlinear systems, in: IFAC Proceedings Volumes (IFAC-PapersOnline), pp. 10219–10224. doi:10.3182/20110828-6-IT-1002.01184.

Fuchs, J.J., 2005. Recovery of exact sparse representations in the presence of bounded noise. IEEE Transactions on Information Theory 51, 3601–3608. doi:10.1109/TIT.2005.855614.

Gavahian, M., Farahnaky, A., Javidnia, K., Majzoobi, M., 2012. Comparison of ohmic-assisted hydrodistillation with traditional hydrodistillation for the extraction of essential oils from thymus vulgaris l. Innovative Food Science And Emerging Technologies 14, 85 – 91. URL: http://www.sciencedirect.com/science/article/pii/S1466856412000033, doi:https://doi.org/10.1016/j.ifset.2012.01.002.

Gavahian, M., Farhoosh, R., Javidnia, K., Shahidi, F., Farahnaky, A., 2015. Effect of applied voltage and frequency on extraction parameters and extracted essential oils from mentha piperita by ohmic assisted hydrodistillation. Innovative Food Science And Emerging Technologies 29, 161 – 169. URL: http://www.sciencedirect.com/science/article/pii/S1466856415000284, doi:https://doi.org/10.1016/j.ifset.2015.02.003. aPPLICATIONS OF PEF FOR FOOD PROCESSING.

Gavahian, M., Lee, Y.T., Chu, Y.H., 2018. Ohmic-assisted hydrodistillation of citronella oil from taiwanese citronella grass: Impacts on the essential oil and extraction medium. Innovative Food Science And Emerging Technologies 48, 33 – 41. URL: http://www.sciencedirect.com/science/article/pii/S1466856418303771, doi:https://doi.org/10.1016/j.ifset.2018.05.015.

Gavahian, M., Sastry, S., Farhoosh, R., Farahnaky, A., 2019. Ohmic heating as a promising technique for extraction of herbal essential oils: Understanding mechanisms, recent findings, and associated challenges, Academic Press. Advances in Food and Nutrition Research. URL: http://www.sciencedirect.com/science/article/pii/S1043452619300750, doi:https://doi.org/10.1016/bs.afnr.2019.09.001.

Gawde, A., Cantrell, C.L., Zheljazkov, V.D., Astatkie, T., Schlegel, V., 2014. Steam distillation extraction kinetics regression models to predict essential oil yield, composition, and bioactivity of chamomile oil. Industrial Crops and Products 58, 61 – 67. URL: http://www.sciencedirect.com/science/article/pii/S0926669014001927, doi:https://doi.org/10.1016/j.indcrop.2014.04.001.

Goro, O., Anderson, B., 2001. Model Reduction for Control System Design. Springer-Verlag London.

Guardabassi, G.O., Savaresi, S.M., 2000. Virtual reference direct design method: an off-line approach to data-based control system design. IEEE Transactions on Automatic Control 45, 954–959. doi:10.1109/9.855559.

Hashemi, S.M.B., Nikmaram, N., Esteghlal, S., Khaneghah, A.M., Niakousari, M., Barba, F.J., Roohinejad, S., Koubaa, M., 2017. Efficiency of Ohmic assisted hydrodistillation for the extraction of essential oils from oregano (Origanum vulgare subsp. viride) spices. Innovative Food Science & Emerging Technologies 41, 172–178. doi:10.1016/j.ifset.2017.03.003.

Hedengren, J.D., Shishavan, R.A., Powell, K.M., Edgar, T.F., 2014. Nonlinear modeling, estimation and predictive control in apmonitor. Computers and Chemical Engineering 70, 133 – 148. doi:https://doi.org/10.1016/j.compchemeng.2014.04.013. manfred Morari Special Issue.

van Heusden, K., Karimi, A., Bonvin, D., 2009. Data-driven controller validation. IFAC Proceedings Volumes 42, 1050 – 1055. URL: http://www.sciencedirect.com/science/article/pii/S1474667016387882, doi:https://doi.org/10.3182/20090706-3-FR-2004.00174. 15th IFAC Symposium on System Identification.

van Heusden, K., Karimi, A., Bonvin, D., 2011. Data-driven model reference control with asymptotically guaranteed stability. International Journal of Adaptive Control and Signal Processing 25, 331–351. URL: https://onlinelibrary.wiley.com/doi/abs/10.1002/acs.1212, doi:10.1002/acs.1212, arXiv:https://onlinelibrary.wiley.com/doi/pdf/10.1002/acs.1212.

Hou, Z.S., Wang, Z., 2013. From model-based control to data-driven control: Survey, classification and perspective. Inf. Sci. (Ny). 235, 3–35. URL: http://linkinghub.elsevier.com/retrieve/pii/S0020025512004781, doi:10.1016/j.ins.2012.07.014.

Howell, J., 1992. Fundamentals of Engineering Thermodynamics. McGraw-Hill.

Jacobsen, L.T., Spivey, B.J., Hedengren, J.D., 2013. Model predictive control with a rigorous model of a solid oxide fuel cell, in: 2013 American Control Conference, pp. 3741–3746. doi:10.1109/ACC.2013.6580409.

Kammer, L.C., Bitmead, R.R., Bartlett, P.L., 2000. Direct iterative tuning via spectral analysis. Automatica 36, 1301 – 1307. URL: http://www.sciencedirect.com/science/article/pii/S0005109800000406, doi:https://doi.org/10.1016/S0005-1098(00)00040-6.

Karimi, A., Galdos, G., 2010. Fixed-order h-infinity controller design for nonparametric models by convex optimization. Automatica 46, 1388 – 1394. doi:https://doi.org/10.1016/j.automatica.2010.05.019.

Karimi, A., van Heusden, K., Bonvin, D., 2007. Non-iterative data-driven controller tuning using the correlation approach, in: 2007 European Control Conference (ECC), pp. 5189–5195. doi:10.23919/ECC.2007.7068802.

Karimi, A., Miskovic, L., Bonvin, D., 2002. Convergence analysis of an iterative correlation-based controller tuning method. IFAC Proceedings Volumes 35, 413 – 418. URL: http://www.sciencedirect.com/science/article/pii/S1474667015385712, doi:https://doi.org/10.3182/20020721-6-ES-1901.00150. 15th IFAC World Congress.

Kergus, P., Olivi, M., Poussot-Vassal, C., Demourant, F., 2019. From reference model selection to controller validation: Application to loewner data-driven control. IEEE Control Systems Letters 3, 1008–1013. doi:10.1109/LCSYS.2019.2920208.

Knirsch, M.C., dos Santos, C.A., de Oliveira Soares Vicente, A.A.M., Penna, T.C.V., 2010. Ohmic heating - a review. Trends in Food Science & Technology 21, 436 – 441. URL: http://www.sciencedirect.com/science/article/pii/S0924224410001494, doi:https://doi.org/10.1016/j.tifs.2010.06.003.

Krausz, M., 2014. Lavender and lavandin: world production, strengths and weaknesses, in: IFEAT Conference, Rome, Italy.

Kusuma, H.S., Altway, A., Mahfud, M., 2018. Solvent-free microwave extraction of essential oil from dried patchouli (Pogostemon cablin Benth) leaves. J. Ind. Eng. Chem. 58, 343–348. URL: http://dx.doi.org/10.1016/j.jiec.2017.09.047, doi:10.1016/j.jiec.2017.09.047.

Landau, I., Rey, D., Karimi, A., Voda, A., Franco, A., 1995. A flexible transmission system as a benchmark for robust digital control*. European Journal of Control 1, 77 – 96. doi:https://doi.org/10.1016/S0947-3580(95)70011-5.

Lanzon, A., Lecchini, A., Dehghani, A., Anderson, B.D.O., 2006. Checking if controllers are stabilizing using closed-loop data, in: Proceedings of the 45th IEEE Conference on Decision and Control, pp. 3660–3665. doi:10.1109/CDC.2006.377549.

Lecchini, A., Campi, M., Savaresi, S., 2002a. Virtual reference feedback tuning for two degree of freedom controllers. International Journal of Adaptive Control and Signal Processing 16, 355–371. URL: https://onlinelibrary.wiley.com/doi/abs/10.1002/acs.711, doi:10.1002/acs.711.

Lecchini, A., Campi, M.C., Savaresi, S.M., 2002b. Virtual reference feedback tuning for two degree of freedom controllers. Int. J. Adapt. Control Signal Process. 16, 355–371. doi:10.1002/acs.711.

Ljung, L., 1999. System Identification: Theory for the User. second ed., Prentice Hall Inc, Upper Saddle River, NJ, USA.

Loizzo, M.R., Menichini, F., Conforti, F., Tundis, R., Bonesi, M., Saab, A.M., Statti, G.A., de Cindio, B., Houghton, P.J., Menichini, F., Frega, N.G., 2009. Chemical analysis, antioxidant, antiinflammatory and anticholinesterase activities of Origanum ehrenbergii Boiss and Origanum syriacum L. essential oils. Food Chem. 117, 174–180. URL: http://dx.doi.org/10.1016/j.foodchem.2009.03.095, doi:10.1016/j.foodchem.2009.03.095.

Lu, J., DePoyster, M., 2002. Multiobjective optimal suspension control to achieve integrated ride and handling performance. Control Systems Technology, IEEE Transactions on 10, 807–821.

Masango, P., 2005. Cleaner production of essential oils by steam distillation. J. Clean. Prod. 13, 833–839. doi:10.1016/j.jclepro.2004.02.039.

Matsuo, R., Yubai, K., Yashiro, D., Hirai, J., 2013. Tuning of controller parameters by FCbT with stability constraints for non-minimum phase plants, in: International Conference on Control, Automation and Systems, pp. 1736–1740. doi:10.1109/ICCAS.2013.6704217.

Milanese, M., Norton, J., Piet-Lahanier, H., Walter, E., 1996. Bounding Approaches to System Identification. Plenum Press, New York.

Milanese, M., Novara, C., 2004. Set membership identification of nonlinear systems. Automatica 40/6, 957–975.

Milanese, M., Novara, C., 2011. Unified set membership theory for identification, prediction and filtering of nonlinear systems. Automatica 47, 2141 – 2151. URL: http://www.sciencedirect.com/science/article/pii/S000510981100344X, doi:https://doi.org/10.1016/j.automatica.2011.03.013.

Milanese, M., Ruiz, F., Taragna, M., 2010. Direct data-driven filter design for uncertain lti systems with bounded noise. Automatica 46, 1773–1784.

Milanese, M., Taragna, M., 2005. $\mathcal{H}_\infty$ set membership identification: A survey. Automatica 41, 2019–2032.

Novara, C., 2012. Sparse identification of nonlinear functions and parametric set membership optimality analysis. IEEE Transactions on Automatic Control 57, 3236–3241. doi:10.1109/TAC.2012.2202051.

Novara, C., 2016. Sparse set membership identification of nonlinear functions and application to fault detection. International Journal of Adaptive Control and Signal Processing 30, 206–223. doi:10.1002/acs.2539, arXiv:https://onlinelibrary.wiley.com/doi/pdf/10.1002/acs.2539.

Novara, C. (Ed.), 2019. Data-Driven Modeling, Filtering and Control: Methods and applications. Control, Robotics; Sensors, Institution of Engineering and Technology. URL: https://digital-library.theiet.org/content/books/ce/pbce123e.

Novara, C., Fagiano, L., Milanese, M., 2013a. Direct feedback control design for nonlinear systems. Automatica 49, 849–860. URL: http://dx.doi.org/10.1016/j.automatica.2013.01.002, doi:10.1016/j.automatica.2013.01.002.

Novara, C., Ruiz, F., Milanese, M., 2013b. Direct filtering: A new approach to optimal filter design for nonlinear systems. Automatic Control, IEEE Transactions on 58, 86–99.

Patel, K., Mehta, A., 2019. Discrete-time sliding mode protocols for leader-following consensus of discrete multi-agent system with switching graph topology. European Journal of Control URL: http://www.sciencedirect.com/science/article/pii/S0947358019300457, doi:https://doi.org/10.1016/j.ejcon.2019.06.011.

Piga, 2009. A convex relaxation approach to set-membership identification. Ph.D. thesis. Politecnico di Torino.

Previde, F., Belloli, D., Cologne, A., Savaresi, S., 2010. Virtual reference feedback tuning (vrft) design of cascade control systems with application to an electro-hydrostatic actuator. IFAC Proceedings Volumes 43, 626 – 632. URL: http://www.sciencedirect.com/science/article/pii/S1474667015375467, doi:https://doi.org/10.3182/20100913-3-US-2015.00033. 5th IFAC Symposium on Mechatronic Systems.

Rojas, D., 2011. Extensions and applications of the Virtual Reference Feedback Tuning. Ph.D. thesis. Universidad Autónoma de Barcelona.

Roohi, R., Hashemi, S.M.B., 2019. Experimental and computational fluid dynamics modeling of satureja khuzestanica essential oil extraction during ohmic-hydrodistillation. Journal of Food Process Engineering 42, e13083. URL: https://onlinelibrary.wiley.com/doi/abs/10.1111/jfpe.13083, doi:10.1111/jfpe.13083, arXiv:https://onlinelibrary.wiley.com/doi/pdf/10.1111/jfpe.13083.

Ruiz, F., Novara, C., Milanese, M., 2010. Direct design from data of optimal filters for LPV systems. Systems & Control Letters 59, 1 – 8.

Safdarnejad, S.M., Hedengren, J.D., Baxter, L.L., 2015a. Plant-level dynamic optimization of cryogenic carbon capture with conventional and renewable power sources. Applied Energy 149, 354 – 366. doi:https://doi.org/10.1016/j.apenergy.2015.03.100.

Safdarnejad, S.M., Hedengren, J.D., Lewis, N.R., Haseltine, E.L., 2015b. Initialization strategies for optimization of dynamic systems. Computers and Chemical Engineering 78, 39 – 50. doi:https://doi.org/10.1016/j.compchemeng.2015.04.016.

Sakr, M., Liu, S., 2014. A comprehensive review on applications of ohmic heating (oh). Renewable and Sustainable Energy Reviews 39, 262 – 269. URL: http://www.sciencedirect.com/science/article/pii/S1364032114005139, doi:https://doi.org/10.1016/j.rser.2014.07.061.

Sala, A., Esparza, A., 2005. Extensions to "virtual reference feedback tuning: A direct method for the design of feedback controllers". Automatica 41, 1473–1476. URL: http://linkinghub.elsevier.com/retrieve/pii/S0005109805000804, doi:10.1016/j.automatica.2005.02.008.

Savaresi, S.M., Bittanti, S., Silani, E., Porciani, N., 2003. On performance evaluation methods and control strategies for semiactive suspension systems, in: Proc. IEEE Conference on Decision and Control, Maui, Hawaii.

Seidi Damyeh, M., Niakousari, M., Golmakani, M.T., Saharkhiz, M.J., 2016. Microwave and ohmic heating impact on the in situ hydrodistillation and selective extraction of satureja macrosiphonia essential oil. Journal of Food Processing and Preservation 40, 647–656. URL: https://onlinelibrary.wiley.com/doi/abs/10.1111/jfpp.12644, doi:10.1111/jfpp.12644, arXiv:https://onlinelibrary.wiley.com/doi/pdf/10.1111/jfpp.12644.

Simoes, A., 2018. The observatory of economic complexity. https://atlas.media.mit.edu/en/. MIT Media Lab.

Skogestad, S., Postlethwaite, I., 2005. Multivariable feedback control: analysis and design. second ed., John Wiley & Sons, Chichester, UK.

Soderstrom, T., Stoica, P., 1983. Instrumental variable methods for system identification. Berlin:Springer.

Sovová, H., 2005. Mathematical model for supercritical fluid extraction of natural products and extraction curve evaluation. Journal of Supercritical Fluids 33, 35–52. doi:10.1016/j.supflu.2004.03.005.

Stashenko, E.E., 2009. Aceites Esenciales. Division de publicaciones UIS.

Tanaskovic, M., Fagiano, L., Novara, C., Morari, M., 2015. On-line direct control design for nonlinear systems. IFAC-PapersOnLine 48, 144 – 149. doi:https://doi.org/10.1016/j.ifacol.2015.12.115. 17th IFAC Symposium on System Identification SYSID 2015.

Thompson, D.W., 1987. Fluid mechanics and transfer processes, j. m. kay and r. m. nedderman, 1985, 602 pages. published by cambridge university press, $69.50 us (hardcover), $29.95 us (paperback). The Canadian Journal of Chemical Engineering 65, 526–527. URL: https://onlinelibrary.wiley.com/doi/abs/10.1002/cjce.5450650328, doi:10.1002/cjce.5450650328, arXiv:https://onlinelibrary.wiley.com/doi/pdf/10.1002/cjce.5450650328

Tropp, J.A., 2004. Greed is good: algorithmic results for sparse approximation. IEEE Transactions on Information Theory 50, 2231–2242. doi:10.1109/TIT.2004.834793.

Tropp, J.A., 2006. Just relax: convex programming methods for identifying sparse signals in noise. IEEE Transactions on Information Theory 52, 1030–1051. doi:10.1109/TIT.2005.864420.

Turner, G.W., Gershenzon, J., Croteau, R.B., 2000. Distribution of peltate glandular trichomes on developing leaves of peppermint. Plant Physiol. 124, 655–664. doi:10.1104/pp.124.2.655.

Usami, H., 2010. Correlation-based Direct Tuning of 2DOF Controller by Least Squares, in: 11th IEEE International Workshop on Advanced Motion Control, pp. 637–642.

Valderrama, F., 2018. Ohmic heater for extracting essential oils from aromatic plants. Scientia et Technica 23, 160 – 167. URL: http://revistas.utp.edu.co/index.php/revistaciencia/article/view/16931/11751, doi:http://dx.doi.org/10.22517/23447214.16931.

Valderrama, F., Ruiz, F., 2014. Controller design from data under UBB noise. Proc. Am. Control Conf. , 5103–5108doi:10.1109/ACC.2014.6858626.

Valderrama, F., Ruiz, F., 2018. An optimal control approach to steam distillation of essential oils from aromatic plants. Computers & Chemical Engineering 117, 25 – 31. URL: http://www.sciencedirect.com/science/article/pii/S0098135418301352, doi:https://doi.org/10.1016/j.compchemeng.2018.05.009.

Valderrama, F., Ruiz, F., 2019. A comparative study of vrft and set-membership data-driven controller design techniques: active suspension tuning case, in: Data-Driven Modeling, Filtering and Control: Methods and applications. Institution of Engineering and Technology. Control, Robotics and amp; Sensors, pp. 165–188. URL: https://digital-library.theiet.org/content/books/10.1049/pbce123e_ch9, doi:10.1049/PBCE123E_ch9.

Valderrama, F., Ruiz, F., Patino, D., 2019. Evaluation of set-membership approaches for data-driven tuning of two-degree-of-freedom controllers, in: 2019 American Control Conference (ACC), pp. 5668–5673. doi:10.23919/ACC.2019.8814372.

van Heusden, K., Karimi, A., Bonvin, D., 2007. Data-driven estimation of the infinity norm of a dynamical system, in: 2007 46th IEEE Conference on Decision and Control, pp. 4889–4894. doi:10.1109/CDC.2007.4434184.

Van Heusden, K., Karimi, A., Bonvin, D., 2011a. Data-driven model reference control with asymptotically guaranteed stability. International Journal of Adaptive Control and Signal Processing 25, 331–351. URL: https://onlinelibrary.wiley.com/doi/abs/10.1002/acs.1212, doi:10.1002/acs.1212, arXiv:https://onlinelibrary.wiley.com/doi/pdf/10.1002/acs.1212.

Van Heusden, K., Karimi, A., Söderström, T., 2011b. On identification methods for direct data-driven controller tuning. International Journal of Adaptive Control and Signal Processing 25, 448–465.

Vargas A, B.E., 2008. Estudio De La Composición Química De Los Aceites Esenciales De Seis Especies Vegetales Cultivadas.

Wächter, A., Biegler, L.T., 2006. On the implementation of an interior-point filter line-search algorithm for large-scale nonlinear programming. Mathematical Programming 106, 25–57. doi:10.1007/s10107-004-0559-y.

Waki, H., Kim, S., Kojima, M., Muramatsu, M., Sugimoto, H., 2008. Algorithm 883: Sparsepop - a sparse semidefinite programming relaxation of polynomial optimization problems. ACM Transactions on Mathematical Software 35. doi:10.1145/1377612.1377619.

Yubai, K., Usami, H., Hirai, J., 2009. Correlation-based Direct Tuning of MIMO Controllers by Least-squares and Its Application to Tension-and-speed Control Apparatus. Design , 931–936.

Zhou, K., Doyle, J.C., 1998. Essentials of Robust Control. Prentice Hall Inc, Upper Saddle River, NJ, USA.